AFML-TR-75-191

F.G.

12

ADA025365

FURTHER DEVELOPMENT OF RELIABILITY ANALYSIS APPLICATION TO STRUCTURAL FATIGUE EVALUATION

Boeing Commercial Airplane Company

January 1976

TECHNICAL REPORT AFML-TR-75-191

Final Report for Period February 1974—October 1975

Approved for public release; distribution unlimited

AIR FORCE MATERIALS LABORATORY
Air Force Wright Aeronautical Laboratories
AIR FORCE SYSTEMS COMMAND
Wright-Patterson Air Force Base, Ohio 45433

NOTICE

When Government drawings, specifications, or other data are used for any purpose other than in connection with a definitely related Government procurement operation, the United States Government thereby incurs no responsibility nor any obligation whatsoever; and the fact that the Government may have formulated, furnished, or in any way supplied the said drawings, specifications, or other data, is not to be regarded by implication or otherwise as in any manner licensing the holder or any other person or corporation, or conveying any rights or permission to manufacture, use, or sell any patented invention that may in any way be related thereto.

This technical report has been reviewed and is approved for publication. This report has been reviewed by the appropriate Office of Information (OI) and is releasable to the National Technical Information Service (NTIS). At NTIS, it will be available to the general public, including foreign nations.

ROBERT C. DONAT

Project Engineer

FOR THE COMMANDER

VINCENT J. RUSSO
Metals Behavior Branch
Metals and Ceramics Division
Air Force Materials Laboratory

Copies of this report should not be returned unless return is required by security considerations, contractual obligations, or notice on a specific document.

AIR FORCE - 17 MAY 76 - 150

Unclassified

SECURITY CLASSIFICATION OF THIS PAGE (When Data Entered)

19

REPORT DOCUMENTATION PAGE

READ INSTRUCTIONS BEFORE COMPLETING FORM

18

1. REPORT NUMBER
AFML-TR-75-191

2. GOVT ACCESSION NO.

3. RECIPIENT'S CATALOG NUMBER

9

6

4. TITLE (and Subtitle)
FURTHER DEVELOPMENT OF RELIABILITY ANALYSI
APPLICATION TO STRUCTURAL FATIGUE EVALUATI

5. TYPE OF REPORT & PERIOD COVERED
Final Report,
15 Feb[redacted]74—15 Oct[redacted]75

6. PERFORMING ORG. REPORT NUMBER

10

7. AUTHOR(s)
I. C. Whittaker [redacted] S. C. Saunders

15

8. CONTRACT OR GRANT NUMBER(s)
F33615-74-C-5037

NEW

9. PERFORMING ORGANIZATION NAME AND ADDRESS
Boeing Commercial Airplane Company
P.O. Box 3707
Seattle, Wash[redacted] 98124

16

AF-7351, AF-7367

17

10. PROGRAM ELEMENT, PROJECT, TASK AREA & WORK UNIT NUMBERS
Project 7351 Project 1367
Task 735106, [redacted] 136703

11. CONTROLLING OFFICE NAME AND ADDRESS
Air Force Materials Laboratory (LLN)
Wright-Patterson Air Force Base, Ohio 45433

11

12. REPORT DATE
Jan[redacted]76

13. NUMBER OF PAGES
92

14. MONITORING AGENCY NAME & ADDRESS (if different from Controlling Office)

12 101 p.

15. SECURITY CLASS. (of this report)
Unclassified

15a. DECLASSIFICATION/DOWNGRADING SCHEDULE

16. DISTRIBUTION STATEMENT (of this Report)
Approved for public release; distribution unlimited

17. DISTRIBUTION STATEMENT (of the abstract entered in Block 20, if different from Report)

18. SUPPLEMENTARY NOTES

19. KEY WORDS (Continue on reverse side if necessary and identify by block number)

Structural reliability	Fail-safe	Estimation theory
Fatigue performance	Residual strength	Simulation
Preflaw	Censored data	
Detectable size	Distribution function	

20. ABSTRACT (Continue on reverse side if necessary and identify by block number)

Three parameter symmetric distributions have been investigated for application as a fatigue life distribution model. Maximum likelihood (ML) estimator, and simulation procedures for maximum variance unbiased estimates and confidence bounds have been developed for analysis of censored data. A technique for testing the hypothesis of two censored samples having a common parent population is also presented. The effect on airplane structural reliability resulting from differing levels of fatigue performance

DD FORM 1 JAN 73 1473 EDITION OF 1 NOV 65 IS OBSOLETE

Unclassified

SECURITY CLASSIFICATION OF THIS PAGE (When Data Entered)

390 145

from nominally identical structures is discussed, and a preflaw model was developed and incorporated in a reliability analysis method. Parametric studies were conducted using the reliability method to obtain qualitative information on the impact and interaction in terms of structural reliability, of several variables such as preflaws, loads environment, material, structural configuration, and designed residual strength.

FOREWORD

The research work reported herein was conducted at the Boeing Commercial Airplane Company, P.O. Box 3707, Seattle, Washington. The contract was initiated by the Metals and Ceramics Division, Air Force Materials Laboratory, Air Force Systems Command, Wright-Patterson Air Force Base, Ohio, and was performed under contract F33615-74-C-5037 through project 7351, "Metallic Materials," task 735106, "Behavior of Metals." Support was also provided by the Air Force Flight Dynamics Laboratory through project 1367, "Structural Integrity for Military Aerospace Vehicles," task 136703, "Fatigue, Fracture and Reliability Analyses and Design Methods for Aerospace Vehicles." Mr. R. C. Donat (AFML/LLN) was the project engineer.

The research work was performed within the Boeing Commercial Airplane Company Structures Technology Staff, Stress and Fatigue Research Groups, Fail-Safe and Fatigue Section. Mr. J. P. Butler acted as the program manager. Mr. I. C. Whittaker was the principal investigator, while Dr. S. C. Saunders of Washington State University developed the statistical formulation, and Dr. C. M. Carlson of Boeing Computer Services, Inc., provided computing assistance. Work began 15 February 1974 and was completed in October 1975. This report was submitted by the authors in January 1976.

TABLE OF CONTENTS

Page

TABLE OF CONTENTS (Concluded)

Page

LIST OF ILLUSTRATIONS

LIST OF ILLUSTRATIONS (Concluded)

LIST OF TABLES

LIST OF ABBREVIATIONS AND SYMBOLS

Abbreviations

E	Mathematical expectation
exp	Exponential function
kc	Kilocycle
ℓn	Natural logarithm
ML	Maximum likelihood
MLE	Maximum likelihood estimate
p( )	Probability of that event described within parenthesis
var	Mathematical variance
sgn	Signum function; value is 1 for $x > 0$, -1 for $x < 0$, and 0 for $x = 0$

Symbols

Ξ	Special class of functions
ξ	Disposable function expressing a reciprocal relationship
ϵ	Element of a set, such as in $\xi \epsilon \Xi$
$\omega(x)$	Disposable function for ℓn-life variates
α, γ, μ	Flexure, scale, and location parameters for the ℓn-life model
Φ	Standard normal distribution
L	Likelihood function
P, R	Product and ratio functions of certain derivatives of ω
σ	Standard deviation
s	Sample standard deviation
T, U	Statistics based on the location and scale parameters
V	A statistic based on the scale parameter
F( ), G( )	Symbols of time-to-failure distribution functions

r	Number of ordered failure observations in sample
n	Sample size
τ	Size of detectable flaw or damage
ζ	Standard normal variate at specific probability level
ν	Exponent of flaw size density distribution
$\hat{}$	Maximum likelihood point estimate, as in $\hat{\gamma}$
$\hat{\hat{}}$	Point estimate that is free of bias, as in $\hat{\hat{\gamma}}$
$*$	Point estimate obtained from the STAR estimator as in α^*
$\overline{}$	Average value, as in $\overline{\alpha}$
$\tilde{}$	An unbiased average value, as in $\tilde{\gamma}$
$\sim$	Follows a specified distribution, as in $Z \sim N(0,1)$

1.0 INTRODUCTION

Aircraft structural systems must meet stringent strength demands, as well as requirements, for durability and integrity during their operational lifetime. As part of the related research and development work for materials, the Air Force Materials Laboratory (AFML) has sponsored considerable research concerned with the application of reliability technology to the problem of assessing and assuring the fatigue performance of structural materials. This present study further develops one phase of that work on applying reliability methodology to the fatigue performance of aircraft structures.

At best, fatigue behavior is a complex one. It concerns not only the spectrum of variables like loads, geometry, structural response, manufacture, etc., all affecting the initiation and extension of fatigue damage, (i.e., the fatigue crack) but also the coincident material behavior. Of particular note is the variability in the response of materials to this complicated total environment. Scatter in the fatigue performance of materials, exposed to a given load environment, is an observation well-documented in the annals of structural mechanics ever since fatigue behavior was first identified. The early unpredicted appearance of fatigue damage as a detectable crack, followed by its subsequent propagation to cause failure if undetected, has a potentially detrimental effect on the function and safety of operational structures, not to mention the serious economic consequences. However, with the development of the science of fracture mechanics during the last 20 years, a means has evolved by which a structural material's fatigue performance can be characterized for the conditions of crack propagation and residual strength.

Obviously, the measured time to fatigue crack initiation in a structural system is a function of the detection capability for the crack as well as the complicated cumulative response to its environment. The crack growth rate and fracture toughness of a material are physical parameters identifying the other important properties necessary to assess the durability and integrity of a structure during its operational lifetime. These three fatigue-related properties exhibit variability and depend on experimental determination. Accordingly, this empiric nature of the fatigue process makes it a ready candidate for application of statistical techniques and reliability technology.

As a matter of coincident interest, the strength properties of materials are treated with a well tested and widely accepted reliability methodology in defining the mechanical properties of strength. A normal distribution is assumed for a particular property like ultimate tensile strength. This mechanical property is measured and distribution parameters estimated from the data, allowing a reliable level of strength to be established. Thus, sampling techniques and the selection of some degree of assurance provide a confidence and probability level with which the specific alloy and condition will demonstrate the desired strength property.

However, the task of applying the material to a structural configuration introduces some additional difficulties. Major portions of the structural system fulfill a multiple role of providing aerodynamic properties and function and structural capability at very

stringent levels of structural efficiency. This situation can introduce some hazards in the design process. Nevertheless, ultimate strength goals usually present only minimal difficulties in matching a prescribed load envelope to a structural capability. A well-developed analysis technology backed by an experimental strength verification procedure of static testing generally assures achieving a specified strength goal. Structural strength deficiencies uncovered during this process are usually resolvable by effective modifications, often simple, to achieve the specified strength levels within the production fleet.

On the other hand, attaining durability is a more difficult task. It has a more complex design and verification process, since it is subject to unexpected and unidentified operational exposure than that presumed during design. Furthermore, the analysis process apparently seems neither as well developed nor as universally understood as the comparable static strength design procedures. Likewise, remedial steps are not as simple as those for static strength because of the cumulative aspects rather than the single discrete response to a load. A simple corrective effort may introduce other fatigue sensitive details and thus be only temporary in nature. Additionally, fatigue damage initiation and propagation are continuing hazards over the total operational life of the structural system. Hence, the capability for analysis must not only encompass the initial paper-to-hardware development phase but also need to be capable of coping with results from the operational phase. However, despite the very local nature of fatigue damage and its difficulty of detection in structural details, some degree of damage tolerance built into the surrounding area can provide the opportunity to extend the serviceability of the structure beyond the first bell-ringer incident of fatigue crack initiation.

Approaches compensating for fatigue life variability in aircraft structural systems have ranged from selecting arbitrary scatter factors, like 2 or 4, to using computational procedures based on theory. As in the ultimate strength problem, the primary emphasis on developing a rationale to characterize the scatter in fatigue behavior has been to fit a statistical distribution function to observed data. With an identified distribution function and estimated parameters, the likely performance and the associated factor of safety to assure an acceptable level of fatigue performance are determinable. The measure of success of this approach is the accuracy with which the selected distribution and its parameters replicate the observed scatter in fatigue performance. The particular advantage (i.e., gaining structural efficiency) in this approach is the reduction in tolerance gained through identifying only the shape and scale parameters of the distribution function. For each structural detail, the determination of the location parameter is always necessary. Added assurance is gained on the likely performance as more data are acquired to estimate the location parameter (i.e., the mean or other characteristic life). Then the probabilistically determined scatter factor applied to characteristic life provides a practical way to attain reliability in fatigue.

There are several problems associated with this approach to the fatigue damage initiation prediction previously described. First, identification of the distribution is done empirically, although the central tendency (the mean, median, or characteristic life) is reasonably identified by a few test values. However, for a large group of identical structures in a specific operating environment, the operational condition of the group is

more closely identified by the time-to-first failure (or subsequent early failures) of a detail rather than the average behavior. Consequently, to determine the adequacy of the fit of the distribution, the quantity of test data must be sufficient to verify the accuracy of the toe of the distribution. Accordingly, hundreds or even thousands of detail fatigue test results are necessary to recognize and estimate the probability of the early failure in the group of parts. Collecting such extensive data may be practically and economically impossible for a particular structure. Another facet of the problem concerns the very nature of a statistical behavior; the actual life of a part is not predictable on a part-to-part basis but instead only by the probable performance as determined by a general distribution. Thus, the hazards of population identification from samples must be resolved directly after incidents occur. Alternatively, the parts may be replaced on the basis of an acceptable probability of failure from a safe life reliability analysis scheme. Of course this makes some assumptions about the expected usage of a part. However, a fail-safe or damage-tolerant structural design process provides a practical opportunity to treat fatigue crack initiation on a part-to-part basis if unanticipated damage does initiate prior to predicted goals.

Some of the early work sponsored by AFML explored the variability of the initiation of fatigue damage in terms of statistical and related reliability concepts. This led to an examination of the time-to-first failure rather than a factored "average" time to assess fatigue performance. In reference 1, characteristics of the log-normal, Weibull, and gamma distributions were studied relative to the first failure for a range of sample (i.e., fleet) sizes. A further development on the application of this first failure concept to a fleet was reported in reference 2. This latter investigation developed the concept involving specific structural details in relation to the task of design, manufacture, and subsequent operational exposure. This study considered the associated practices of fatigue life estimation, supported by developmental and verification testing of the aircraft structural system. Primary emphasis focused on the application of the log-normal and Weibull distributions, describing fatigue damage initiation variability. Scale parameters were determined by examining test data from many groups, mostly small ones, of various types of specimens. A standard deviation of 0.14 was derived for the log-normal distribution shape parameter, while the value 4.0 was appropriate for the Weibull distribution. Using the Weibull distribution function, an application of the time-to-first failure concept was made to a tanker transport type of aircraft subdivided by usage into a number of different fleets. Eight different details, which had laboratory identified fatigue performance during the design stage, were investigated for their subsequent behavior in the operational fleets. A promising correlation was found between the predicted fatigue performance and service results available at that time.

In reference 3, the problem of identifying a representative distribution to characterize fatigue scatter was explored for aluminum alloy materials as well as titanium and steel. A technique for normalizing and utilizing the data from many groups of tests was applied. This process made available thousands of test points and provided an insight into the extreme behavior of the normalized test data. The Weibull distribution appeared to fit the tendency of the data to flare out at very low probabilities. Other subsequent studies were made on the application of this reliability technology scheme to another type of cargo airplane and a fighter aircraft, references 4 and 5, respectively. Both of these studies indicated that the early failure concept provided a corroboration

with fleet performance. However, the Weibull distribution provided a more conservative estimate of fatigue damage initiation than the log-normal distribution. Furthermore, the fatigue results demonstrated by laboratory-programmed loading tests indicated scale factors less than the standardized values of reference 2. This is not a contradiction, since it is the result of statistical assessment of observed data and the related problem of sampling.

In the reference 5 study, two other concepts were explored for application of the reliability analysis scheme utilizing the first failure approach. One proposed determination of the scatter factor as the ratio of two random quantities, namely the test life and service life from a Weibull population. This approach is different from the previously proposed scheme which samples a population to estimate its location parameter and calculates the likely occurrence of the first or early failure. The smaller scatter factor of the former estimation scheme is illustrative of the different approach. A second variation was the definition of a joint scatter factor to combine the effects of fatigue and usage. In the reference 2 approach, the characteristic or mean life is treated as an input, principally because of the very nature of cumulative fatigue damage response of materials. It is of pertinent interest to note that both references 4 and 5 had illustrations in which prediction did not correlate with service results. However, this observation is not unique to those two investigations. Hence, the introduction of a joint scatter factor for fatigue and use is not included in the basic reliability analysis scheme. Certainly, additional work seems necessary to evaluate and judge the part played by measured usage in terms of cumulative acceleration counts and the responding cumulative damage.

Considering further the choice of a representative distribution to simulate the variability in time-to-fatigue crack initiation under a given loading environment, an experimental study, summarized in references 6, 7, and 8, generated order-statistic test data from multidetail specimens. A graphical study of all the data (refs. 7 and 8) did not indicate an obviously superior fit of the experimental external data by either the Weibull or log-normal form of distribution. However, the Weibull distribution generally predicted an earlier, more conservative estimate of the first failure than did the log-normal. This was particularly apparent as the level of reliability varied from 0.50 to 0.95 for the early failures.

As noted in a preceding paragraph, the log-normal and two-parameter Weibull statistical distributions were compared with empirical distributions obtained from a considerable amount of normalized fatigue test data (ref. 3). These empirical distributions were observed to have a tendency toward symmetry between the upper and lower halves when plotted on normal probability paper, and also to have a flexure mode. This latter behavior disagrees with the characteristics of the log-normal distribution, whereas the former symmetry condition is not found in results generated from a Weibull model. However by transforming the basic two-parameter Weibull distribution, a new "symmetric-Weibull" distribution was obtained, which had the basic form of the empirically obtained fatigue test distribution.

Subsequent to this investigation, it was determined that the modified or symmetric-Weibull distribution belonged to a new class of statistical distributions

(ref. 9) that contained certain reciprocal properties (ref. 10). It was clear, therefore, that other distributions within this class should be examined to determine if a more suitable fatigue life distribution model was available. In this context the term suitable is not necessarily limited to an evaluation based on data correlation but must include aspects of ease of application, philosophic rationale, etc. For example, the fatigue distribution model that would show the most correlation with the data is one formed empirically from the data. This would contain many more parameters (ref. 11) and would thus become extremely difficult if not impossible to apply to typical problems such as parameter estimation from censored observations, determination of confidence bounds, and so forth.

It should be realized that an airplane designer is frequently guided by the past performance, either operational or test, of similar components to the one presently being designed or modified. Operational fatigue data are, without exception, of the extreme event type, and as such information needs to be assessed it is necessary to have an estimation procedure, preferably giving unbiased values, for the general case of censored data. Consequently it is advisable, for reasons of practicality, to keep the numbers of parameters or variables to a minimum.

The correct interpretation of operational data is further confounded by the fact that all of the limited information may not be completely identical, but come from nominally different subsets; e.g., small differences in failure locations, structural operation, etc. It is, therefore, most desirable to have the capability of: (1) obtaining bounded estimates of the distribution parameters from the censored data and (2) testing the hypothesis that different censored data subsets actually do or don't come from the same parent population.

While fatigue crack initiation is a key milestone in the usable life of a structural system, the presence of fail-safe or damage-tolerant capabilities in structures introduces concepts of crack growth, inspection control for detection of initiated cracks before the deterioration of structural safety, and the upper limit of crack growth as dictated by the residual strength capability of the fatigue-damaged structure. These elements of fatigue performance of a structural system are all a part of the basic reliability plan of this current investigation. This multidiscipline structural reliability method, initially described in reference 12 and subsequently revised and expanded in references 13 and 14, recognizes that the time-to-crack initiation and its growth is a random event. However, current Air Force philosophy (ref. 15) reflects an approach based on the preexistence of a flaw at a critical detail in the structure when it enters operational service. Hence, some accounting for the concept of an undetected flaw at time zero is also a desirable element of this reliability analysis scheme.

This report discusses the findings from an investigation of the topics mentioned in the preceding paragraphs. The new class of distributions is discussed in section 2.0, and four distributions from this class are highlighted. Section 3.0 discusses the development of parameter estimation procedures, both censored and uncensored data, for one of the described distributions. An efficient method, which is believed to be a major advance, of obtaining unbiased estimates and confidence bounds for censored data is also described in this section. Additionally, a means of testing the hypothesis that two independent

data samples belong to the same parent population is presented. Finally these developed procedures have been applied for illustrative purposes to some real samples of censored fatigue data.

The discussion given in section 4.0 of this report covers the rationale for development of the preflaw model; section 5.0 describes the model and its application to the existing reliability analysis system given in references 12 and 13. Finally, section 6.0 covers the results of some parametric studies made using the expanded reliability system.

Two other sections complete the document. Section 7.0 discusses structural data input considerations, and section 8.0 gives the conclusions reached from this investigation and lists some recommendations.

2.0 THE ADVANCED DISTRIBUTIONS

2.1 A NEW CLASS OF ADVANCED DISTRIBUTIONS FOR FATIGUE DATA

A considerable amount of fatigue test data was collected and normalized in an earlier investigation (ref. 3). These normalized results were then used to define empirical distributions which, when plotted on normal probability paper, demonstrated both a flexure at the tails and a symmetry between upper and lower halves.

A transformation of the two-parameter Weibull into a symmetrical-Weibull distribution was developed and was found to have the characteristics of the empirical distribution. Subsequently, it was established that the symmetric-Weibull distribution belonged to a new advanced class of distributions that had certain reciprocal properties (refs. 9 and 10).

The following initial study considers four distribution functions from within this new class of distributions. The first is the log-normal distribution that can be used as the reference baseline, and another for obvious reasons is the symmetric-Weibull. Two other distributions are those from reference 10 and are labelled as the hyperbolic sine and the inverse hyperbolic sine distributions.

These distributions, described in the following paragraphs, are based on three parameters. In their application to modeling fatigue performance, it is assumed that a flexure parameter will represent material behavior; a scale parameter will reflect such variables as configuration, size, type of loading, etc., which are characteristics of the specimen and the fatigue test; and finally a location parameter which will depend primarily on the magnitude of the loads to which the test specimen is subjected.

2.1.1 THE ξ-NORMAL DISTRIBUTION

Let Ξ be a class of real valued functions so that if $\xi \epsilon \Xi$ then it satisfies the functional equation

$$\xi(t) = -\xi(1/t) \quad \text{for } t > 0 \qquad (2.1.1\text{-}1)$$

If T is a nonnegative random variable so that there exists constants $\alpha, \beta > 0$ and $\xi \epsilon \Xi$, for which

$$\frac{1}{\alpha}\xi\left(\frac{T}{\beta}\right) \sim \text{Normal}\,(0,1)$$

then by adopting a nomenclature analogous to that of the log-normal distribution, it can be said that T is ξ-normal.

Thus if T is ξ-normal with parameters $\alpha, \beta > 0$ and has a distribution F then

$$F(t) = \Phi\left[\frac{1}{\alpha}\xi(t/\beta)\right] \quad \text{for } t > 0$$

where

$$\Phi(x) = \frac{1}{\sqrt{2\pi}} \int_{\infty}^{x} e^{-t^2/2} dt \qquad (2.1.1\text{-}2)$$

To facilitate comparison with currently available plotted data that are so frequently in terms of the logarithm of the number of cycles, consider the log-life variate $X = \ell nT$ and take its distribution G to be of the form

$$G(x) = \Phi\left[\frac{1}{\alpha}\omega(x-\mu)\right] \quad -\infty < x < \infty \qquad (2.1.1\text{-}3)$$

where $\mu = \ell n\beta$; $\omega(x) = \xi(e^x)$ for all x.

Now consider a class of functions Ω defined as follows:

$$\omega \epsilon \Omega \text{ iff } \omega' > 0,\ \omega' > \omega'' \text{ and } \omega \text{ is odd, checking that } \omega\epsilon\Omega \text{ iff } \xi\epsilon\Xi$$
$$\text{when } \omega(x) = \xi(e^x) \quad -\infty < x < \infty \qquad (2.1.1\text{-}4)$$

Examining now the closure properties of Ω. Assuming that if

$$\omega_1, \omega_2\ \epsilon\Omega \text{ then } \omega_1 + \omega_2\ \epsilon\Omega$$

and moreover if

$$\omega\epsilon\Omega \text{ and } a > 0, 0 < b < 1$$

then both

$$\omega_1, \omega_2\ \epsilon\Omega \text{ where } \omega_1(x) = a\omega(x) \text{ and } \omega_2(x) = \omega(bx) \quad \text{for } -\infty < x < \infty$$

As a consequence, for any given $\omega\epsilon\Omega$, a three-dimensional parametric family of distributions of the log-life can be generated, namely,

$$G(x: \alpha,\gamma,\mu) = \Phi\left[\frac{1}{\alpha}\omega\left(\frac{x-\mu}{\gamma}\right)\right] \quad -\infty < x < \infty \tag{2.1.1-5}$$

where $\alpha > 0, \gamma > 0, -\infty < \mu < \infty$.

In this notation, μ is the location parameter, γ is the scale parameter, and α is the flexure parameter. The flexure and scale both together control the shape. (Note that if it is required that $\omega' \geq \omega''$, a restriction $\gamma > 1$ must apply to ensure the closure properties.)

Examples of such functions ω, which correspond to known parametric families, for $-\infty < x < \infty$, are:

$$\omega_1(x) = \sinh x$$

$$\omega_2(x) = \omega_1^{-1}(x) = \ell n(x+\sqrt{x^2+1})$$

which corresponds to the distributions of Birmbaum-Saunders, and

$$\omega_3(x) = \Phi^{-1}[F(x)]$$

where

$$F(x) = \frac{1-\text{sgn } x}{2} + (\text{sgn } x) \exp\left\{-(\ell n 2)e^{-|x|}\right\}$$

which corresponds to the symmetric-Weibull distribution.

Finally for comparison, a well-known and commonly used fatigue life distribution is taken as

$$\omega_4(x) = x$$

which corresponds with the log-normal distribution as it was shown earlier that $X = \ell nT$.

2.1.2 DISCUSSION OF EXPLORATORY APPLICATION AND RESULTS

The typical behavior of this class of distributions is illustrated in figures 1 through 4. These show cumulative frequency plots of the four statistical models, discussed previously, for several arbitrary values of the flexure parameter α. It is clear from these

illustrations that the log-normal model (fig. 1) plots linearly and thus does not have the flexure which has been observed to be characteristic of fatigue data. The other three selected models are all seen to flex with the hyperbolic sine distribution, (fig. 2), flexing in a direction opposite to either the inverse hyperbolic sine or the symmetric-Weibull distributions, figures 3 and 4, respectively. These latter three figures also vividly demonstrate the importance of the flexure parameter α, because it is obvious how the frequency plot can go from almost linear to highly flexed depending upon the magnitude of α. Finally the scale parameter γ is seen to govern the slope of the plots and is thus analogous to the standard deviation parameter of a normal distribution.

A large amount of aluminum fatigue data was normalized and plotted on normal probability in reference 3. These data have been reproduced in this report in figure 5 using the α-ordinate, γ-abscissa format of figures 1 through 4. The amount of flexure exhibited by the data is immediately obvious, and the almost "mirror image" nature of the lower and upper halves of the curve is also clear. The best log-normal and symmetric-Weibull distribution values are superimposed on the data-curve. This chart demonstrates that the log-normal plots linearly as expected and the symmetric-Weibull does follow the data trend and flex, although not enough to exactly match the data at the extreme tails.

Figure 6 shows the comparison of the Birmbaum-Saunders inverse hyperbolic sine distribution with the aluminum data curve. A value of $\alpha = 0.74$ was used to compute the curve shown in this figure. It is clear from figure 6 that this distribution model can virtually duplicate the empirical distribution, with only a small mismatch in the extreme upper tail at approximately the upper two- or three-tenths of 1%.

It had been presumed at the beginning of this investigation that the flexure parameter α would be a material parameter and that the scale parameter γ would reflect stochastic differences resulting from variations in specimen geometry, testing methods, etc. Thus, it can be anticipated that the flexure parameter found to produce a good fit with all the aluminum data will be found to be close to the individual values obtained after analysis of the separate data subsamples. Furthermore, in order to facilitate the development of the subsequent estimation theory and its application, it was decided at this time to concentrate on the inverse hyperbolic sine distribution.

3.0 DISTRIBUTION PARAMETER ESTIMATION

3.1 THE ESTIMATION OF PARAMETERS

Suppose that there is a complete sample of failure data $(x_1, \ldots, x_n)$ from the distribution

$$G(x) = \Phi\left[\frac{1}{\alpha}\,\omega\left(\frac{x-\mu}{\gamma}\right)\right] \qquad -\infty < x < \infty$$

where ω is known but the parameters α, γ, μ are unknown. The density of each observation is

$$g(x) = \Phi'\left[\frac{1}{\alpha}\omega\left(\frac{x-\mu}{\gamma}\right)\right]\frac{1}{\alpha\gamma}\,\omega'\left(\frac{x-\mu}{\gamma}\right)$$

and thus

$$\ell n\, g(x) = \frac{-\ell n(2\pi)}{2} - \frac{1}{2\alpha^2}\omega^2\left(\frac{x-\mu}{\gamma}\right) - \ell n(\alpha\gamma) + \ell n\,\omega'\left(\frac{x-\mu}{\gamma}\right)$$

The log-likelihood then is

$$L = \sum_1^n \ell n\, g(x_i)$$

which, except for a constant independent of the parameters, is

$$L = \sum_1^n \left\{-\ell n(\alpha\gamma) - \frac{1}{2\alpha^2}\omega^2\left(\frac{x_i-\mu}{\gamma}\right) + \ell n\,\omega'\left(\frac{x_i-\mu}{\gamma}\right)\right\} \tag{3.1-1}$$

In order to maximize the likelihood consider

$$\frac{\partial L}{\partial \mu} = \sum_1^n \left\{\frac{1}{\alpha^2\gamma}\omega\left(\frac{x_i-\mu}{\gamma}\right)\omega'\left(\frac{x_i-\mu}{\gamma}\right) - \frac{1}{2}\,\frac{\omega''\left(\frac{x_i-\mu}{\gamma}\right)}{\omega'\left(\frac{x_i-\mu}{\gamma}\right)}\right\} \tag{3.1-2}$$

$$\frac{\partial L}{\partial \gamma} = \sum_1^n \left\{-\frac{1}{\gamma} + \frac{1}{\alpha^2}\omega\left(\frac{x_i-\mu}{\gamma}\right)\omega'\left(\frac{x_i-\mu}{\gamma}\right)\left(\frac{x_i-\mu}{\gamma^2}\right) - \frac{\omega''\left(\frac{x_i-\mu}{\gamma}\right)}{\omega'\left(\frac{x_i-\mu}{\gamma}\right)}\left(\frac{x_i-\mu}{\gamma^2}\right)\right\} \tag{3.1-3}$$

$$\frac{\partial L}{\partial \alpha} = \sum_1^n \left\{-\frac{1}{\alpha} + \frac{\omega^2\left(\frac{x_i-\mu}{\gamma}\right)}{\alpha^3}\right\} \tag{3.1-4}$$

Now the joint solution of $\partial L/\partial\mu = 0$, $\partial L/\partial\gamma = 0$, $\partial L/\partial\alpha = 0$ will yield the maximum likelihood (ML) estimators $\hat{\alpha}$, $\hat{\gamma}$, and $\hat{\mu}$. Thus, the simultaneous solution to the following equations in the variables (α, γ, μ) is sought:

$$\frac{1}{\alpha^2}\sum_1^n \omega\left(\frac{x_i-\mu}{\gamma}\right)\omega'\left(\frac{x_i-\mu}{\gamma}\right) = \sum_1^n \frac{\omega''\left(\frac{x_i-\mu}{\gamma}\right)}{\omega'\left(\frac{x_i-\mu}{\gamma}\right)} \tag{3.1-5}$$

$$\frac{1}{\alpha^2 n}\sum_1^n \left(\frac{x_i-\mu}{\gamma}\right)\omega'\left(\frac{x_i-\mu}{\gamma}\right)\omega\left(\frac{x_i-\mu}{\gamma}\right) - \frac{1}{n}\sum_1^n \left(\frac{x_i-\mu}{\gamma}\right)\frac{\omega''\left(\frac{x_i-\mu}{\gamma}\right)}{\omega'\left(\frac{x_i-\mu}{\gamma}\right)} = 1 \tag{3.1-6}$$

$$\alpha^2 = \frac{1}{n}\sum_1^n \omega^2\left(\frac{x_i-\mu}{\gamma}\right) \tag{3.1-7}$$

As a notational convenience, define as implicit functions of μ and γ the values

$$y_i = \frac{x_i-\mu}{\gamma} \qquad i = 1, \ldots, n$$

and introduce, for any function f, the averaging operator

$$\langle f(y_i)\rangle = \frac{1}{n}\sum_1^n f(y_i)$$

Define the functions of (μ, γ):

$$\tilde{H} = \frac{\langle P(y_i)\rangle}{\langle \omega^2(y_i)\rangle} - \langle R(y_i)\rangle$$

and

$$H^* = \frac{\langle y_i P(y_i)\rangle}{\langle \omega^2(y_i)\rangle} - \langle y_i R(y_i)\rangle - 1$$

where the ratio and product functions are defined by:

$$R = \omega''/\omega', \quad P = \omega\omega' \tag{3.1-8}$$

and both R and P are odd.

3.1.1 MAXIMUM LIKELIHOOD ESTIMATE (MLE) ITERATION METHOD

The iteration method for the situation when three parameters are unknown is as follows. For $j = 0, 1, 2, \ldots$

Step 1: **Given μ_j, solve for γ in the equation**

$$H^*(\mu_j, \gamma) = 0$$

Call the solution γ_j

Step 2: **Given γ_j solve for μ in the equation**

$$\overline{H}(\mu, \gamma_j) = 0$$

Call the solution μ_{j+1}

Set

$$\mu_0 = \bar{x} \text{ and } \hat{\mu} = \lim_{j\to\infty} \mu_j, \quad \hat{\gamma} = \lim_{j\to\infty} \gamma_j$$

then set

$$\hat{\alpha} = \left\langle \omega^2\left(\frac{x_j - \hat{\mu}}{\hat{\gamma}}\right)\right\rangle^{\frac{1}{2}}$$

where

$$\langle f(x) \rangle \text{ is the averaging operator } = \frac{1}{n}\left(\sum_1^n f(x_j)\right)$$

To apply the Newton-Raphson technique above to solve the equation $f(x) = 0$ for the single variable set

$$x_{j+1} = x_j - \frac{f(x_j)}{f'(x_{j-1})} \quad j = 0, 1, 2, \ldots$$

then $\lim_{j\to\infty} x_j = x_0$ will satisfy $f(x_0) = 0$.

Thus, it is necessary to know both partial derivatives

$$\frac{\partial H^*}{\partial \gamma}, \frac{\partial \overline{H}}{\partial \mu}$$

so as to be able to determine their behavior.

Examining first $\partial\overline{H}/\partial\mu$; it is checked that

$$\frac{\partial}{\partial \mu}\langle P(y_i)\rangle = -\frac{1}{\gamma}\langle P'(y_i)\rangle \qquad (3.1.1\text{-}1)$$

$$\frac{\partial}{\partial \mu}\langle R(y_i)\rangle = -\frac{1}{\gamma}\langle R'(y_i)\rangle$$

$$\frac{\partial}{\partial \mu}\langle \omega^2(y_i)\rangle = -\frac{2}{\gamma}\langle P(y_i)\rangle$$

$$\gamma\frac{\partial \overline{H}}{\partial \mu} = -\frac{\langle \omega^2(y_i)\rangle\ \langle P'(y_i)\rangle + 2\langle P(y_i)\rangle^2}{\langle \omega^2(y_i)\rangle^2} + \langle R'(y_i)\rangle$$

Similarly it is found that

$$\gamma\frac{\partial H^*}{\partial \gamma} = -\frac{\langle \omega^2(y_i)\rangle\ \langle y_i^2 P'(y_i) + y_i P(y_i)\rangle + 2\langle y_i P(y_i)\rangle^2}{\langle \omega^2(y_i)\rangle^2} + \langle y_i^2 R'(y_i) + y_i R(y_i)\rangle$$

$$\gamma\frac{\partial H^*}{\partial \gamma} = -(H^*+1) - \frac{\langle y_i^2 P'(y_i)\rangle}{\langle \omega^2(y_i)\rangle} + \frac{2\langle y_i P(y_i)\rangle^2}{\langle \omega^2(y_i)\rangle^2} + \langle y_i^2 R'(y_i)\rangle \qquad (3.1.1\text{-}2)$$

3.1.2 DISCUSSION OF EXPLORATORY APPLICATION AND RESULTS

The initial task in testing the MLE equations and the Newton-Raphson iterative techniques (sec. 3.1.1) was the selection of some suitable data. A large number of such samples are listed in appendix III of reference 2. In order to facilitate the initial estimates, it was decided to select data of sample size ≥ 10 specimens. The first such acceptable uncensored test sample comprising 10 specimens was selected from reference 2, and the described MLE methodology was applied. Unfortunately at this initial attempt at estimating the distribution parameters, it was found that the estimators did not exhibit convergence and so no solution was obtained.

An understanding of the nature of this problem was most important, and so it was decided to generate several values of the partial derivatives $\partial L/\partial\mu = 0$ and $\partial L/\partial\gamma = 0$, (see sec. 3.1). The plotted results shown in figure 7 demonstrate that both quantities appear to be approaching their respective asymptotic values without ever intersecting; i.e., no common value as would be necessary for an MLE solution. Thus it seems that for some quite typical fatigue data, as evidenced by the test results given in figure 7, problems would be encountered using the present form of the MLE equations.

To obviate the difficulty encountered in this numerical analysis, equivalent forms of the MLE equations were tried but without any more success. Attempts at redefining or reparameterizing the equations also proved fruitless. Subsequent additional studies then showed that in certain cases the simultaneous MLE's of all three parameters do not exist.

3.2 NONEXISTENCE OF THREE MLE'S IN CERTAIN CASES

In section 3.1.2, mention was made of the lack of an MLE solution for a fairly typical sample of fatigue data. The data values and the estimator results were shown plotted in figure 7. Consider how the behavior of the likelihood function when ω is S-shaped as shown in the schematic below:

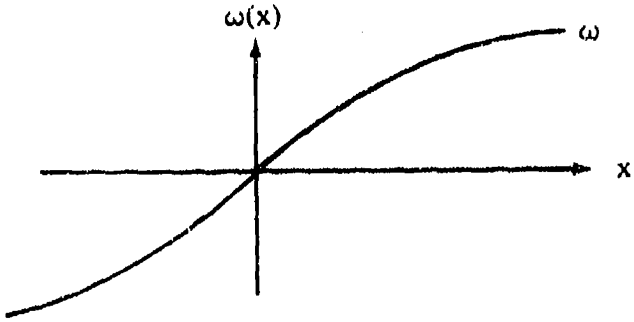

Now ω is S-shaped if

$$1 \geqslant \frac{\omega(x)}{x} \geqslant \omega'(x) > 0 \qquad \omega'(0) = 1 \tag{3.2-1}$$

and

$$\omega'(x) \text{ and } \frac{\omega(x)}{x} \text{ both decrease as } |x| \text{ increases} \tag{3.2-2}$$

Consider the joint log-likelihood equation involving only the parameters μ, γ having previously eliminated α. Then write

$$L(\mu,\gamma) = -\ell n(\alpha\gamma) - \frac{1}{2n\alpha^2}\sum_{i=1}^{n} \omega^2\left(\frac{x_i-\mu}{\gamma}\right) + \frac{1}{n}\sum_{i=1}^{n} \ell n\omega'\left(\frac{x_i-\mu}{\gamma}\right)$$

where α is a function of μ, γ given by

$$\alpha^2 = \frac{1}{n}\sum_{i=1}^{n} \omega^2\left(\frac{x_i-\mu}{\gamma}\right)$$

After substitution and simplification it is found that

$$L(\mu,\gamma) = -\frac{1}{2}\ell n\left\{\frac{1}{n}\sum_{i=1}^{n}\left[\gamma\omega\left(\frac{x_i-\mu}{\gamma}\right)\right]^2\right\} -\frac{1}{2}+\frac{1}{n}\sum_{i=1}^{n} \ell n\omega'\left(\frac{x_i-\mu}{\gamma}\right) \qquad (3.2\text{-}3)$$

Now set

$$y_i = x_i-\mu$$

$$i = 1, \ldots, n,$$

$$a = \max_{i=1}^{n} |y_i|$$

Thus from equation (3.2-1) for i=1, . . ., n

$$[\gamma\omega(y_i/\gamma)]^2 > y_i^2[\omega'(y_i/\gamma)]^2 > y_i^2[\omega'(a/\gamma)]^2$$

Upon substitution it is found that

$$L(\mu,\gamma) + \frac{1}{2}\ln\left\{\frac{1}{n}\sum_{i=1}^{n} y_i^2\right\} + \frac{1}{2} \leq -\ln\omega'(a/\gamma)$$

On the other hand from the bound in equation (3.2-1)

$$[\gamma\omega(y_i/\gamma)]^2 = y_i^2\left[\frac{\omega(y_i/\gamma)}{y_i/\gamma}\right]^2 \leq y_i^2 \quad \text{for } i = 1, \ldots, n$$

and thus

$$L(\mu,\gamma) \geq -\frac{1}{2}\ln\left\{\frac{1}{n}\sum_{i=1}^{n} y_i^2\right\} - \frac{1}{2} + \frac{1}{n}\sum_{i=1}^{n} \ln\omega'(y_i/\gamma) \tag{3.2-4}$$

From equation (3.2-2) it is known that

$$\omega'(y_i/\gamma) \geq \omega'(a/\gamma) \qquad \text{for } i = 1, \ldots, n$$

and thus from equation (3.2-4) it follows

$$L(\mu,\gamma) + \frac{1}{2}\ln\left\{\frac{1}{n}\sum_{i=1}^{n} y_i^2\right\} + \frac{1}{2} \geq \ln\omega'(a/\gamma)$$

As a result it may be remarked that the log-likelihood is bounded by:

$$\ln\omega'(a/\gamma) \leq L(\mu,\gamma) + \frac{1}{2}\ln\left\{\frac{1}{n}\sum_{i=1}^{n} (x_i-\mu)^2\right\} + \frac{1}{2} \leq -\ln\omega'(a/\gamma)$$

where

$$a = \max_{i=1}^{n} |x_i - \mu|$$

It follows, of course, that in the limit as $\gamma \to \infty$ the log-likelihood approaches a limit for which the maximum value of μ is at $\bar{x}$. Moreover those ω's chosen for study show that this limit is reached very quickly. In addition computation also indicates that with ω defined as shown earlier, that with μ fixed, $L(\mu,\gamma)$ is an increasing function of $\gamma > 0$. Thus the likelihood is maximum at $\hat{\mu} = \bar{x}$, and $\bar{x}$ is an unbiased estimate of μ. But the maximum likelihood of γ does not exist.

The problem of characterizing the class of ω's for which $L(\mu,\gamma)$ is an increasing function of γ seems to be difficult. It must be that as $\gamma \to \infty$ the second term of equation (3.2-3) increases while the first term, which decreases, is completely dominated.

Faced with the fact that for some ω's, which are of practical interest, the MLE's of all three parameters may not exist, it is now necessary to seek some alternate method of estimating the flexure parameter. This follows in the next section.

3.3 A SIMPLIFIED ESTIMATOR FOR UNCENSORED DATA

The discovery that, for some fairly typical samples of data, MLE's of all three parameters do not exist meant a revision to the planned approach. Now it was believed that if one of the three parameters could be assumed to have a known fixed value, then MLE's could be made of the remaining two parameters. The most likely candidate for having least variation was considered to be the flexure parameter α, and so some means were necessary to determine its probable value.

In order to facilitate this development stage of the investigation, it was decided to concentrate on the fairly large uncensored samples of data from reference 2 in the determination of the distribution parameters. Keeping the problems of the MLE in mind, some consideration was given to the development of moment estimators as a simpler means of obtaining parameter estimates from fatigue test results. Unfortunately, a general method suitable for all distributions within the class of distributions studied was not determined. Even conventional estimators such as the method of least squares did not result in computable estimates of all the location, scale, and flexure parameters simultaneously.

However, a fairly simple estimator, which has been labelled the "STAR" estimator, was developed by combining the moment and MLE's. The application of this estimator was limited to the Birmbaum-Saunders inverse hyperbolic sine distribution and has shown itself capable of consistently solving for all three parameters from fairly large samples of uncensored fatigue data. For example, considering the distribution given as:

$$\omega_2(x) = \sinh^{-1}(x) \quad \text{(see sec. 2.0)}$$

Then letting

$$\mu^* = \bar{x}$$

and the solution of the two equations in α, γ; namely,

$$s^2 = \gamma^2\left(\frac{e^{2\alpha^2}-1}{2}\right) \tag{3.3-1}$$

$$\alpha^2 = \frac{1}{n}\sum_{i=1}^{n} \omega_2{}^2\left(\frac{x_i-\bar{x}}{\gamma}\right) \tag{3.3-2}$$

Now solve for the solution γ^* in the equation in γ

$$\frac{1}{2}\ell n\left[1+2\left(\frac{s}{\gamma}\right)^2\right] = \frac{1}{n}\sum_{i=1}^{n} \omega_2{}^2\left(\frac{x_i-\bar{x}}{\gamma}\right)$$

by some iteration method. Then

$$\alpha^* = \left\{\frac{1}{2}\ell n\left[1+2\left(\frac{s}{\gamma^*}\right)^2\right]\right\}^{\frac{1}{2}}$$

It is known that μ^* is unbiased and consistent, and so α^* and γ^* are consistent estimators and have been found to converge quite readily.

3.3.1 DISCUSSION OF EXPLORATORY APPLICATION AND RESULTS

Samples of fatigue data have been selected from appendix III of reference 2 and analyzed using the STAR estimator. Only uncensored samples of size $n \geq 6$ specimens per sample were selected. Initially it had been the intent not to consider any samples comprising less than 10 observations, but this did not provide a sufficiently large data base, and so additional smaller sized samples had to be considered.

The results of the data analyses have been plotted in the form of cumulative frequency versus flexure parameter graphs (figs. 8 and 9). It must be noted that emphasis has been given to the flexure parameter for reasons mentioned previously, although all three parameters were in fact computed by the procedure described in section 3.3.

The 184 samples of fatigue test data, which were collected and analyzed, came from a multitude of original sources and contained several variables (table 1). These data were consequently grouped in several different categories of interest, and their flexure parameter characteristics were compared. These comparisons are illustrated in figures 8 and 9. It is readily apparent that there are no fundamental differences in the results presented. All show that the large majority of the population falls within a narrow

range of values of the flexure parameter. This small variation over the central portion and the somewhat larger variations at the extremities are most probably sampling error, although this has not yet been established. Furthermore, it is noted that the weighted mean values of the flexure parameters of the various subgroups are all very similar, thereby providing additional support to the hypothesis of an acceptably constant value for this parameter. It must be emphasized that the data selected for this study covered a considerable range in the extent of the sample scatter. For example, using the parameter of standard deviation of logarithms (base 10) as a measure of variability, the largest standard deviation within the analyzed data samples had a value of $s = 1.304$. However, in spite of gross scatter such as this, the flexure parameter was not too influenced, thereby demonstrating its relative insensitivity to variability in test results.

Finally based on the results of the 164 aluminum alloy test samples that have been analyzed, the weighted average value of the flexure parameter is $\bar{\alpha}^* = 0.64$. Furthermore having determined that the flexure parameter remains almost constant, the three-parameter distribution model being investigated can be treated justifiably as a model with one known constant and two unknown parameters which require estimating. The estimation task is then substantially simplified and, therefore, facilitates the application of MLE procedures thus providing the necessary capability of evaluating smaller sample sizes and, more importantly, censored data.

3.4 ML ESTIMATION FOR TWO PARAMETERS USING CENSORED DATA

Assume a data sample comprising both real life length observations $x_1, \ldots, x_k$ and censored life lengths $x_{k+1}, \ldots, x_n$. In these circumstances the value x_i is taken to indicate that the ith component was alive at time x_i for $i = k+1, \ldots, n$.

Assuming that the life length observations are from the distribution

$$G(x) = \Phi\left[\omega\left(\frac{x-\mu}{\gamma}\right)\right] \qquad -\infty < x < \infty$$

where ω is a known odd function, but the location and scale parameters, μ and γ, respectively, are unknown.* Then the density of each observation is

$$g(x) = \Phi'\left[\omega\left(\frac{x-\mu}{\gamma}\right)\right]\omega'\left(\frac{x-\mu}{\gamma}\right)\cdot\frac{1}{\gamma} \qquad -\infty < x < \infty$$

*The flexural parameter is taken as being constant and known and omitted in this development by assuming a value of unity.

and so

$$\ell n g(x) = -\frac{\ell n(2\pi)}{2} - \frac{1}{2}\,\omega^2\left(\frac{x-\mu}{\gamma}\right)\ell n\gamma + \ell n\omega'\left(\frac{x-\mu}{\gamma}\right)$$

The probability of an "alive-time" of value x, is

$$P(X > x) = 1 - G(x) = \Phi\left[\omega\left(\frac{\mu - x}{\gamma}\right)\right]$$

with the last equality following since ω is odd.

It follows from this that the log-likelihood for the set of complete data $(x_1, \ldots, x_n)$ is

$$L = \sum_{i=1}^{k} \ell n g(x_i) + \sum_{i=k+1}^{n} \ell n\Phi\left[\omega\left(\frac{\mu - x_i}{\gamma}\right)\right]$$

Defining the cumulative hazard as

$$Q(x) = -\ell n\Phi(-x)$$

gives

$$L = \sum_{i=1}^{k}\left\{-\ell n\gamma - \frac{1}{2}\omega^2\left(\frac{x_i-\mu}{\gamma}\right) + \ell n\omega'\left(\frac{x_i-\mu}{\gamma}\right)\right\} - \sum_{k+1}^{n} Q\left[\omega\left(\frac{x_i-\mu}{\gamma}\right)\right]$$

Upon taking partial derivatives, it is found that

$$\frac{\partial L}{\partial \mu} = \sum_{i=1}^{k}\left\{\frac{1}{\gamma}\,\omega\left(\frac{x_i-\mu}{\gamma}\right)\omega'\left(\frac{x_i-\mu}{\gamma}\right) - \frac{1}{\gamma}\,\frac{\omega''\left(\frac{x_i-\mu}{\gamma}\right)}{\omega'\left(\frac{x_i-\mu}{\gamma}\right)}\right\}$$

$$+ \sum_{i=k+1}^{n} q\left[\omega\left(\frac{x_i-\mu}{\gamma}\right)\right]\omega'\left(\frac{x_i-\mu}{\gamma}\right)\frac{1}{\gamma}$$

$$\frac{\partial L}{\partial \gamma} = \sum_{i=1}^{k}\left\{-\frac{1}{\gamma} + \omega\left(\frac{x_i-\mu}{\gamma}\right)\omega'\left(\frac{x_i-\mu}{\gamma}\right)\left(\frac{x_i-\mu}{\gamma^2}\right) - \frac{\omega''\left(\frac{x_i-\mu}{\gamma}\right)}{\omega'\left(\frac{x_i-\mu}{\gamma}\right)}\left(\frac{x_i-\mu}{\gamma^2}\right)\right\}$$

$$- \sum_{k+1}^{n} q\left[\omega\left(\frac{x_i-\mu}{\gamma}\right)\right]\omega'\left(\frac{x_i-\mu}{\gamma}\right)\left(\frac{x_i-\mu}{\gamma^2}\right)$$

By utilizing the product and ratio functions, P and R, respectively, originally defined in section 3.1 as

$$P = \omega\omega' \text{ and } R = \omega''/\omega'$$

and setting

$$h(x) = q[\omega(x)]\,\omega'(x)$$

The two equations $\partial L/\partial\mu = 0$ and $\partial L/\partial\gamma = 0$ can be rewritten as

$$\sum_{1}^{k}\left\{P\left(\frac{x_i-\mu}{\gamma}\right)-R\left(\frac{x_i-\mu}{\gamma}\right)\right\}+\sum_{k+1}^{n} h\left(\frac{x_i-\mu}{\gamma}\right)=0 \qquad (3.4\text{-}1)$$

and

$$-\gamma+\frac{1}{k}\sum_{i=1}^{k} x_i\left[P\left(\frac{x_i-\mu}{\gamma}\right)-R\left(\frac{x_i-\mu}{\gamma}\right)\right]+\frac{1}{k}\sum_{i=k+1}^{n} x_i h\left(\frac{x_i-\mu}{\gamma}\right)=0 \qquad (3.4\text{-}2)$$

Thus, to obtain MLE's of the location and scale parameters, it is necessary that equations (3.4-1) and (3.4-2) be solved simultaneously, using some procedure such as the two-dimensional Newton-Raphson. Further, in order to obtain an MLE in the special case when there are no censored data, merely set $k = n$. Then, from equations (3.4-1) and (3.4-2) and by setting $d(x) = P(x) - R(x)$,

$$\sum_{i=1}^{n} d\left(\frac{x_i-\mu}{\gamma}\right) \doteq 0$$

and

$$-\gamma+\frac{1}{n}\sum_{i=1}^{n} x_i d\left(\frac{x_i-\mu}{\gamma}\right)=0$$

need simultaneous solution ot obtain MLE's for μ and γ.

It can be shown, for the case of complete uncensored samples, that the statistics

$$T = \frac{\mu-\hat{\mu}}{\hat{\gamma}} \text{ and } V = \frac{\hat{\gamma}}{\gamma}$$

have a joint distribution which is independent of the parameters μ,γ.

By definition $\hat{\mu},\hat{\gamma}$ satisfy the equations

$$\sum_{i=1}^{n} d\left(\frac{x_i-\hat{\mu}}{\hat{\gamma}}\right)=0, \quad 1=\frac{1}{n}\sum_{1}^{n}\frac{x_i-\hat{\mu}}{\hat{\gamma}}\, d\left(\frac{x_i-\hat{\mu}}{\hat{\gamma}}\right)$$

Now by adding and subtracting μ and letting $y_i = (x_i - \mu)/\gamma$ which is stochastically independent of μ,γ, in distribution yields the two equations in T,V namely:

$$\sum_{i=1}^{n} d\left(\frac{y_i}{V}+T\right)=0, \quad 1=\frac{1}{n}\sum_{i=1}^{n}\left(\frac{y_i}{V}+T\right)d\left(\frac{y_i}{V}+T\right)$$

Clearly the distribution of T,V does not depend upon μ,γ and neither does

$$TV=\frac{\mu-\hat{\mu}}{\gamma}$$

This same result holds in the case when a sample is truncated at the kth ordered observation.

3.4.1 TESTS AND ESTIMATION FROM GROUPS OF DATA

Throughout the following discussion suppose that there are several samples from different populations; i.e., there are m such samples,

$$x_{1,j},\ldots,x_{n,j} \quad \text{for } j=1,\ldots,m$$

where n_j observations are taken from the jth population with parameters $(\alpha_j,\gamma_j,\mu_j)$ for $j = 1,\ldots,m$. Now compute the two sample statistics

$$\bar{x}_j=\frac{1}{n_j}\sum_{i=1}^{n_j} x_{ij} \tag{3.4.1-1}$$

$$s_j^2=\frac{1}{n_j-1}\sum_{i=1}^{n_j}(x_{ij}-\bar{x}_j)^2 \tag{3.4.1-2}$$

where X_{ij} as a normal distribution transformed by ω, with parameters

$$(\alpha_j, \gamma_j, \mu_j) \quad \text{for } i = 1, \ldots, n_j$$

then

$$Z_{ij} = \frac{1}{\alpha_j}\ \omega\left(\frac{X_{ij} - \mu_j}{\gamma_j}\right) \quad i = 1, \ldots, n_j; j = 1, \ldots, m \tag{3.4.1-3}$$

are independent identically distributed standard normal variates. Since ω^{-1} is odd it follows

$$E\left(\frac{X_{ij} - \mu_j}{\gamma_j}\right) = E\,\omega^{-1}(\alpha_j Z_{ij}) = 0$$

and so

$$E X_{ij} = \mu_j$$

and thus $\bar{X}_j$ is an unbiased estimate of μ_j. But note also that

$$E\left[\omega^{-1}(\alpha_j Z_{ij})\right]^2 = E\left(\frac{X_{ij} - \mu_j}{\gamma_j}\right)^2$$

By defining

$$\sigma_j^2 = \text{var}(X_{ij}) \tag{3.4.1-4}$$

then

$$\sigma_j^2 = \gamma_j^2\, E\,\omega^{-1}(\alpha_j Z_{ij})^2 \tag{3.4.1-5}$$

and it is known that an unbiased estimate of σ_j^2 is the sample standard deviation squared s_j^2.

Thus it is seen that this family of distributions separates the variance into the product of two factors. The first factor is the scale parameter, γ, while the second factor, say $B(\alpha)$, is determined by the flexure parameter, α, and the family characterization function ω; i.e.,

$$B(\alpha) = E\omega^{-1}(\alpha Z)^2 = \int_{-\infty}^{\infty} \omega^{-1}(y)^2\, d\Phi\left(\frac{y}{\alpha}\right)$$

Thus the equation, valid for only large samples, of

$$s_j^2 = \gamma_j^2 B(\alpha_j)$$

forces the utilization of an independent method for estimating α_j.

In one case, namely when

$$\omega(x) = \sinh^{-1}(x) = \ln(x + \sqrt{x^2+1})$$

$B_\omega(\alpha)$ may be computed explicitly.

Let $X \sim N(0,\alpha^2)$, recalling that

$$E(e^{tX}) = e^{\frac{t^2\alpha^2}{2}}$$

then

$$B_\omega(\alpha) = E(\sinh X)^2 = \frac{E(e^{2X} - 2 + e^{-2X})}{4}$$

and finally

$$B_\omega(\alpha) = \frac{1}{2}(e^{2\alpha^2} - 1)$$

from above

$$s_j^2 = \gamma_j^2 \left(\frac{e^{2\alpha^2}-1}{2}\right)$$

thus for samples large enough that $s_j^2 \doteq \sigma_j^2$,

$$\hat{\alpha}_j = \left[\frac{1}{2}\ln\left(2\left(\frac{\sigma_j}{\gamma_j}\right)^2 + 1\right)\right]^{\frac{1}{2}}$$

3.4.2 DISCUSSION OF EXPLORATORY APPLICATION AND RESULTS

Four data samples were selected for initial evaluation of the ML estimator just described. These trial cases, all of size n = 10 observations, were chosen because of the dissimilarities in their estimated parameters based on the STAR estimator. These data and their estimated parameters are given in table 2; the behavior of the estimator for the first data sample is shown in figure 10. It is interesting to compare figures 7 and 10. In both cases the generated values of the partial derivatives $\partial L/\partial\mu = 0$ and $\partial L/\partial\gamma = 0$ have been plotted for the identical fatigue data sample. It is readily apparent that in figure 7, when the flexure parameter was treated as an unknown, no clear cut solution appears to exist as both the plotted curves run more or less parallel with each other toward some asympototic value. However, in the case of the known flexure parameter $\alpha = 0.64$, there is an obvious singularity resulting in unique solutions for both the location (μ) and scale (γ) parameters.

Next a censored sample comprising 16 failure observations and 32 censored times was investigated. The results of this test and the data are given in figure 11. Again a clear singularity is shown, demonstrating that the MLE procedure is functioning for the censored case also. It was also noted that convergence was rapid.

The ready convergence of the MLE solutions, when given the value of the flexure parameter, has been convincingly demonstrated. Therefore, the data previously investigated to establish this parameter were reevaluated using the value of $\alpha = 0.64$ and MLE's obtained for the scale and location parameters. These results have been tabulated in tables 3 and 4.

A study of tables 3 and 4 shows that the flexure parameters remain almost constant regardless of comparisons made between life lengths, types of specimens, or loading procedures. Considering first the life length comparison, it is seen from these tables that although the data have been subdivided into groups depending on the magnitude of their respective location parameters, the resultant weighted average flexure value for each subset is almost identical. In table 3, the weighted average ℓn-normal standard deviations for the same data groups are also shown for comparison, and it is seen that the trend of the deviation values is to increase with increasing values of the location parameter. In table 4, the flexure parameter estimates of the investigated data are grouped according to specimen types and loading procedures; once more it is noted that this parameter remains uninfluenced by such variables. However, the scale parameter estimates are seen to have more variation both overall and when comparing specimen types or loading procedures.

These observations, therefore, have given some substance to the initial hypotheses of: (1) a flexure parameter that is constant and independent of life length, geometry, and loading considerations; and (2) a scale parameter that reflects geometry, loading, or other such variables. It must be pointed out that this study has not included, to date, other materials such as titanium or steel because of the difficulty in readily obtaining sufficient suitable data. The comments just noted have been based solely on aluminum alloy information and may, therefore, require some adjustment when further data are evaluated. It should be emphasized here that aluminum fatigue data with both very

little and extremely large scatter were included in this investigation, and no systematic differences in their estimated flexure parameters were observed when compared with estimates from more typical looking test results. Therefore, it is believed that the value of the flexure parameter will not alter by much for materials such as titanium and steel.

Tables 3 and 4 also give the comparison of results obtained from the STAR and MLE estimators; it is quite clear that both methods produced almost identical estimates with regard to the location parameter, μ, values. In the case of the scale parameter, γ, the difference in the MLE and STAR results, although still small, was more noticeable. The scale parameter is, to some extent, dependent on the magnitude of the flexure parameter. As a result, when the constant MLE flexure value is less than or larger than the STAR estimated flexure parameter, then the MLE scale parameter is larger than or lesser than, respectively, the STAR-estimated scale values (see table 2).

Finally, it was noted that there was a tendency toward a small lowering of the MLE scale parameters with regard to the STAR scale estimates. This can be seen in the results given in both tables 3 and 4. Nevertheless, the overall trend of the results obtained by the MLE method is the same as that given by the STAR estimator, and the imposition of a fixed value for the flexure parameter does not appear to alter the behavior of the other two parameters.

3.5 SIMULATION METHODOLOGY TO GENERATE SPECIFIED r ORDERED OBSERVATIONS OUT OF A SAMPLE OF SIZE n

The structural performance of a fleet of airplanes is typically based on the performance of the weakest airframes, with the result that the extreme, isolated incidents become the basis of the information for subsequent operation and/or modification of the airplane. Therefore, consideration must be given to the important problem of simulating fleet performance; i.e., the generation of the first (early) failures (damage) among a larger number of identical components that are exposed to the same operational and loading environments and that are assumed to be independent.

One way to do this, if, for example, the first r observations in a sample of size n were desired, would be to generate the n observations, sort them, and then discard all but the first r ordered observations. It can be seen that this procedure is both inelegant and inefficient, and when repeated a large number of times—typical of simulation procedures—it becomes very costly. Alternatively, the problem can be formulated mathematically as follows.

Generate the first r ordered observations out of n, given the density $f(x)$ for $0 < x < \infty$ of each independent observation. The joint density of the first r ordered observations, say $(X_1, X_2, \ldots, X_r)$, is

$$g(x_1, x_2, \ldots, x_r) = \frac{n!}{(n-r)!} \prod_{i=1}^{r} f(x_i) [\bar{F}(x_r)]^{n-r} \quad 0 < x_1 < \ldots, < x_r < \infty \tag{3.5-1}$$

where the distribution and survival distribution are defined, respectively, by

$$F(x) = \int_0^x f(t)dt, \quad \bar{F}(x) = 1 - F(x), \quad \text{for } x > 0$$

By setting $r = 1$, it can be seen that the marginal density of the first, smallest observation is

$$g(x_1) = nf(x_1)[\bar{F}(x_1)]^{n-1} \quad 0 < x_1 < \infty \tag{3.5-2}$$

It is found by use of the calculus of probabilities that the conditional density of the $(j+1)$st ordered observation, given the value of the jth, is

$$g(x_{j+1})(x_j) = \frac{(n-j)f(x_{j+1})[\bar{F}(x_{j+1})]^{n-j-1}}{[\bar{F}(x_j)]^{n-j}} \qquad x_j < x_{j+1} < \infty \tag{3.5-3}$$

checking that

$$g(x_1, x_2, \ldots, x_r) = g(x_1)\,\Pi_{j=1}^{r-1}\, g(x_{j+1} \mid x_j)$$

which is in agreement with equation (3.5-1).

Now define the hazard function and the hazard rate, respectively, by

$$H = -\ell n\bar{F}, \; h = H'$$

for the variate with survival distribution $\bar{F}$.

The formula for the generation of the first r ordered observations out of n, with $r \leq n$, in terms of transformations by the hazard function of linear combinations of independent, identically distributed exponential variates with unit mean, is now given:

If H is strictly monotone, and so has an inverse, and $Y_1, Y_2, \ldots, Y_r$ are independent, identically distributed exponential variates with unit mean, then

$$X_k = H^{-1}\left[\sum_{i=1}^{k} \frac{Y_i}{(n+1-i)}\right] \quad k = 1, 2, \ldots, r \tag{3.5-4}$$

are the first r ordered observations out of n independent life lengths, each with survival distribution

$$\bar{F}(x) = \exp\{-H(x)\} \quad \text{for } x > 0$$

By letting k = 1, and showing that $Y_1 = n\,H(X_1)$, which implies that X_1 has the density given in equation (3.5-2), it can be found that

$$P[X_1 > x_1] = \exp\{-nH(x_1)\}$$

Differentiating this to obtain the density of X_1, it is seen that the density is that given in equation (3.5-2).

Supposing that equation (3.5-4) has been verified for k = 1, 2, . . ., j and

$$H(X_j) = \sum_{i=1}^{j} \frac{Y_i}{(n+1-i)} \qquad (3.5\text{-}5)$$

it follows from the conditional density of equation (3.5-3) that for a given x_j

$$Y_{j+1} = (n-j)[H(X_{j+1}) - H(x_j)]$$

is exponential with unit mean. Thus,

$$H(X_{j+1}) = H(x_j) + \frac{Y_{j+1}}{n-j}$$

and, therefore, from equation (3.5-5)

$$H(X_{j+1}) = \sum_{i=1}^{j} \frac{y_i}{n+1-i} + \frac{Y_{j+1}}{n-j}$$

where

$$H(x_j) = \sum_{i=1}^{j} \frac{y_i}{n+1-i}$$

is regarded as being given. Therefore, unconditionally

$$H(X_{j+1}) = \sum_{i=1}^{j+1} \frac{Y_i}{n+1-i}$$

which is the result claimed.

It is worth repeating that the practical method for simulating censored data, developed above, applies only to the technique of censoring by number; i.e., where, after the first few failure observations have been obtained, the data gathering is suspended or aborted. Thus, all the nonfailure values are identical and, furthermore, must be equal to or exceed the last observed failure value.

3.5.1 APPLICATION

The simulation method described in the preceding paragraphs can also be applied to distributions other than the ones being used in the following examples. For consistency, it has been assumed here that X is a ξ-normal variate. Then, by definition

$$P[X > x] = \Phi\left[-\frac{1}{\alpha}\xi\left(\frac{x}{\beta}\right)\right] = e^{-H(x)} \quad \text{for } x > 0$$

where

$$\Phi(x) = \frac{1}{\sqrt{2\pi}} \int_{-\infty}^{x} e^{-t^2/2}\,dt \quad -\infty < x < \infty$$

is the standard normal distribution.

Thus, it can be found that

$$H(x) = -\ell n\Phi\left[-\frac{1}{\alpha}\xi\left(\frac{x}{\beta}\right)\right] \quad x > 0$$

and

$$H^{-1}(y) = \beta\xi^{-1}\left[-\alpha\Phi^{-1}(e^{-y})\right] \quad y > 0$$

The particular case of interest, as before, is the ξ-normal distribution defined as

$$\xi(x) = \sqrt{x} - (1/\sqrt{x}) \quad \text{for } x > 0$$

Consider now the three statistics, T, U, and V, defined as follows:

$$T = \frac{\mu - \hat{\mu}}{\gamma}$$

$$V = \frac{\hat{\gamma}}{\gamma}$$

$$U = \frac{T}{V}$$

which are known to be invariant with regard to their parameters. The distributions of these statistics are obtained empirically by first generating censored data, using the developed MLE methodology to estimate the parameters and then computing T, U, and V. Finally, this procedure is repeated many times, and the results are ordered to form the empirical distributions.

3.5.2 DISCUSSION OF EXPLORATORY APPLICATION AND RESULTS

Several samples of censored data (ref. 16) are listed in table 5. These particular data have been selected as examples because they are fairly large samples and also are of the properly censored type. It is noted from table 5 that the extent of censoring ranges from 20% to 90%, and that sample sizes range from 46 to 54 specimens.

Figures 12 through 14 illustrate some results obtained by using the simulation procedure described previously. Figure 12 is a simulation of the first sample listed in table 5 and presents the simulated sampling distributions of the T and V statistics for a sample of size 52 where 79% comprised failure observations and 21% were nonfailure censored values. For comparison, the empiric distributions of the T and V statistics for uncensored samples of the same size as the number of failure observations—in this example 42 specimens—have been superimposed in the figure as dotted lines. A study of this figure shows the slight increase in the spread of the solid line which represents the censored case.

Figures 13 and 14 present simulated distributions representative of other samples from table 5. A comparison of these figures clearly illustrates the increase in the amount of bias in the distributions of both the T and V statistics as the level of censoring becomes larger. This bias is believed to be a result of first the extent of the censoring of the data and second the limited size of the sample. Again returning to the figures, it is readily apparent that the bias in each uncensored sample's V-statistic distribution is less than that exhibited by the complementary censored sample. Furthermore, it can be noted that bias does increase as the sample size decreases, except for the T-statistic distributions of the uncensored cases which, as expected, appear fairly unbiased.

Finally, figure 15 is presented to illustrate the relative impact on the T and V distributions of the absolute number of failure observations and the level of censoring. This has been achieved by maintaining the ratio of failure to suspended observations but doubling the sample size. For this example, the data already shown in figure 14 were selected as the reference; i.e., a sample comprising eight failure observations and 40 suspensions. Now, by doubling this to 16 failures and 80 suspensions, the level of censoring has been maintained at the original 83%, but the absolute number of failure observations has been increased by eight data points. A study of figure 15 shows that the level of censoring becomes correspondingly less important as the number of observed values increases.

One additional check was conducted and is presented in figure 16. It should be noted that all the preceding figures have been based on a flexure parameter ($\alpha = 0.64$). Therefore, in order to check whether variation in the value of this parameter should be

a consideration, the first two data samples of table 5 were again simulated using different values of α; the results were plotted in figure 16. It is readily apparent from this figure that significant differences in the distributions were not observed.

A direct result of this developed and demonstrated simulation methodology is the ability to obtain bounds for parameter estimates made from censored data. This is readily apparent from the figures where the deviation of the estimated values from the true values is clearly illustrated. For example, from figure 12 can be seen that the scale parameter 90% bounds are 0.76 at the 5th percentile and 1.25 at the 95th percentile.

3.6 DEVELOPMENT OF UNBIASED MINIMUM VARIANCE ESTIMATORS FROM THE ML ESTIMATORS OBTAINED FROM CENSORED FATIGUE DATA

The following discussion is based on the assumptions that the variate X denotes the logarithm of fatigue life, (i.e., $X = \ln N$, (see sec. 2.1), that the appropriate transform (sec. 2.1.2) is taken to be

$$\omega^{-1}(x) = \ln(x+\sqrt{x^2+1}) \quad -\infty < x < \infty$$

and that the shape (or flexure) parameter is known, but the location and scale parameters, μ and γ, respectively, are unknown (sec. 3.3.1).

Assume that a censored sample of the first r ordered observations out of n is given. The computational procedures described in section 3.4 are known to solve the implicit ML equations necessary to obtain the MLE's, $\hat{\mu}$ and $\hat{\gamma}$. Therefore, for any particular sample of size (r,n), the statistics

$$T = \frac{\mu-\hat{\mu}}{\gamma}$$

$$V = \frac{\hat{\gamma}}{\gamma}$$

$$U = \frac{T}{V}$$

are known to be invariant with respect to the parameters, but their sampling distributions must be found by the simulation technique given in section 3.5. Thus by generating a sequence of observations, the distribution of the statistics

$$(T_i, V_i) \quad \text{for } i = 1, \ldots, m$$

can be described when m is large. Furthermore, the sampling bias can also be obtained by computing the expectations, valid only for large samples

$$ET = \frac{1}{m} \sum_{i=1}^{m} T_i = a$$

and

$$EV = \frac{1}{m} \sum_{i=1}^{m} V_i = \frac{1}{b}$$

The variance of these statistics is given by

$$E(T\text{-}abV)^2 = \frac{1}{m} \sum_{i=1}^{m} T_i^2 - \frac{2ab}{m} \sum_{i=1}^{m} T_iV_i + \frac{(ab)^2}{m} \sum_{i=1}^{m} V_i^2 = t^2$$

$$\text{var}(V) = \frac{1}{m} \sum_{i=1}^{m} V_i^2 - \frac{1}{b^2} = \sigma^2$$

Thus, for any real sample of censored fatigue data of the same sample size (r,n) as the simulation, the ML estimators, $\hat{\mu}$ and $\hat{\gamma}$ can be used to construct unbiased estimators of the true parameters μ and γ by:

$$\hat{\hat{\mu}} = \hat{\mu} + ab\hat{\gamma}$$

$$\hat{\hat{\gamma}} = b\hat{\gamma}$$

It follows that these estimates are unbiased since

$$E(\hat{\hat{\mu}} - \mu) = \gamma E\left(\frac{\hat{\mu} - \mu}{\gamma}\right) + ab\gamma EV = 0$$

$$E\hat{\hat{\gamma}} = b\gamma EV = \gamma$$

3.6.1 DISCUSSION OF EXPLORATORY APPLICATION AND RESULTS

Several censored data samples from reference 16 were analyzed using the techniques just specified. An attempt was made to only work with sample sizes that were both similar and large. The data used for this example are listed in table 5; it is seen that the extent of censoring varies between 20% and 90%. Figure 17 presents the scale parameter sampling bias results obtained by simulation for these data and clearly illustrates the increased bias that occurs with fewer real observations. Two extra points have been spotted on this curve to show the effects of decreased total sample sizes. In

each case, it is noted that the bias is increased with the smallest sample showing, relatively, the most bias. Figure 18 shows the location parameter sampling bias results for the same set of data samples, and the trend is obviously similar to that noted for the scale parameter.

These initial results show a promising consistency which suggests that a matrix of factors might well be a practical goal. This would then circumvent the need to do a data simulation every time an unbiased estimate is made of the distribution parameters from a data sample.

3.7 SIMULATION OF THE DISTRIBUTION OF ESTIMATED POPULATION PARAMETERS OF CENSORED DATA

Assume that a data sample of size (r,n) is one which has been truncated at the r ordered observation out of n. Given values of r and n, a collection of m different data sets must be generated, each one being the first r out of n ordered observations drawn from the standard distribution. In this application the standard distribution is defined by $\mu = 0$ and $\gamma = 1$.

The jth set of these r values is denoted by

$$y_{1j}, \ldots, y_{rj} \quad \text{for } j = 1, \ldots, m$$

Solving for the MLE's of the location and scale parameters for these values allows the determination of the statistics

$$T_j = \frac{\mu - \hat{\mu}}{\gamma}; \; U_j = \frac{\mu - \hat{\mu}}{\hat{\gamma}}; \; V_j = \frac{\hat{\gamma}}{\gamma}; \quad \text{for } j = 1, \ldots, m$$

Thus, if m is large, the empiric frequency distributions of these statistics can be described.

Now consider a second different data sample of size $(r^{\dagger}, n^{\dagger})$. By repeating the above procedure the corresponding statistics

$$T_j^{\dagger}, U_j^{\dagger}, V_j^{\dagger} \quad \text{for } j = 1, \ldots, m$$

are computed.

The following ratio

$$V_j / V_j^{\dagger} \quad \text{for } j = 1, \ldots, m$$

is calculated, and its cumulative frequency distribution is determined.

Thus, it can be seen that by this process the joint bounds of the statistics V_j and $V_j^{\dagger}$ have been generated. Furthermore, it follows that if the two censored samples of size (r,n) and $(r^{\dagger},n^{\dagger})$ both have the same true scale parameter (i.e., $\gamma = \gamma^{\dagger}$), then their ratio is simply the ratio of estimated scale parameters $\hat{\gamma}$ and $(\hat{\gamma})^{\dagger}$. Therefore, by calculating the actual ratio of the scale parameter estimates for the two samples and comparing this ratio with the simulated distribution, it is possible to test the hypothesis that the two sets of data come from a population with the same scale parameter (i.e., with the same unknown γ, but possibly different μ's).

For example, assume that it is necessary to test the hypotheses of equivalent scale parameters at the 10% level; i.e., to test whether

$$H_0 : \gamma = \gamma^{\dagger}, H_1 : \gamma \neq \gamma^{\dagger}$$

Now compare the ratio of the MLE's, $\hat{\gamma}$ and $\hat{\gamma}^{\dagger}$, for the two real data samples with the simulated distribution, and note whether the ratio falls outside the 5th and 95th percentiles. If it does, H_0 is rejected at the 10% level, asserting a 90% certainty that the true-scale parameters of the two data samples are different.

A similar process to test the hypothesis that the two samples (r,n) and $(r^{\dagger},n^{\dagger})$ also have the same true location parameter μ has been developed for application to those samples that pass the γ test. Here, a simple relationship between the MLE's of the samples' location parameters will not suffice as the prior test has already demonstrated that both samples most likely have the same true, but unknown, scale parameter γ. Thus, a comparison should be made between estimates of the two samples' location parameters, which have been based on this true scale parameter. Consequently, the empiric distribution of the "T" statistic ($T = (\mu - \hat{\mu})/\gamma$) is of interest for the location parameter hypothesis test. The following relationship

$$T_j - T_j^{\dagger} \quad \text{for } j = 1, 2, \ldots, m$$

is calculated, and its cumulative frequency distribution is determined in a similar manner to the V ratio already described.

The value of the scale parameter, which must be common to both data samples (r,n) and $(r^{\dagger},n^{\dagger})$ in order to test the hypothesis of equality of the location parameters, is computed in the following manner. The empiric distributions resulting from the simulation of the V and $V^{\dagger}$ statistics are used to obtain the bias factors b and $b^{\dagger}$ and the spread factors s and $s^{\dagger}$ which are the spread of the V and $V^{\dagger}$ distributions, respectively, at some fixed percentile. Recalling the presumption that $\gamma = \gamma^{\dagger} = \gamma$ which is unknown, the minimum variance unbiased estimate of γ, based on the statistics γ and $\gamma^{\dagger}$, is given by:

$$\tilde{\gamma} = c\hat{\hat{\gamma}} + c^{\dagger}\hat{\hat{\gamma}}^{\dagger} = cb\hat{\gamma} + c^{\dagger}b^{\dagger}\hat{\gamma}^{\dagger}$$

where

$$c_i = (b_i s_i)^{-2} / \sum_{j=1}^{2} (b_j s_j)^{-2} \quad i = 1, 2$$

where $c_1 = c$, $c_2 = c^{\dagger}$

Note that s is assumed to be proportional to σ the standard deviation of the V statistic.

This estimate can, of course, be generalized for the case $\gamma_1 = \gamma_2 = \ldots = \gamma_{\ell} = \gamma$ for any $\ell > 2$. Under these conditions

$$\mathrm{var}(\bar{\gamma}) = \sum_{1}^{\ell} c_i^2 b_i^2 \gamma^2 s_i^2 = \gamma^2 / \sum_{1}^{\ell} (b_i s_i)^{-2} .$$

This is, in fact, the minimum variance estimator since by the Cauchy inequality; i.e.,

$$(\sum C_i^2)(\sum B_i^2) \geqslant (\sum C_i B_i)^2$$

it follows that

$$\sum_{1}^{\ell} (c_i b_i s_i)^2 \cdot \sum_{1}^{\ell} (b_i s_i)^{-2} \geqslant 1$$

for any set of $c_i \geqslant 0$ so that

$$\sum_{1}^{\ell} c_i = 1$$

It should be noted that the spread s or $s^{\dagger}$ rather than the variance has been adopted for the sake of computational expediency. However, it is presumed that the minimum variance unbiased estimate, $\bar{\gamma}$, will produce a common value so close to the true value of γ that the empiric distribution of T can be used justifiably in this investigation for tests or confidence bounds on the location parameter μ. Although this approximation may not be exact, the actual difference is unlikely to vitiate any of the conclusions reached while improving the basic capability of the reliability analysis method to treat censored data.

3.7.1 DISCUSSION OF EXPLORATORY APPLICATION AND RESULTS

Several samples of censored fatigue data from table 5 have been paired for comparison according to the methods described in the previous paragraphs, and the results are presented in figures 19 through 22.

Figure 19a and 19b present the simulation-generated cumulative frequency distributions of the V and T joint statistics for two censored samples of size (41,52) and (33,53). From these figures it is clear how bounds for the "V-ratios" and "T-differences" can be established. For example, it can be seen that the 90% bounds for the V-ratio for two samples of size (41,52) and (33,53) are

$$\left(\frac{V_{41,52}}{V_{33,53}}\right)_{0.05} = 0.695 \text{ and } \left(\frac{V_{41,52}}{V_{33,53}}\right)_{0.95} = 1.45$$

In a similar way the values -0.25 and 0.232 are the 90% bounds for the joint statistic $(T_{41,52}-T_{33,53})$.

Table 6 gives the MLE's of the scale and location parameters for the various data samples examined. It is noted that the estimated scale parameter of the first test sample (of size 41,52) has a value of $\hat{\gamma}_1 = 0.40$ and the second test sample (of size 33,53) has a value of $\hat{\gamma}_2 = 0.696$. Therefore, the ratio $(\hat{\gamma}_1/\hat{\gamma}_2) = 0.575$.

Returning to the results of figure 19, discussed earlier, it was noted that the low value of the 90% bound of the V-ratio was 0.695. Therefore, it can be concluded that it is 90% certain that the true scale parameters of the censored data samples 1 and 2 are different.

Referring once more to table 5, it is seen that sample 3 is also the same size as sample 2 (i.e., r=33, n=53), and so the simulation results are equally applicable to either the (sample 1/sample 2) or (sample 1/sample 3) ratios. From table 6 it is found that $\hat{\gamma}_{\text{sample 3}} = 0.535$ and, therefore, the ratio $(\hat{\gamma}_1/\hat{\gamma}_3) = 0.748$. Thus, in this case the test data ratios fall within the 90% tolerance bounds of figure 19, and the hypothesis that the same true-scale parameter applies to both samples 1 and 3 cannot be rejected at this level.

Figures 20 and 21 illustrate the joint-scale and joint-location statistics obtained through simulation of two other combinations of samples. Figure 20 is interesting because it represents the expected variability between two independent and identically sized samples, such as items 2 and 3 of table 5. From figure 20, it can be found that the hypothesis of the scale equality of samples 2 and 3 cannot be rejected at the 90% level.

Figure 21 applies to data samples 4 and 6, and from those results the hypothesis of scale equality of samples 4 and 6 is not rejected at the previously selected test level of 90%. This figure is interesting because sample 6 is over 90% censored. Consequently, there is considerable bias to the estimates of its scale and location parameters as is apparent in the "V" and "T" plots of figure 21.

This discussion has covered the comparison of paired samples based on the estimated scale parameters, and for the examples tested, it was found that the sample pairings such as 1 and 3, 2 and 3, and 4 and 6 were not rejected. The minimum variance unbiased estimate of the scale parameter of each of these three paired samples was calculated, and then the MLE of the location parameters of each sample, with specified flexure and scale parameters, was computed. These results are shown in table 7 together with the differences of the revised location parameters. The difference values were then compared to the location parameter bounds shown in figures 19, 20, and 21; it was clear that the hypothesis of location equality for each paired sample could not be rejected at the 90% level selected earlier.

It is believed that the few examples discussed in the preceding paragraphs are sufficient for illustrating the developed procedure for testing whether or not censored samples could have come from the same parent population. It has been noted that the testing procedure is able to either reject or not reject the hypothesis of scale equality and subsequent location equality.

4.0 SIGNIFICANCE OF MIXED POPULATIONS

4.1 THE INITIAL FLAW CONCEPT

The structural design goals and subsequent operation of the airplane are based on the rationale that each structure is manufactured similarly. The performance of each structure should, therefore, be consistent. However, the tolerances that are necessary both during the production of the material and its subsequent manufacture into a structural detail or component do cause a variation in the performance of individual structures. This variability is usually taken into account during the design by the assumption of some average level of performance which is then downgraded through use of various factors to a more representative performance level.

Therefore, in a roundabout manner, procedures such as the above presuppose the existence of a statistical population which can be simply described by central tendency and variability parameters. Thus, for example, the fatigue performance of any structure reflects the performance in terms of time or cycles to a detectable crack of the typical structure, i.e., it comes from the same parent population.

However, there are data available, such as that collected, analyzed, and presented in reference 17, leading to the hypothesis that a number of early structural incidents belong to a population that is both different and worse than the population from which the typical structures come. This means that if sufficient data were available, the frequency of plotted times-to-crack initiation would appear bimodal with the lower mode representing the fatigue observations resulting from initial flaws, manufacturing damage, etc., and the second mode representing the average fatigue performance of the typical structure. It follows then that the present method of fatigue performance prediction, based on the behavior of the typical structure, cannot predict the very early incidents that occur as the result of an inadvertent flaw. Under this circumstance, the analysis of the reliability of a structure, based on the single typical population, will be unconservative, especially during the early life of the structure prior to a routine inspection. Therefore, it is important to recognize the initial flaw population so that the inspection procedures can be adjusted accordingly and a high level of reliability maintained. Furthermore, the current Air Force philosophy (ref. 15) is oriented to the concept of the initial or preflaw for the analysis of damage-tolerant structure. However, not all details are necessarily preflawed, and one of the tasks of this study is the extension of the reliability analysis methodology to assess the effect of the presence of details with a reduced level of fatigue performance in a fleet of aircraft. Hence, for the purposes of this investigation, the possibility is considered for some structural details or components entering service with an existing flaw or damage of magnitude equal to or greater than some specified minimum detectable size.

The model that has been developed accounts for both the probable frequency of flawed structures entering service and the probable flaw or damage size in the structure. It is realized that there may be considerable difficulty in obtaining suitable information on the likelihood of flaws or damage in new structure and the probable magnitude of these flaws or damage.

Nevertheless, work such as that of reference 17 already provides indications that applicable input information can be obtained. If not, perhaps judicious selection of input values may be done. Consequently, the development of an intial flaw model and its inclusion in a structural reliability analysis system should provide an added measure of realism to the ensuing results.

5.0 THE RELIABILITY MODEL

5.1 STRUCTURAL RELIABILITY ANALYSIS METHOD

An analysis method to estimate the structural reliability of an airplane structure based on the interaction of cumulative and maximum operational loads, residual strength of fatigue damaged structure, and routine inspection and crack detection and repair of the structure was developed in earlier investigations and reported in references 12 and 13. Some of the design variables that were included in this reliability system were the central tendency time to initiation of a detectable crack and its variability, the size of the detectable crack, and the central tendency crack growth rate and its variability. Monte Carlo simulation techniques are then used to generate a time to a detectable crack of specified size and, subsequently, to grow the crack until it is either arrested by a crack stopper or the part is failed.

This reliability system was based on the principle of the single typical population, as discussed in section 4.0, from which random initiation times are selected. Obviously, such a model could generate some crack initiation times approaching or at "zero time" depending on the values of the central tendency and variability parameters initially input into the reliability system. However, this would be as a direct result of the typical component population's tail and not representative of the nontypical structure with the flaw. Consequently, it was decided to expand the reliability system of references 12 and 13, and thereby increase its comprehensiveness to include the initial or preflaw model discussed in the following pages.

5.2 FLAW SIZE DENSITY

Given that flaws of differing sizes are distributed randomly in structural materials, it is assumed that this flaw size density is exponentially decreasing.

Let Υ denote the random initial flaw size with parameters p_τ and τ, related by the constraint

$$P[\Upsilon < \tau_0] = p_\tau$$

Here τ_0 is some practical minimum detectable flaw/damage size, and p_τ, $0 < p_\tau < 1$, is that portion of the area under the density curve representative of the flaws that are below τ_0 in size and therefore not detectable.

Now assume:

$$\Upsilon \sim \sigma\,|Z|^{\nu}$$

where Z is the standardized normal variate with zero mean and unit deviation and σ is the correlation parameter between the minimum detectable flaw/damage size and its frequency, as represented by the following relationship:

$$\sigma = \tau_0 / \zeta_\alpha{}^{\nu}$$

where ζ_α is the standard normal quantile at a given probability level, α, with α taken as $(1+p_\tau)/2$; and, ν is the magnitude at which flaw size density in the structure is exponentially decreasing.

Flaws or damage, in a structural component, of size $< \tau_0$ are considered to be typical, and the standard operational procedure is to compute the time to initiation of a crack of size τ_0 and, subsequently, to determine crack growth to critical size. However, when flaws or damage of size $\geq \tau_0$ exist, the structural component is considered to be preflawed and only the subsequent crack growth in the structure need be considered. The procedure for this operation follows:

Generate $Z \sim N(0,1)$; test whether $Z < \zeta_\alpha$ where α is the probability level as before.

Now if this is the case, then no flaw or damage of detectable size exists in the structure and the time-to-crack initiation must be computed. However, if $Z \geq \zeta_\alpha$ then a flaw or damage of size

$$\Upsilon = \sigma\, |Z|^{\nu} > \tau_0$$

is already present in the structural component so that only the subsequent crack growth in the structure needs to be considered.

From this procedure, it follows

$$P[\Upsilon < \tau_0] = p_\tau$$

and a continuous density for flaw sizes exceeding τ_0 of:

$$f(\tau,\nu) = \sqrt{\frac{2}{\pi}}\, \frac{1}{\nu\sigma}\, \frac{e^{-1/2\left(\frac{\tau}{\sigma}\right)^{2/\nu}}}{\left(\frac{\tau}{\sigma}\right)^{1-1/\nu}} \quad \text{for } \tau > \tau_0 \,;\, \nu > 0$$

Now, let τ_1 be the size of a large initial flaw or crack which has some small probability ϵ of existing in a component entering service. This is given by the following constraint

$$P[\Upsilon = \tau_1] = \epsilon$$

or

$$P[\sigma|Z|^{\nu} = \tau_1] = \epsilon$$

thus

$$P\left[|Z| < (\frac{\tau_1}{\sigma})^{1/\nu}\right] = 1-\epsilon$$

This reduces to

$$(\frac{\tau_1}{\tau_0})^{1/\nu} = \frac{\zeta_\beta}{\zeta_\alpha}$$

where:

$$\beta = 1 - \frac{\epsilon}{2}$$

$$\alpha = \frac{1 + p_\tau}{2}$$

and solving for ν gives

$$\nu = \frac{\ell n(\tau_1/\tau_0)}{\ell n(\zeta_\beta/\zeta_\alpha)}$$

The behavior of the density of the initial flaw sizes exceeding τ_0 varies radically with the value of $\nu > 0$, as shown in the following schematic:

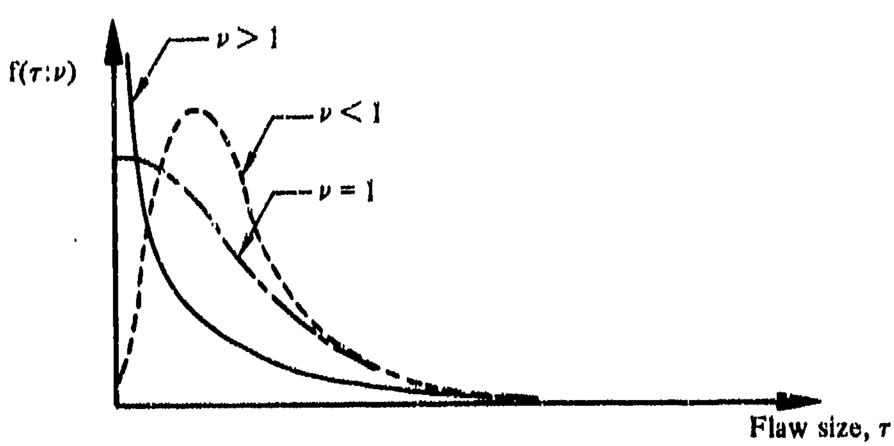

Proof: In all cases, for given $\nu > 0$

$$F(\tau:\nu) = P[T < \tau] = P[|Z| < (\frac{\tau}{\sigma})^{1/\nu}] = 2\Phi[(\frac{\tau}{\sigma})^{1/\nu}]-1$$

where $\Phi(x)$ is the cumulative distribution of the standard normal. It is checked directly that $F(\tau_0:\nu) = p_T$ and by differentiation that

$$f(\tau:\nu) = 2\,\phi[(\frac{\tau_0}{\sigma})^{1/\nu}]\,\frac{1}{\nu\sigma}\,(\frac{\tau}{\sigma})^{1/\nu-1}$$

which reduces to the preceding result.

6.0 INTERACTION OF MATERIAL/ STRUCTURE VARIABILITY WITH RELIABILITY LEVEL

6.1 DISCUSSION OF EXPLORATORY APPLICATION RESULTS

The results of parametric studies using the expanded structural reliability analysis system are discussed in this section. The hypothetical cases that have been investigated are based on the following assumptions:

- The characteristic life to a detectable crack of size 0.03 in. is 120 000 hr.
- The minimum or threshold size for crack detection is 0.02 in.
- The scheduled inspection period is 7500 hr.
- The fail-safe residual strength of a component with a cracked detail is taken to be limit load capability.
- The reference stress intensity factor for aluminum is taken as 16 ksi $\sqrt{\text{in.}}$
- The crack growth rate for aluminum is taken as 1.25×10^{-5} in./cycle.
- The critical stress intensity factor for aluminum is taken as 75 ksi $\sqrt{\text{in.}}$
- The reference stress intensity factor for steel is taken as 20 ksi $\sqrt{\text{in.}}$
- The crack growth rate for steel is taken as 6.5×10^{-6} in./cycle.
- The critical stress intensity factor for steel is taken as 100 ksi $\sqrt{\text{in.}}$

It should be noted that any deviations from these values are indicated in the appropriate figures (23 through 30).

Two different loading cases were also used to describe the mean rates of occurrence of specific structural load levels per hour. These load cases are illustrated in figure 22 and represent exceedance values that may be expected at two different locations of a four-engined jet tanker/transport type airplane on a routine mission.

Figure 23 illustrates the results of comparisons made between several cases with differing preflaw assumptions. The example's structure was assumed to be basically an aluminum skin panel with crack stoppers placed at 14-in. intervals. The preflaw or the initiated fatigue crack was assumed to be located at a central hole between the crack stoppers. The component was assumed to be fail-safe, so that if a crack propagated to the full width of a bay, the remaining structure would still be capable of carrying limit load. The approach used to describe the preflaw density parameters was determined by selecting two flaw sizes and their respective probability levels and then computing the

exponent that would best fit these points. The reference curve at the lower right corner of figure 23 represents the probability of failure, or alternatively, the reliability of the fail-safe component (just described) when exposed to the case A loads of figure 22. The other curves plotted in figure 23 illustrate two things: that component failure probability increases as the probability of an extant detectable flaw at "zero-time" increases; and also that the probable size of the undetected flaw is a significant parameter, since the component reliability decreases with increased flaw size. Another expected observation is that the decreased component reliability which results from an assumption or a preflaw (or damage) condition is most noticeable at the lower lifetimes where several orders of magnitude differentiate between the flawed and unflawed cases.

Figure 24 illustrates the influence of the residual strength on the failure probability of the component. Basically, the two lower curves represent fail-safe structures, whereas the upper curve is for a structural component whose cracked strength is little more than the strength of the detail represented by the single bay. In these examples, the component was assumed to be free of flaws. However, figure 25 presents the same cases except that a high likelihood of preflaws was assumed. It is clear that the combination of high preflaw probability and low fail-safe strength results in an unreliable structure.

Figure 26 is included here to illustrate the importance of the load environment. The results shown in this figure come from the assumption that the structure is exposed to the case B loads of figure 22. Consequently, by comparing the results in figure 23 with those of figure 26, the effects of the load cases A and B, respectively, on structural reliability can be noted. It is clear from this comparison that the load exposure term is an important one; it can alter not only the probability of failure but also the trend of the results. For example, in contrast to the results of figure 23, figure 26 does not show the very large differences in structural reliability between the unflawed and preflawed examples.

Figure 27 illustrates the results of similar studies to those of figure 26 except that in these cases the type of structure is changed. For these examples, the structural component comprises several pinned details, so that loss through cracking of any one detail still leaves the component with sufficient residual strength to sustain limit load. It should be noted that the various parameters used to obtain the results shown were selected specifically to maintain a similar probability of failure curve for the reference unflawed condition as shown in figure 26 for the skin-type structure. A comparison of these two figures clearly illustrates these results.

Figure 28 represents cases identical to those of figure 27 except that the material has been changed from aluminum to steel. Once again, in order to have a reference baseline for comparison with other cases, the parameters were selected to produce a probability of failure curve for the unflawed component, similar to those of figures 26 and 27. The results of the equivalent aluminum and steel cases show that the latter structure is somewhat more sensitive to the preflaw assumptions.

Figures 29 and 30 compare the effects of the residual strength assumptions on the aluminum and steel structural components, respectively. Although it is clear that the trend of both figures is similar, it is equally obvious that the latter steel structure is more sensitive to the residual strength term. However, in both cases it is also clear that maintaining a high level of residual strength in the precracked state, by incorporating fail-safe design procedures, is very important.

It is obvious from these examples and discussions that the reliability anlaysis method can consider and evaluate the influence on reliability of possible flaws in a new structure. Furthermore, the presence of initial flaws or even other conditions leading to mixed (or heterogeneous) populations of fatigue performance in terms of initiation time to detectable crack has a definite effect on the fatigue behavior and reliability of a fleet of aircraft. The combination of the probabilities of an initial flaw and the usually expected flaw-free or damage-free structural detail will tend to develop an S-shaped character to the cumulative distribution function of a group of details as compared to the usual linear function when plotted on normal probability paper with logarithmic abscissa. If there is a positive probability of initial flaws or cracks at time zero, the distribution function would become asymptotic to this probability level. On the other hand, should there be a positive waiting time before flaw or crack initiation occurs, a reversed flexure would cause the initial toe of the distribution to rise more steeply than the expected linear representation. Certainly, the inclusion of the preflaw or mixed-population concept into the reliability analysis scheme is important to the development of inspection control plans and maintenance schedules of an aircraft structural system. As another related point, the effects on structural reliability of cracks, which originate either from a preflaw or initiate in unflawed structure due to fatigue, are sensitive to a number of interdependent variables including loads, materials, structural configurations, residual strength, and crack detectability. Finally, it should be noted that with the inclusion of fail-safe components, the structural reliability of a system can be maintained at a high level even with the assumption of a high probability of a preflaw in a detail.

7.0 STRUCTURAL DATA INPUT CONSIDERATIONS FOR APPLICATION OF RELIABILITY MODEL

The durability and integrity of a structural system exposed to a fatigue environment are responsive to the application of reliability analysis technology. However, the degree of responsiveness of the analysis is really dependent upon the modeling details and the input data. Furthermore, almost every rational scheme which quantifies the elements of the fatigue process provides some measure of insurance, though not necessarily security, against the serious consequence of unexpected fatigue damage. The more realistic the approach, the more insight provided for the task of determining a numerical measure; i.e., the probability of structural survival, to judge progress toward operational structural goals. While this remark suggests that the application of reliability analysis technology alone may not be sufficient to resolve the fatigue problem, the technique has a potential to provide a workable and useful tool for aiding in the resolution of the total fatigue assessment process from design through useful life.

Considerations leading to this somewhat paradoxical comment are those related to the complexities of the fatigue process itself, as well as the applied reliability technology. Primarily, cumulative fatigue damage, whether dealing with crack initiation or stable crack growth, the residual strength of the fatigue-damaged structure, and the coincident actual mechanical and physical environment have shared, to various degrees, in confounding the durability and integrity goals of fatigue critical structures. During the development of the reliability analysis scheme of this study and the preceding exploratory work, the emphasis has been toward relating the reliability analysis methods to recognized or measurable structural fatigue properties of materials in their structural form. For instance, different structural details of the same material can have widely differing fatigue performance levels. Furthermore, identical details in differing loading environments also can exhibit a different response. Recognition and separation of these complex elements are believed necessary to make the application of reliability technology a tractable task. Skill, understanding, experience, and even prescience are some of the ingredients that influence the degree of success in making the cumulative damage prediction process match operational results. Hence, this reliability analysis plan is directed toward utilizing the known and reasonably identifiable material/structures fatigue properties. Although variability of identical structures under a specific load environment is universally observed to respond to statistical treatment, the exact nature of that statistical behavior is not nearly as well defined, particularly in reference to extreme behavior. Nevertheless, this approach offers a means to explain an observable behavior (viz, the initiation of fatigue damage) in a rational manner through reliability analysis techniques. As the important technologies and knowledge pertinent to the cumulative damage process are extended, such a reliability analysis scheme will incorporate those advances.

As an example of the preceding concern, the static strengths of commercially available materials are treated by reliability methods. First, variability is recognized and then characterized by presuming a normal distribution for the specific structural properties,

such as ultimate tensile strength or tensile yield stress. A confidence level, reflecting input knowledge (viz, the number of tests performed to obtain the specific value), has been established for certain materials such as the aluminum alloys. With that baseline, a probabilistic level is selected to determine a strength level that will be equaled or exceeded by that particular alloy. The "A" and "B" material property values of the MIL-HDBK-5 compilation of such structural data illustrate this application of reliability methodology. The universal acceptance and demonstrated usability of this technique are believed reasonable justification for the procedure and encourage its use in the fatigue evaluation process. However, one difficulty in this phase of the application of reliability methodology to fatigue concerns the added dimension of fatigue performance. The collection of the static properties of a material is a rather straight-forward process. For instance, 10 static test specimens from each of 10 different heats of a material can be tested at a reasonable cost. The mere introduction of load cycling and the very local nature of fatigue damage initiation in structural details, particularly in complex components, make the task several orders of magnitude greater in specimen and test cost as compared to characterizing the static strength properties. However, with definition of the nature of the distribution for variability of the particular fatigue properties, statistical estimation procedures for small samples, such as one or two, etc., provide a means to estimate the tolerances in performance unavoidably due to such limited input data.

Continuing the static/fatigue comparison, the determination of the static strength of structures from reliability-determined material properties introduces a further complication. Full-scale static tests of structures made from known materials do not always fulfill their static analysis goals. A natural step is to compare the results of this structural testing with the estimated goal. The discrepancies are then presumed to be variable or statistical quantities that can be treated in a probabilistic manner and then introduced into the strength reliability evaluation process. However, it should be evident that the stress analysis procedures are basically deterministic in nature. Hence, the variation between demonstrated strength and calculated strength is not truly a statistical quantity but rather a problem in analysis procedure. Such miscalculations as an inadequate assessment of local buckling or net section area of a structural component are not a result of the material's structural behavior. Fortunately, the design and production of an aircraft structural system have usually included a demonstration or verification phase, the static test, which effectively ferrets out such errors, if existing. Local structural revisions can correct the static analysis deficiency usually in some reasonable and practical manner. On the other hand, to treat the entire structure with its various load conditions resulting from random variations and usage, analyzing all possible local deficiencies would be virtually impossible and would add a structural weight penalty. Furthermore, this weight penalty cannot always be fully compensated with an increased payload or performance.

A similar difficulty exists in the case of fatigue-critical structure. Fatigue performance, whether in terms of crack initiation, crack growth, and/or residual strength, is a variable resulting from a highly individualistic behavior of a particular bit of material in a specific structural configuration and variable loading environment. Nevertheless, the probable behavior of such material fatigue performance will respond to the nondeterministic approach offered by reliability analysis methods. Unfortunately,

fatigue performance is more sensitive to actual local geometry and repeated loading conditions than the comparable elements of static strength. Furthermore, experience shows that deterministic analysis to predict and interpret fatigue performance is a more difficult task, since it is much less understood than that of static strength design. Nevertheless, it is suggested that analysis procedures for fatigue assessment incorporate some deterministic aspects as well as statistical ones despite the significance of unexpected incidents which occur in new and/or different structural systems. However, careful and knowledgeable treatment of the elements causing fatigue damage can aid in the precision of the deterministic phase of the task. Then further assurance is obtained by recognizing the elements of variability and characterizing their behavior so that the likelihood of damage occurrence is a remote or acceptable possibility.

Inherent in the background of this development is the importance of structural configuration and material selection to fail-safe (i.e., damage-tolerant) concepts and the associated inspection maintenance plans. This consideration provides security in maintaining structural safety and reduces fatigue damage to an economic consideration rather than one of safety.

In continuation, the important feature in the achievement of static structural integrity in aircraft structures has been the practice of design and test verification before a fleet has advanced significantly through a production line. Fatigue performance is responsive to similar treatment but with some reservations. The well-practiced and demonstrated procedures of static stength design are not sensitive to the local strain behavior of actual complex structures. Likewise, the expected use may be established for design purposes, but both the actual use and response of the structural system may depart from the design presumptions. However, the analysis difficulties can be essentially resolved by specific developmental and/or verification testing or by the use of previous experience. Such representative testing provides an estimate of fatigue life distribution location parameters, while reasonable interpretation of other comparable data provides guidance for estimating the necessary shape parameters.

The condition of a structural system can only be determined by inspection. The success of the inspection plan depends upon its sensitivity and thoroughness. The material properties of crack growth rate and residual strength are the most important parameters in the formulation of any such surveillance scheme. The intervals between the time at which a crack is detectable and the time at which the crack has developed to the critical fail-safe size provides the only opportunity to detect the damage. The principles of fracture mechanics provide a means to estimate crack growth and resultant strength of the damaged structure. Furthermore, the generation of crack growth information is a far simpler task than determining time to initiation of a detectable crack in structural details. In addition, the rapid development of fracture mechanics information has provided usable data on crack growth rate and residual strength. Hence, appropriate models can be selected and subsequently verified experimentally. As noted in earlier studies, the intercept and slope both appear to vary when plotted as a function of crack growth rate versus stress intensity factor within the useful range of stress intensity values.

In summary, the key materials/structures fatigue performance input parameters in this proposed application of reliability methodology include the following:

1. Time to detectable crack initiation with its variability identified in a distribution with its parameters determined by the specific detail

2. Crack growth rate with its variability identified by a distribution with its parameters determined by the specific material of construction

3. Residual strength or fracture toughness properties of the detail

Closely associated with these material/structures variability behaviors are complementary deterministic analyses or supportive programs:

1. Cumulative damage analyses for determining crack initiation time and its responsiveness to environmental exposure of the particular detail

2. Cumulative crack growth analyses for the environmental exposure of the particular detail

These input functions or parameters are referenced in terms of specific details. These details may be a particular fitting, a joint, a component, or a typical structural area such as a mechanically fastened skin-stiffener structure or a bonded structure. However, all the concepts are developed with consideration of the properties of metal alloy structures having local fatigue-critical details.

8.0 CONCLUSIONS AND RECOMMENDATIONS

8.1 CONCLUSIONS

There are several goals of the statistical investigation that have been accomplished:

1. The study of a symmetric class of distributions for application as a model for the variability of fatigue damage initiation

2. The development of unbiased estimation procedures for the parameters of the distribution using censored data

3. The development of a technique for testing the hypothesis of two censored samples belonging to a common parent population

Additionally, developmental work pertaining to the reliability of airplane structures with mixed populations resulting from different levels of fatigue performance capability has been incorporated into the structural reliability analysis system. Several parametric evaluations of diverse structural variables were conducted using the reliability analysis system, and the results have been presented and discussed.

Conclusions that may be drawn from this investigation include the following:

1. The symmetric three-parameter distribution does describe the empirically determined fatigue distribution.

2. The flexure parameter of this distribution may be presumed to be a constant,.

3. MLE's of the remaining parameters are computable from censored data.

4. A practical simulation procedure for censored data has been developed, an important step resulting in the capability of:

    - Computing bounds for censored data

    - Obtaining unbiased point estimates from censored data

    - Testing the hypotheses that two independent censored samples have a common parent population

5. Structural reliability is significantly affected by the magnitude and the frequency of initial flaws or damage.

Parametric studies conducted in this investigation have shown that structural reliabiltiy is dependent on several interdependent design variables, such as:

- Loading environment
- Residual strength
- Design configuration
- Material characteristics

Finally, the reliability model with the concept of initial flaws or mixed populations of fatigue performance can reflect the extreme initial behavior shown in the collected groups of experimental fatigue test data. Therein, the empirical cumulative failure distribution when plotted on normal probability paper exhibits a characteristic flexure. If there is a positive probability of an initial crack at time zero, the cumulative distribution will become asymptotic to this value. Furthermore, if there is a waiting time until the crack initiates, the cumulative distribution function will rise more steeply in the early extreme portion than the empiric fatigue performance distribution function. Hence, inspection and maintenance control plans should be based on models that reflect such conditions, and not upon linear extrapolations from data.

8.2 RECOMMENDATIONS

It is recommended that:

1. The reliability analysis system be expanded to consider more complex structural configurations and loading conditions. An initial attempt to evaluate a mechanically fastened skin-stiffener type structure is described in reference 14, and some results are presented. It is proposed that this technology be developed to encompass flaws and fatigue cracks in either the skin or the stiffener, at or away from the fastener holes, under typical flight loads.

2. A corrosion term be included in the reliability analysis system to complement the initial-flaw model as a possible source of early fatigue incidents.

3. A capability to modify selected input parameters during the operational lifetime of a structure be incorporated into the reliability analysis system. This would facilitate the application of the analysis system to fleet evaluation and management tasks.

4. The collection and evaluation of suitable information be undertaken to determine the magnitude and frequency of such preflaws typical of current airplane structures.

5. The data simulation procedures be used to develop a usable matrix of factors which can be used to unbias estimates from censored samples.

6. The statistical methods developed for application to censored data be extended to include other distribution models.

Table 1.—Aluminum Alloy Fatigue Data—Uncensored Samples

Sample size	Number of fatigue test data samples in each category								
	Monolithic notched	Lugs	Structural simulators	Structures	Structural simulators		Constant amplitude		Total
					Constant amplitude	Variable amplitude	Lap joints	Butt joints	
6	12	2	16	14	16		15	1	44
7	5	1	30	2	9	21	7	2	38
8	4	3	6	3	6		3	3	16
9	4		3	1	3			3	8
10	5	2	28	3	14	14	12	2	38
11	1		1		1		1		2
12			3		3		3		3
13			3	2	2	1	2		5
15	1								1
20	5		2		2		2		7
30	1								1
36				1					1

Table 2.—Comparison of STAR Estimator and MLE Results From Four Data Samples

	Fatigue data—lives in cycles			
	A	B	C	D
	228 000	400 000	30	74
	239 000	400 000	35	115
	240 000	498 000	120	118
	254 000	566 000	138	119
	260 000	640 000	450	126
	262 000	663 000	3210	132
	277 000	675 000	3318	140
	300 000	706 000	3459	140
	309 000	759 000	3512	142
	359 000	1 236 000	4135	156
STAR estimator results				
$\mu^* =$	12.51	13.34	6.36	4.82
$\gamma^* =$	0.20	0.37	4.31	0.14
$\alpha^* =$	0.58	0.69	0.43	0.92
MLE results				
$\hat{\mu} =$	12.49	13.35	6.53	4.86
$\hat{\gamma} =$	0.18	0.42	3.02	0.20
$\alpha =$	Assumed known constant value = 0.64			

Table 3.—Comparison of Parameters From Data With Differing Life Lengths

Location parameter range	Number of observations	ℓn-normal standard deviation	STAR estimator parameters		MLE scale parameter ($\hat{\gamma}$) (fixed α = 0.64)
			Flexure (α^*)	Scale (γ^*)	
0 to 10^4	333	0.27	0.62	0.42	0.36
10^4 to 10^5	408	0.35	0.63	0.56	0.48
10^5 to 5.10^5	252	0.33	0.67	0.42	0.40
5.10^5 to 10^6	217	0.38	0.63	0.49	0.46
$>10^6$	202	0.53	0.64	0.77	0.67
0 to 10^3			0.63		
0 to 10^4			0.62		
0 to 10^5			0.62		
0 to 5.10^5			0.63		
0 to 10^6			0.63		
0 to $>10^6$			0.63		

Table 4.—Comparison of Parameters From Different Specimen Types and Loading Conditions

Data description	Number of observations	STAR estimator parameters		MLE scale parameter ($\hat{\gamma}$) (fixed α = 0.64)
		Flexure (α^*)	Scale (γ^*)	
Lap joints—variable amplitude	300	0.62	0.38	0.34
Lap joints—constant amplitude	386	0.64	0.62	0.56
Butt joints—constant amplitude	91	0.63	0.53	0.45
Structures	223	0.62	0.63	0.58
Monolithic notched	381	0.66	0.38	0.38
Structural simulators location parameter range				
0 to $>10^6$	777	0.63		
0 to 10^6	621	0.63		
0 to 10^5	398	0.63		
0 to 10^4	159	0.62		
0 to 10^3	153	0.62		

Table 5.--Samples of Censored Fatigue Test Data

Sample no.	Number of failures	Censoring, %	Fatigue lives, kc						
1	41	21	78	111	128	132	134	141	142
			142	150	156	161	166	171	182
			190	191	191	197	197	198	199
			201	212	214	219	221	222	223
			223	226	229	229	230	235	238
			240	240	248	248	249	250	
			(11 suspensions at 250 kc)						
2	33	38	74	95	103	110	115	119	126
			128	140	140	140	142	146	146
			149	150	154	156	160	163	172
			174	175	176	189	189	190	196
			200	223	236	240	247		
			(20 suspensions at 250 kc)						
3	33	38	101	113	130	134	134	135	137
			139	148	153	164	165	165	168
			172	177	183	187	188	193	208
			212	213	214	215	220	223	234
			237	244	244	246	248		
			(20 suspensions at 250 kc)						
4	29	46	161	163	166	170	178	186	187
			191	200	204	204	206	208	209
			211	[illegible]	227	229	230	233	233
			233	[illegible]	245	247	248	248	248
			250						
			(25 suspensions at 250 kc)						
5	29	37	57	84	100	106	106	112	113
			117	124	125	126	128	142	148
			153	154	177	180	187	197	211
			216	223	227	237	240	245	245
			248						
			(17 suspensions at 250 kc)						
6	10	81	138	180	181	193	200	215	220
			225	236	250				
			(44 suspensions at 250 kc)						
7	5	91	188	196	221	234	246		
			(48 suspensions at 250 kc)						

Table 6.—Scale and Location Parameter Estimates of Censored Test Data Samples

Sample no.	MLE scale parameter	MLE location parameter	Scale parameter ratio
1	0.40044	12.269	0.40044/0.69624 = 0.575
			0.40044/0.53515 = 0.748
2	0.69624	12.226	0.69624/0.53515 = 1.301
3	0.53515	12.314	0.53515/0.29699 = 1.802
4	0.29699	12.414	0.69624/0.29699 = 2.344
5	0.78967	12.262	0.78967/0.29699 = 2.659
6	0.43971	12.692	0.43971/0.29699 = 1.481
7	0.29873	12.710	0.29873/0.78967 = 0.378

Table 7.—Location Parameter Estimates of Paired Censored Test Data Samples

Sample no.	Scale parameter $\tilde{\gamma}$ (for paired sample)	MLE location parameter	Location parameter difference
1 3	0.47	12.268 12.308	0.040
2 3	0.62	12.215 12.319	0.104
4 6	0.39	12.427 12.662	-0.235

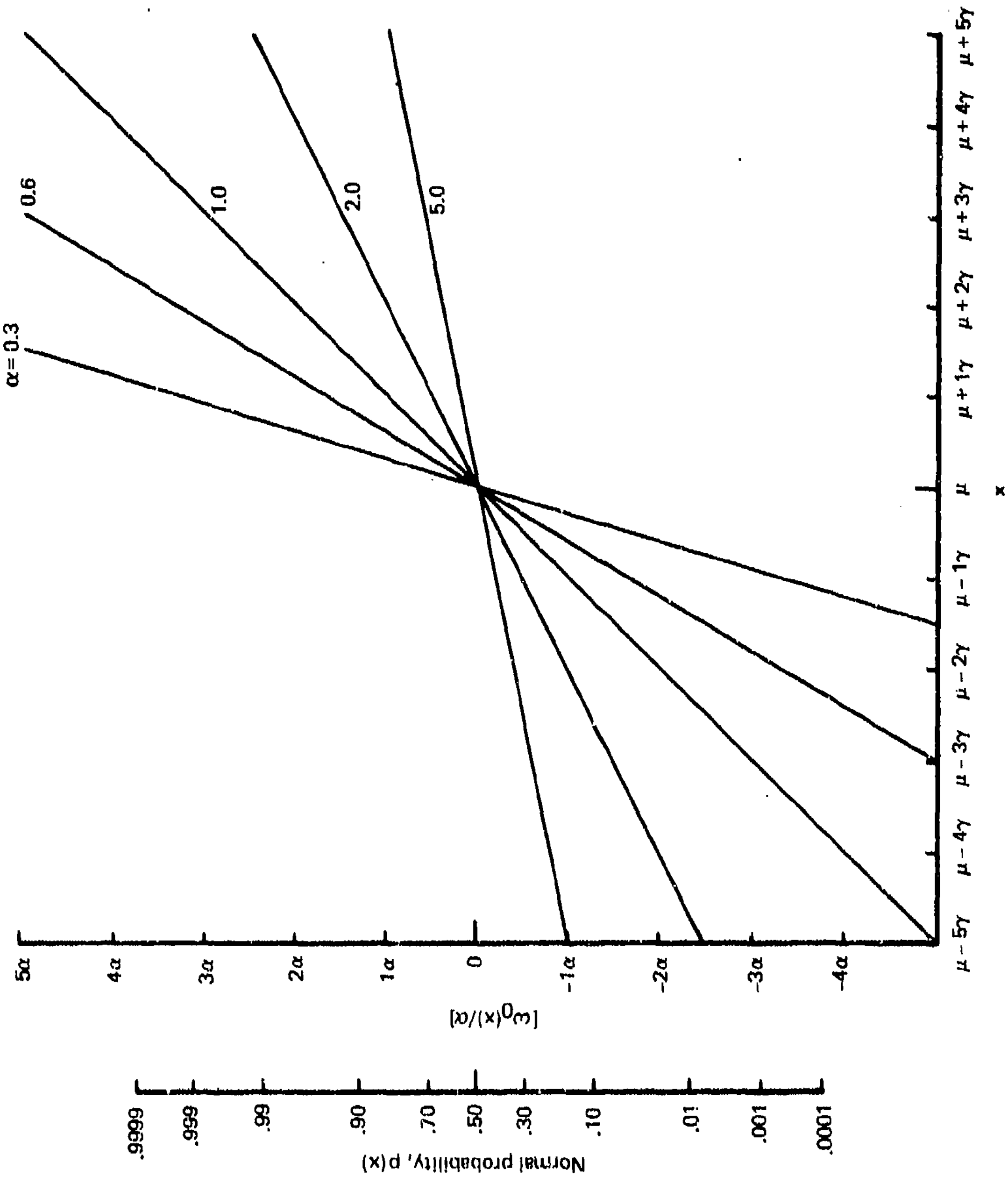

Figure 1.—Log-Normal Distribution—$\omega_0(x) = x$

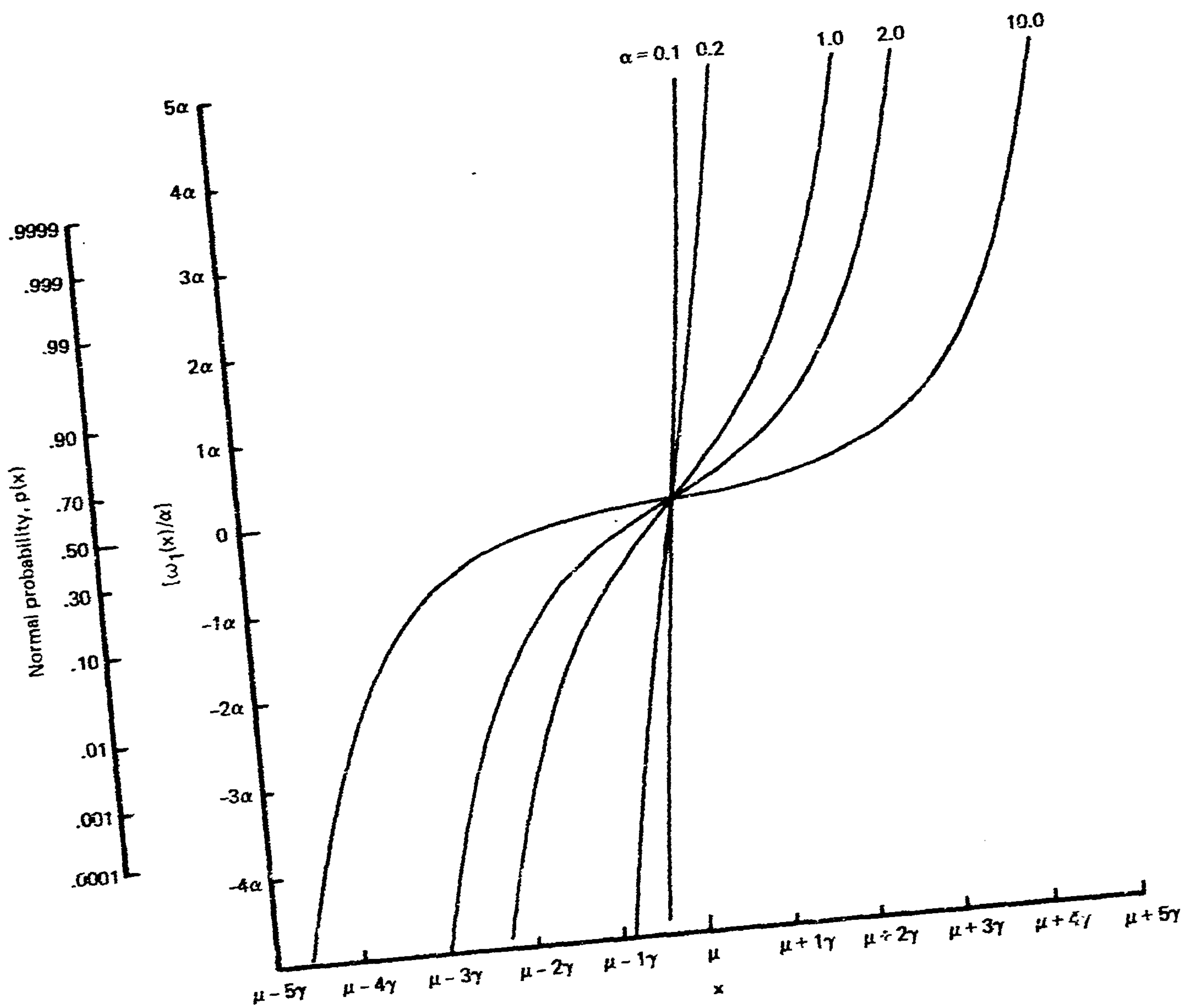

Figure 2.—Hyperbolic Sine Distribution—$\omega_1(x) = \sinh(x)$

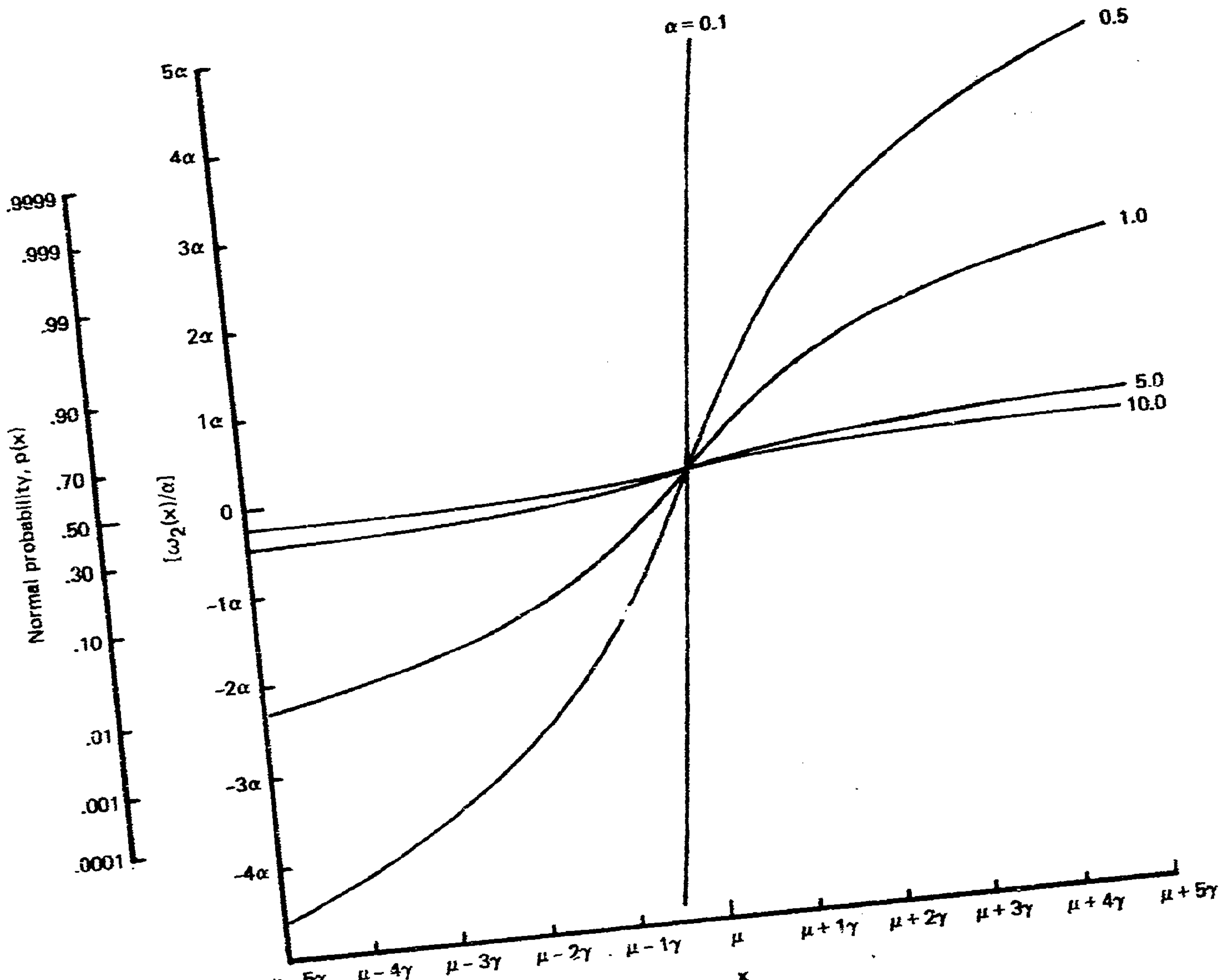

Figure 3.—Inverse Hyperbolic Sine Distribution—$\omega_2(x) = \sinh^{-1}(x)$

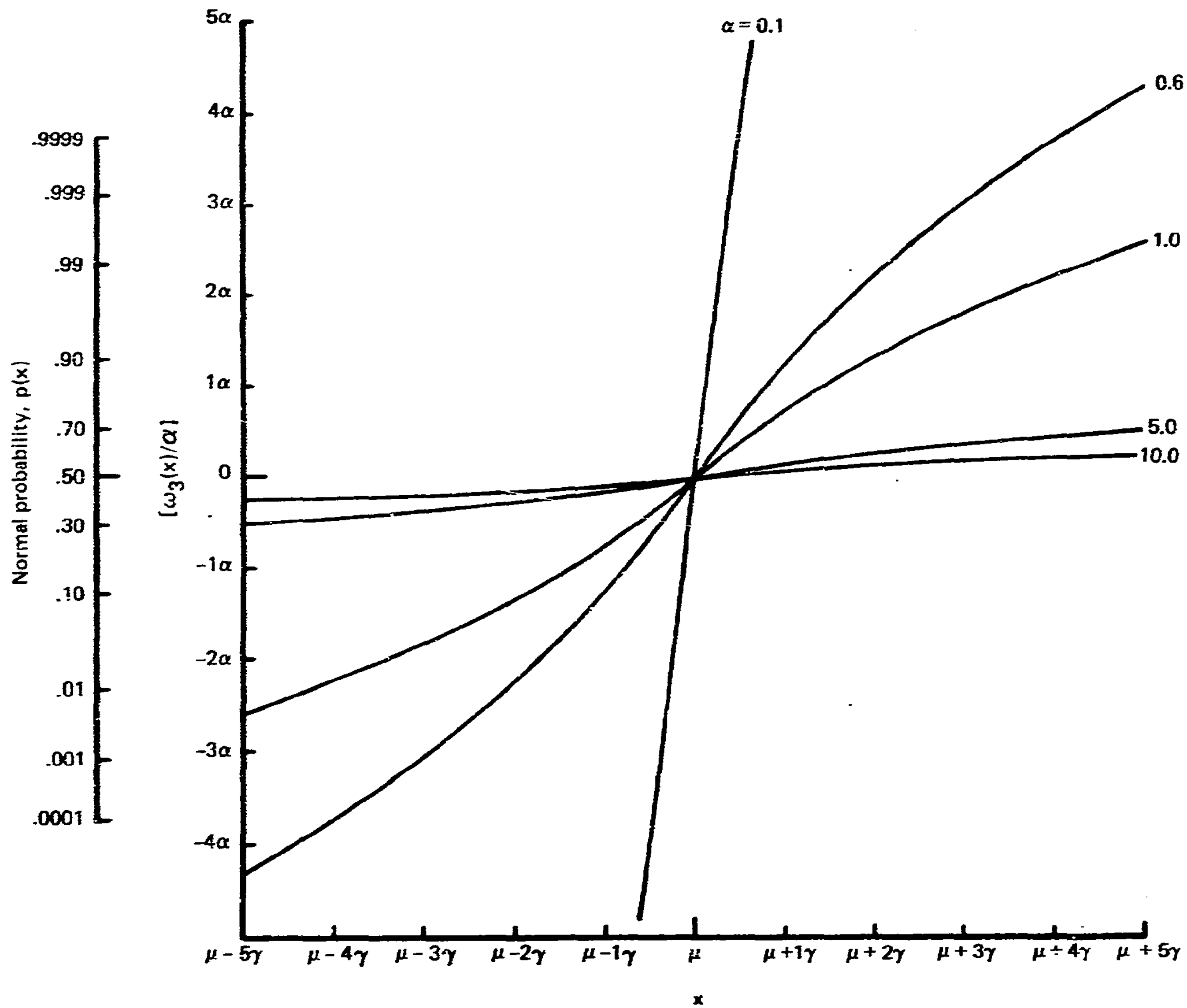

Figure 4.—Symmetric-Weibull Distribution—$\omega_3(x) = \Phi^{-1}\ [F(x)]$

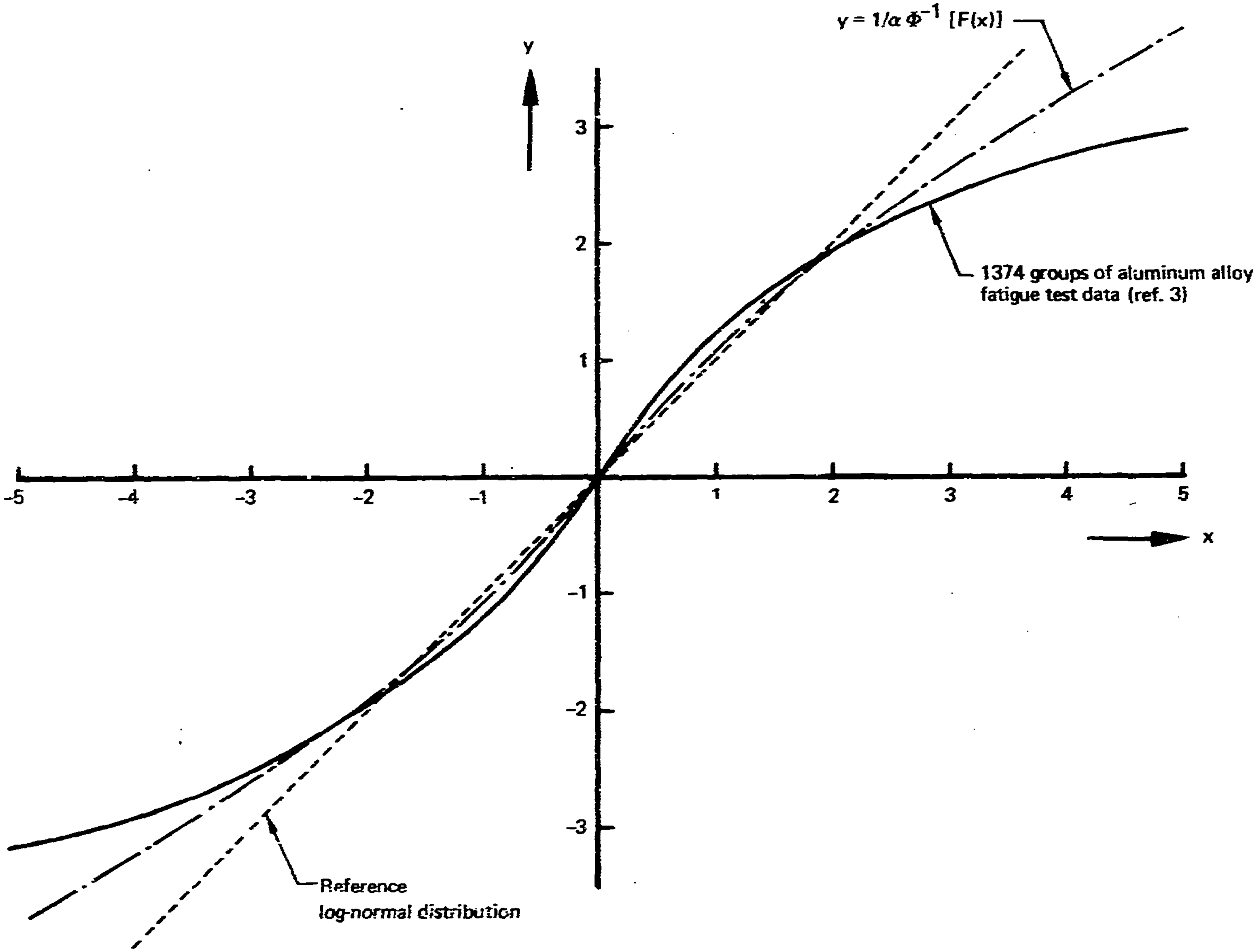

Figure 5.—Comparison of Aluminum Alloy Fatigue Test Data Distribution and the Symmetric-Weibull Distribution

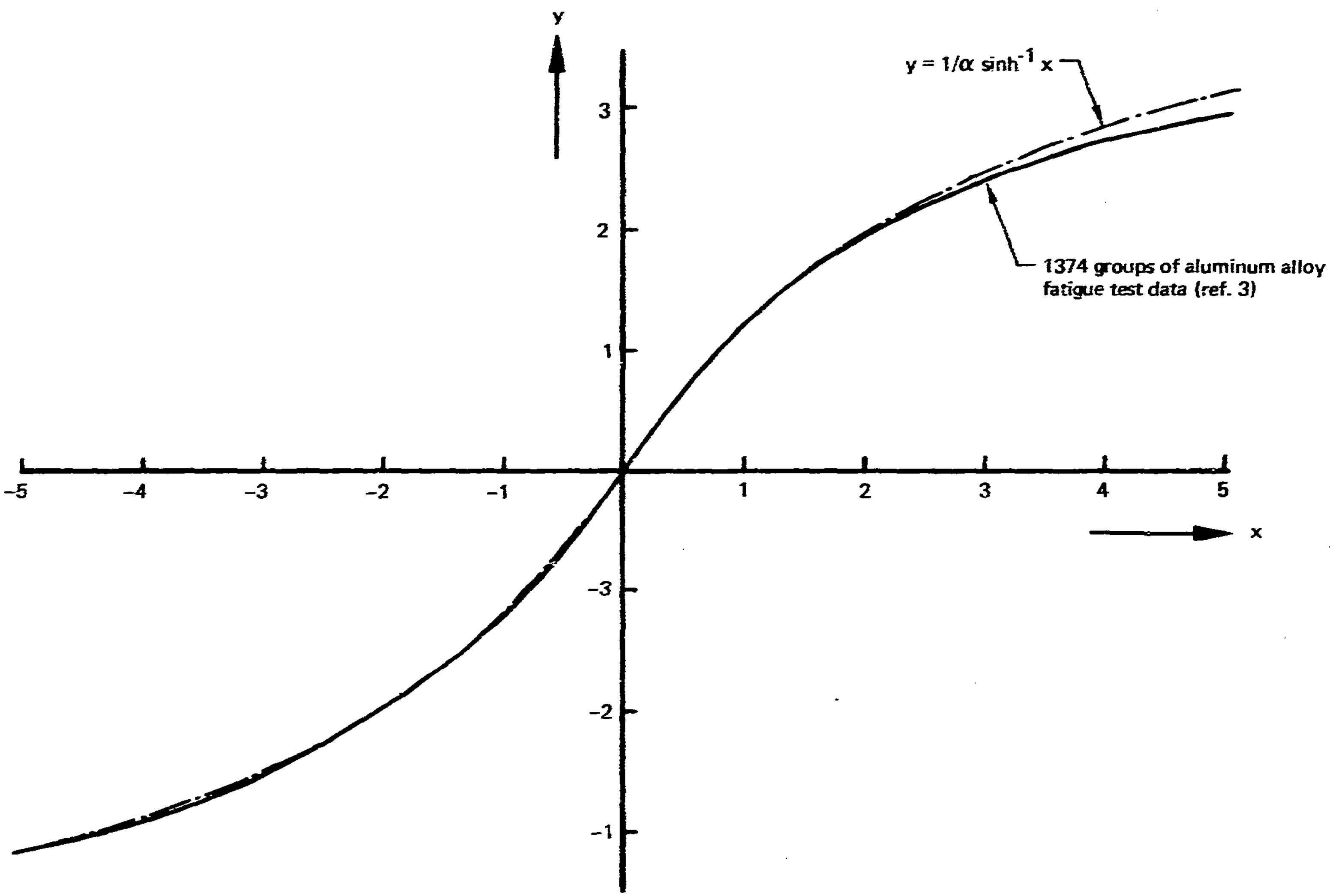

Figure 6.—Comparison of Aluminum Alloy Fatigue Test Data Distribution and the Birmbaum-Saunders Inverse Hyperbolic Sine Distribution

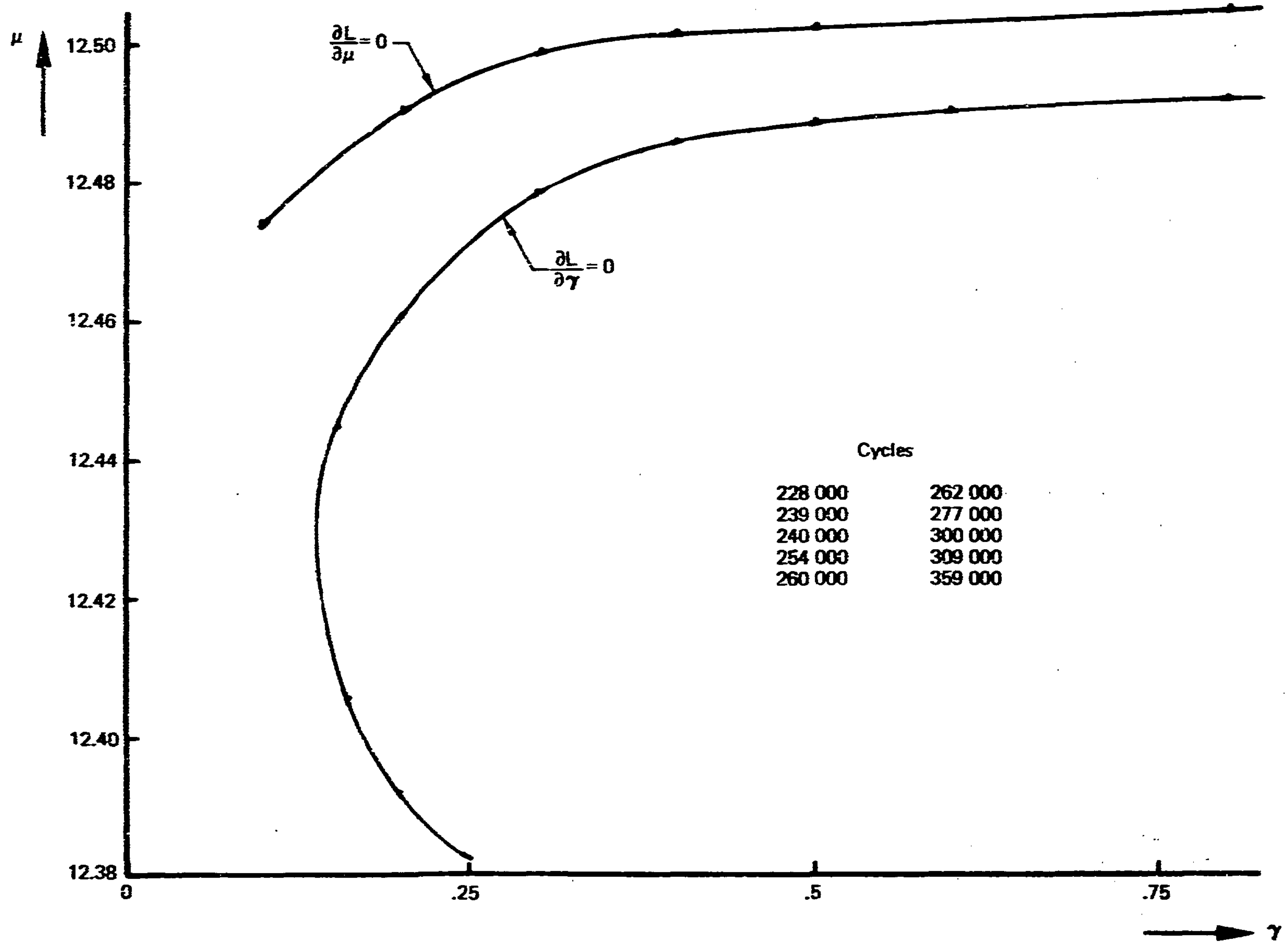

Figure 7.—Iteration Results of Fatigue Data Sample, Open Hole Specimens Randomly Loaded—Sample Size = 10

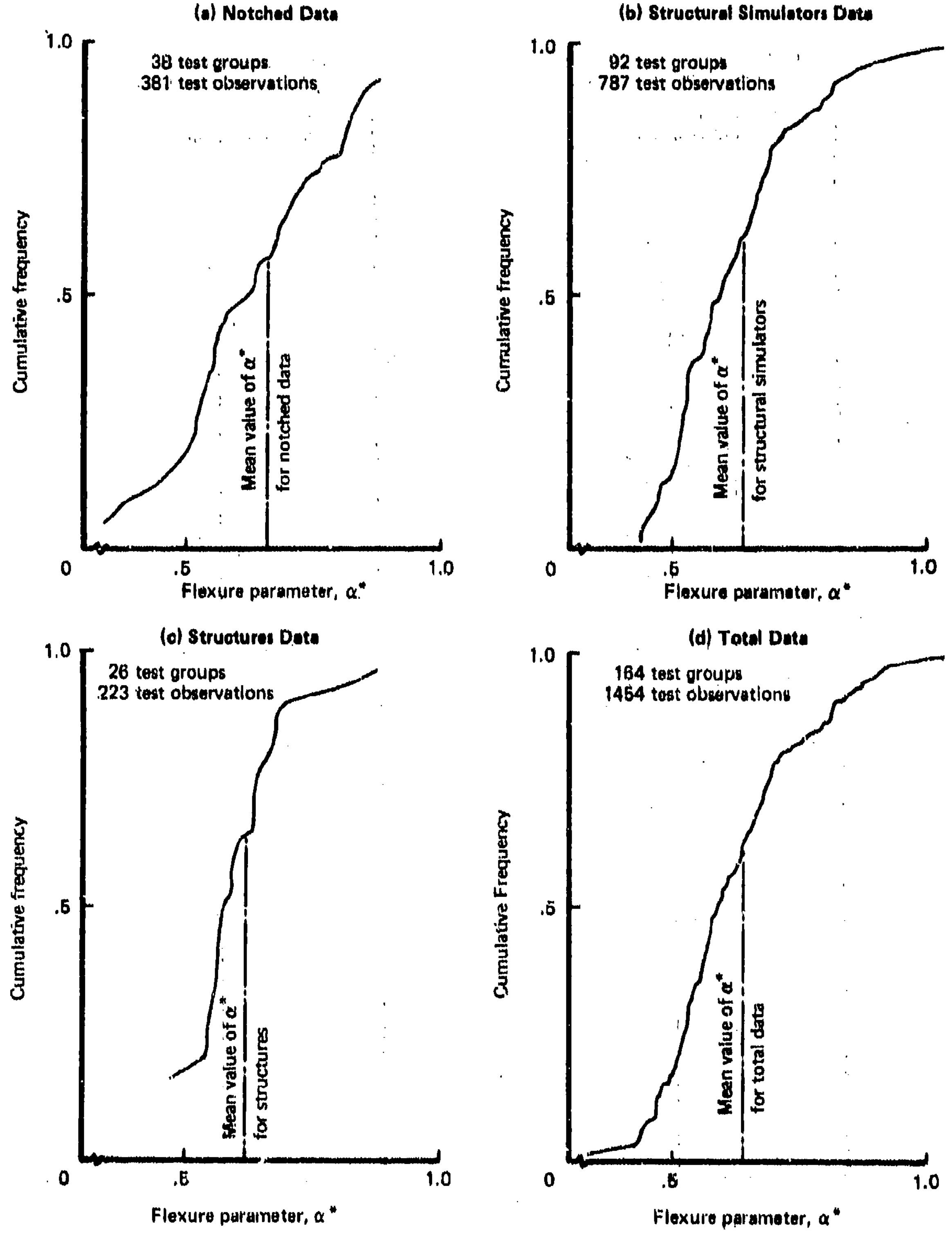

Figure 8.—Comparison of Aluminum Alloy Fatigue Test Specimen Types

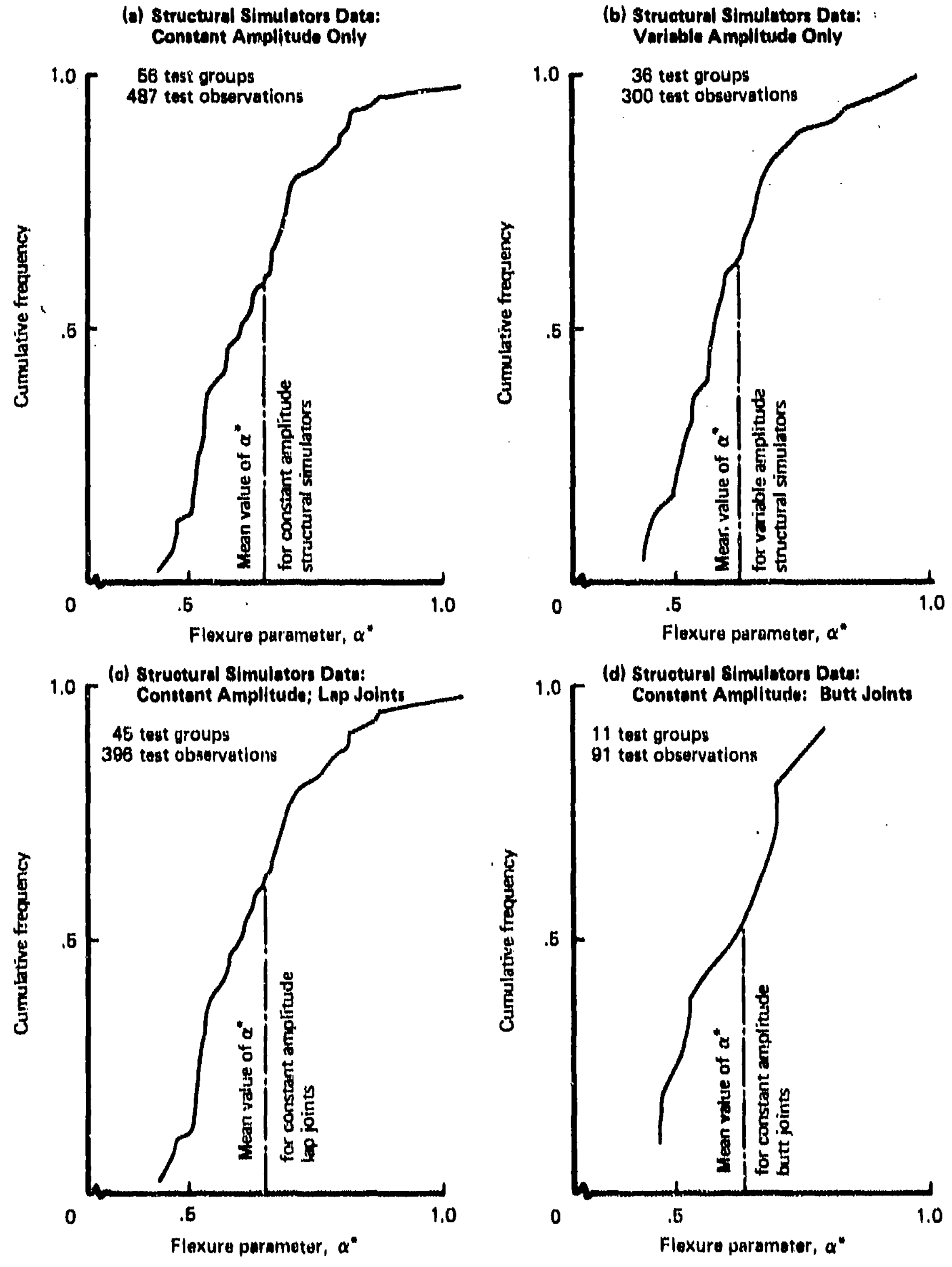

Figure 9.—Comparison of Variables Within One Aluminum Alloy Fatigue Test Specimen Type

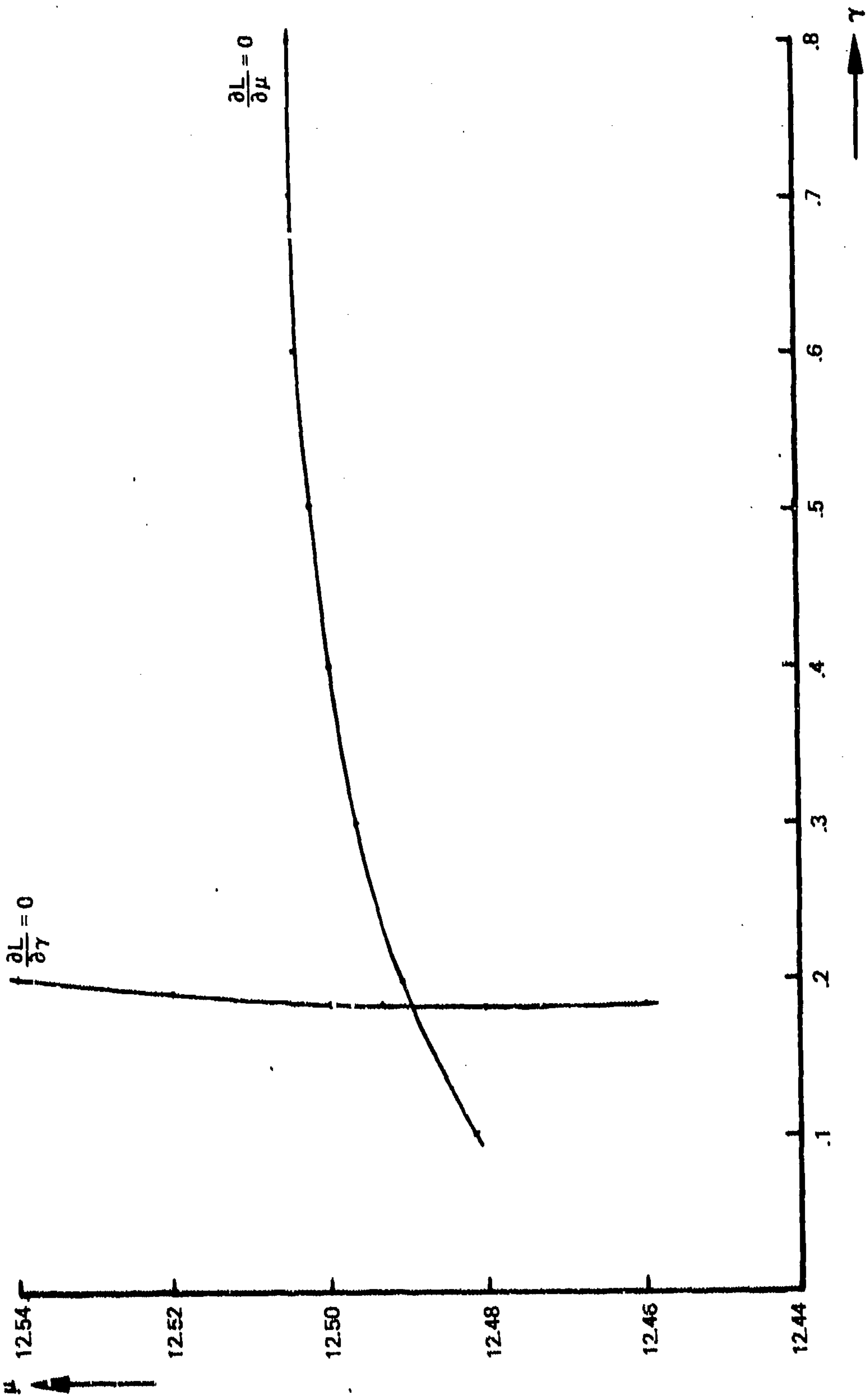

Figure 10.—Iteration Results of Fatigue Data Sample A

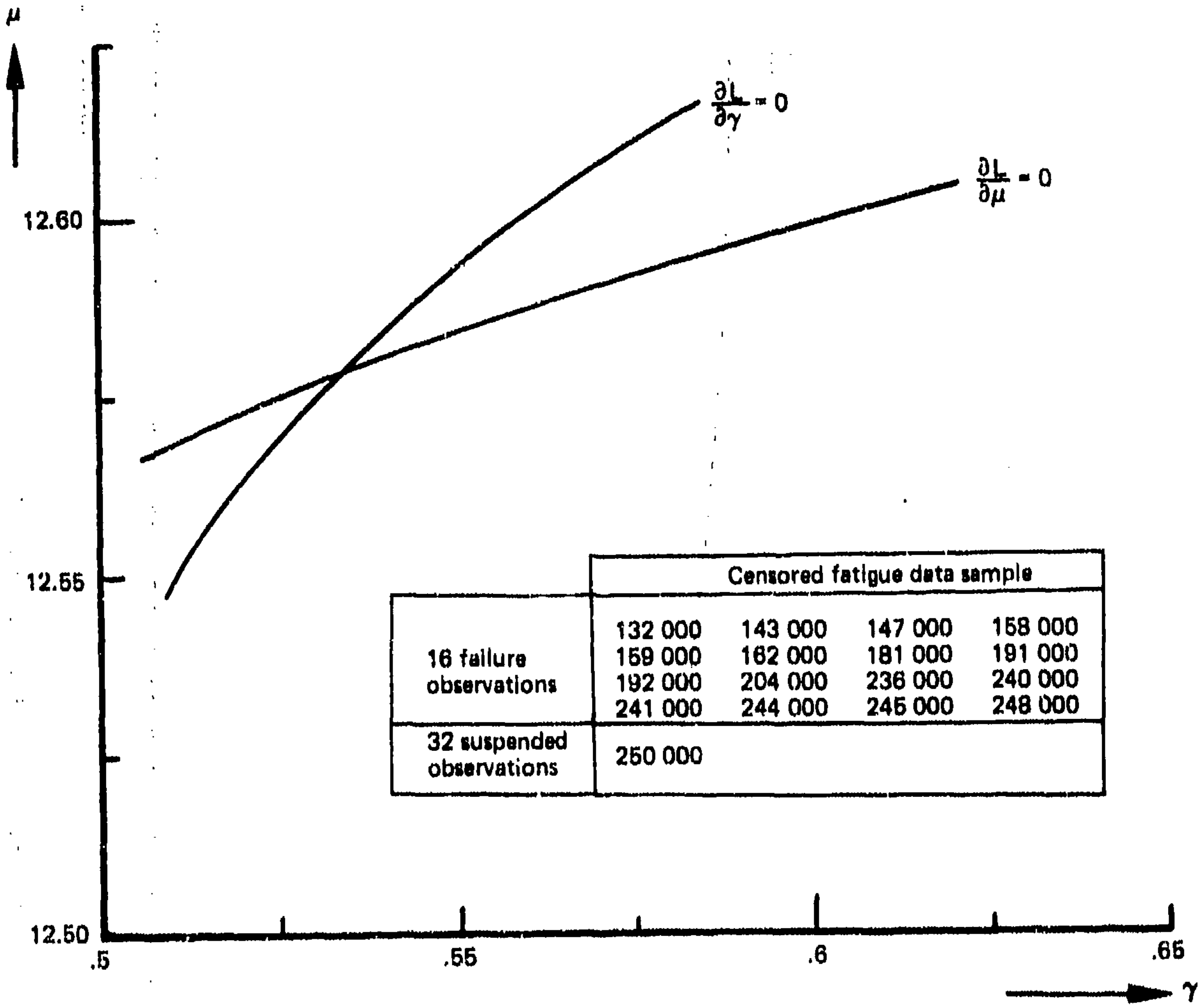

	Censored fatigue data sample			
16 failure observations	132 000	143 000	147 000	158 000
	159 000	162 000	181 000	191 000
	192 000	204 000	236 000	240 000
	241 000	244 000	245 000	248 000
32 suspended observations	250 000			

Figure 11.—Iteration Results From Censored Data

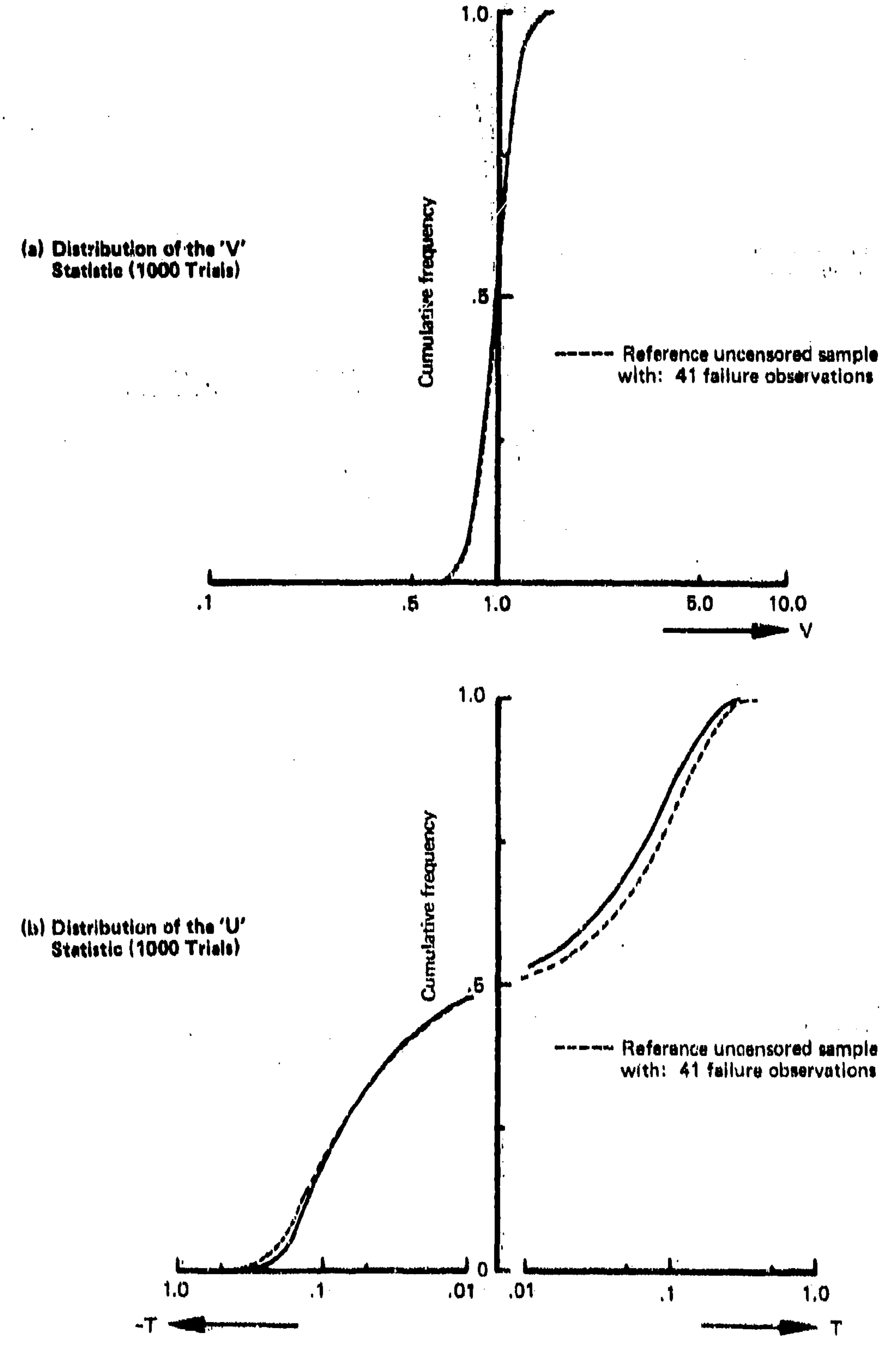

Figure 12.—Simulation of Censored Sample With: 41 Failure Observations; 11 Censored Observations

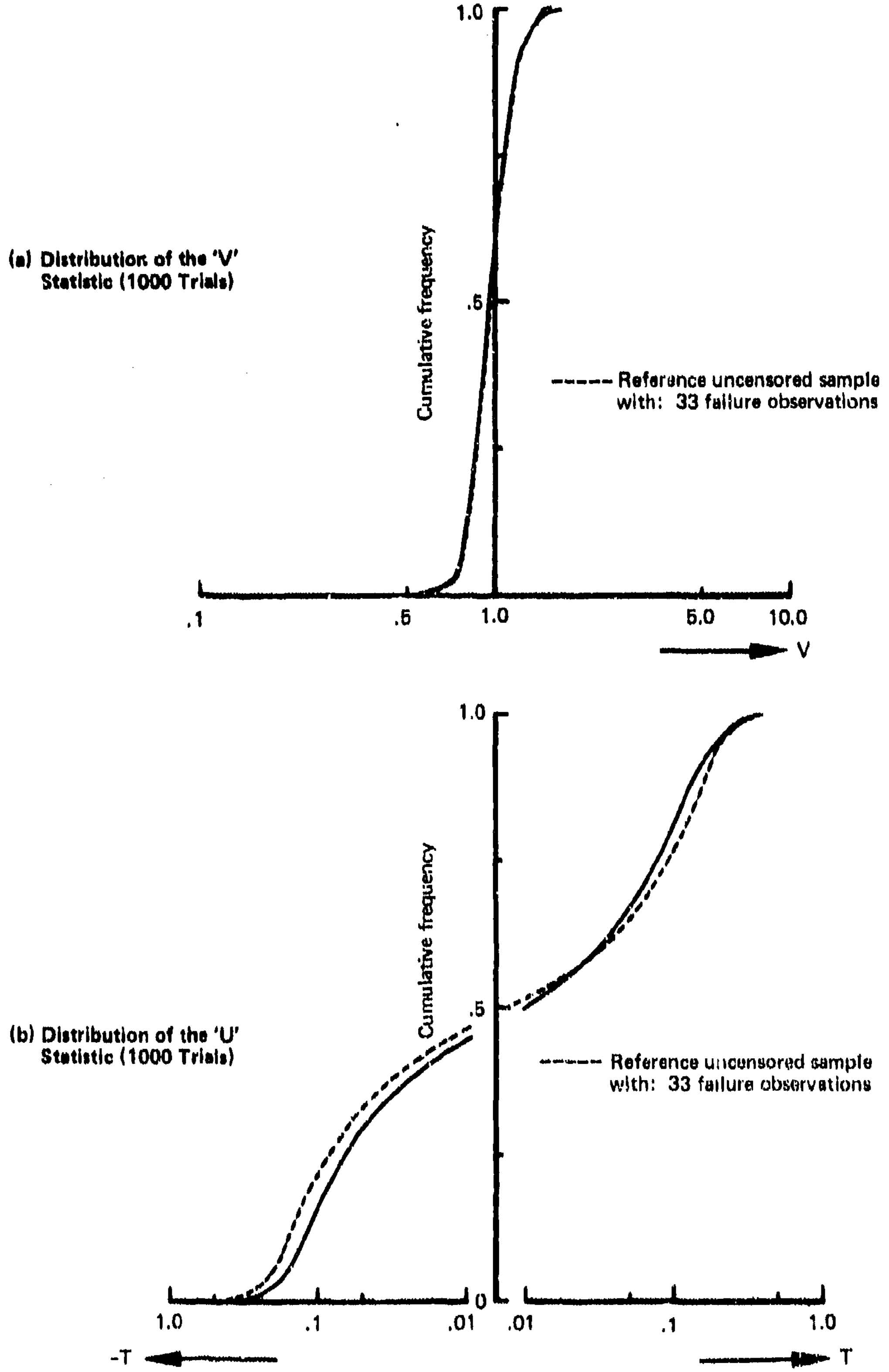

Figure 13.—Simulation of Censored Sample With: 33 Failure Observations; 20 Censored Observations

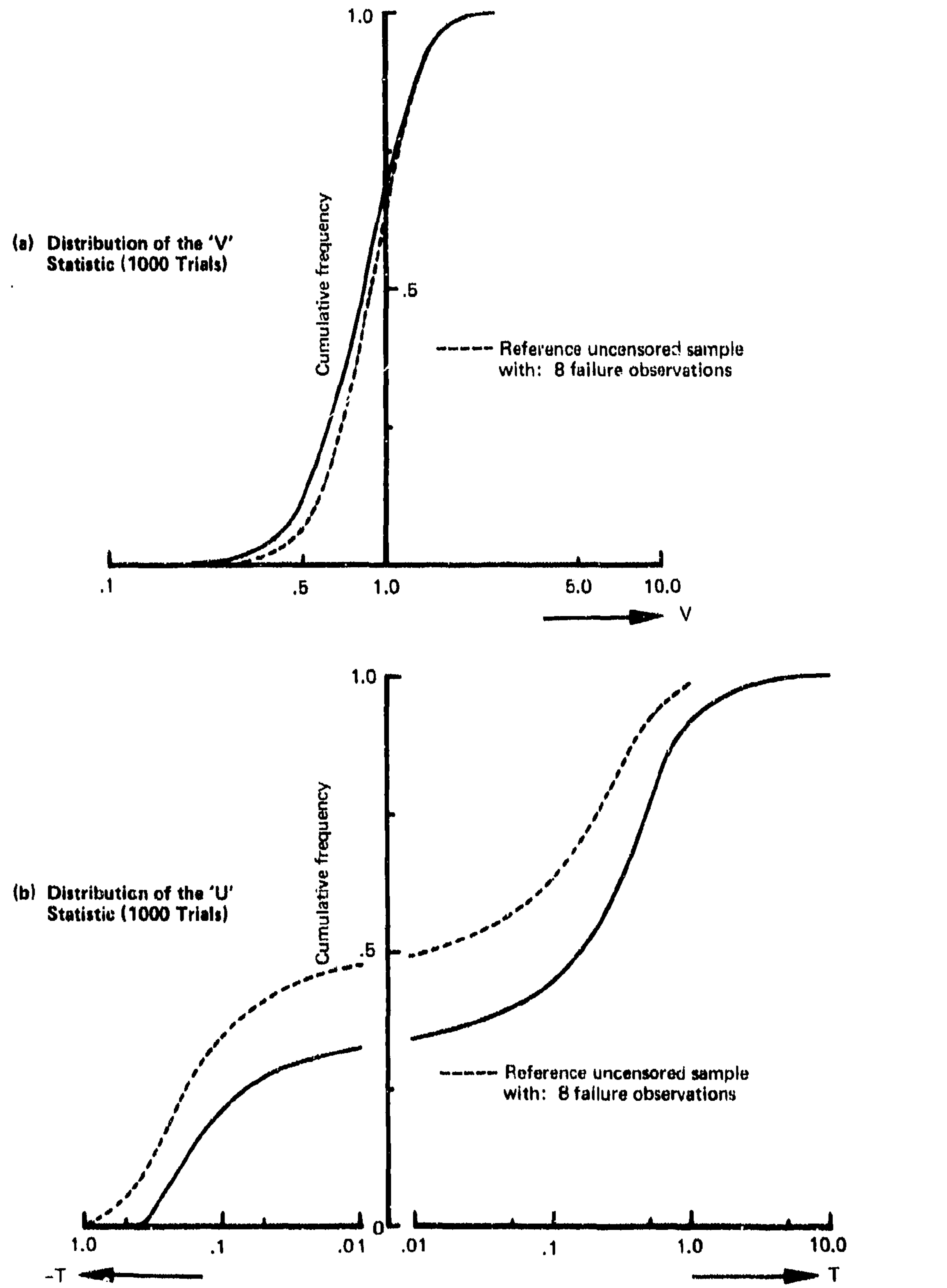

Figure 14.--Simulation of Censored Sample With: 8 Failure Observations; 40 Censored Observations

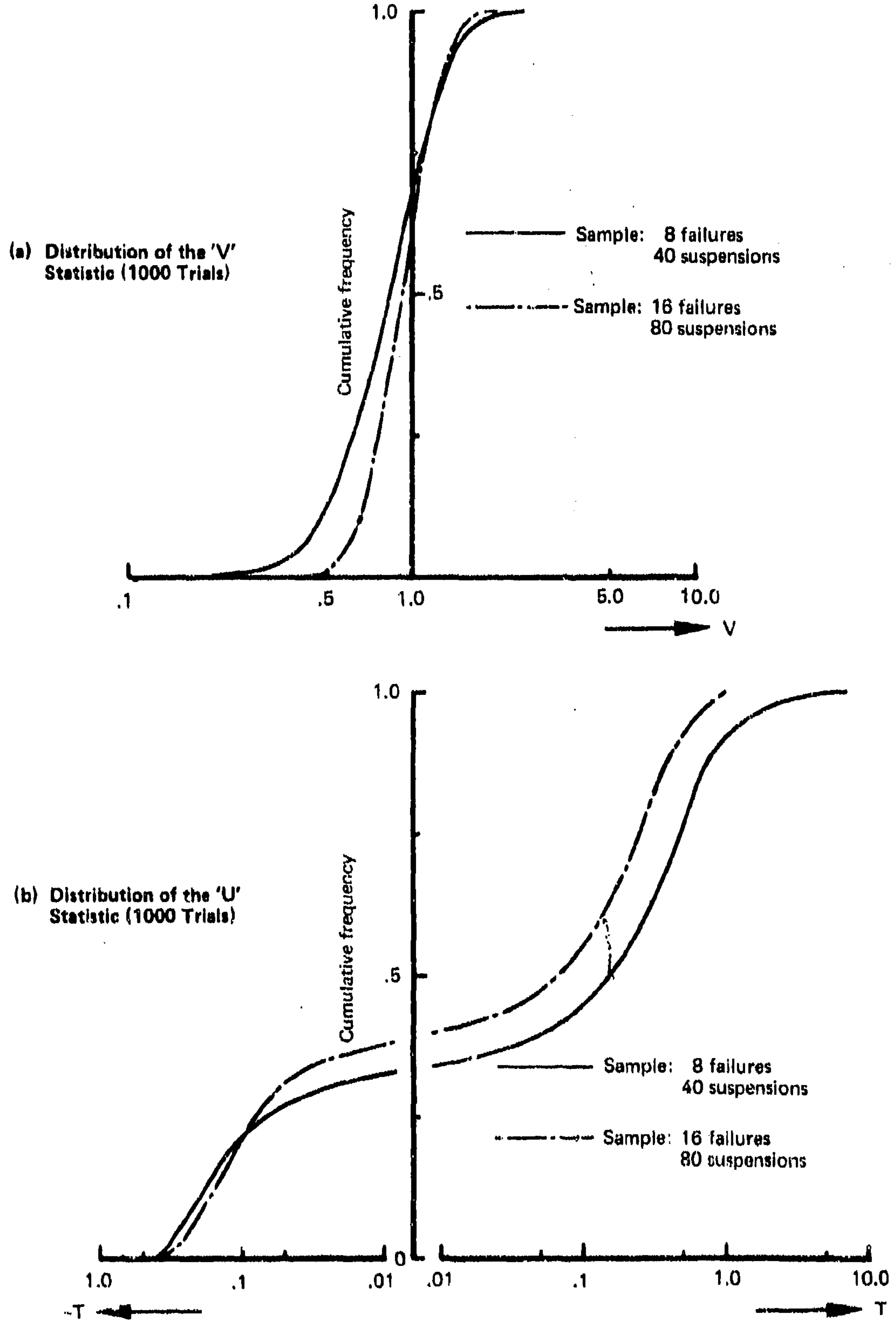

Figure 15.—Simulation of Censored Samples With 83% Censoring

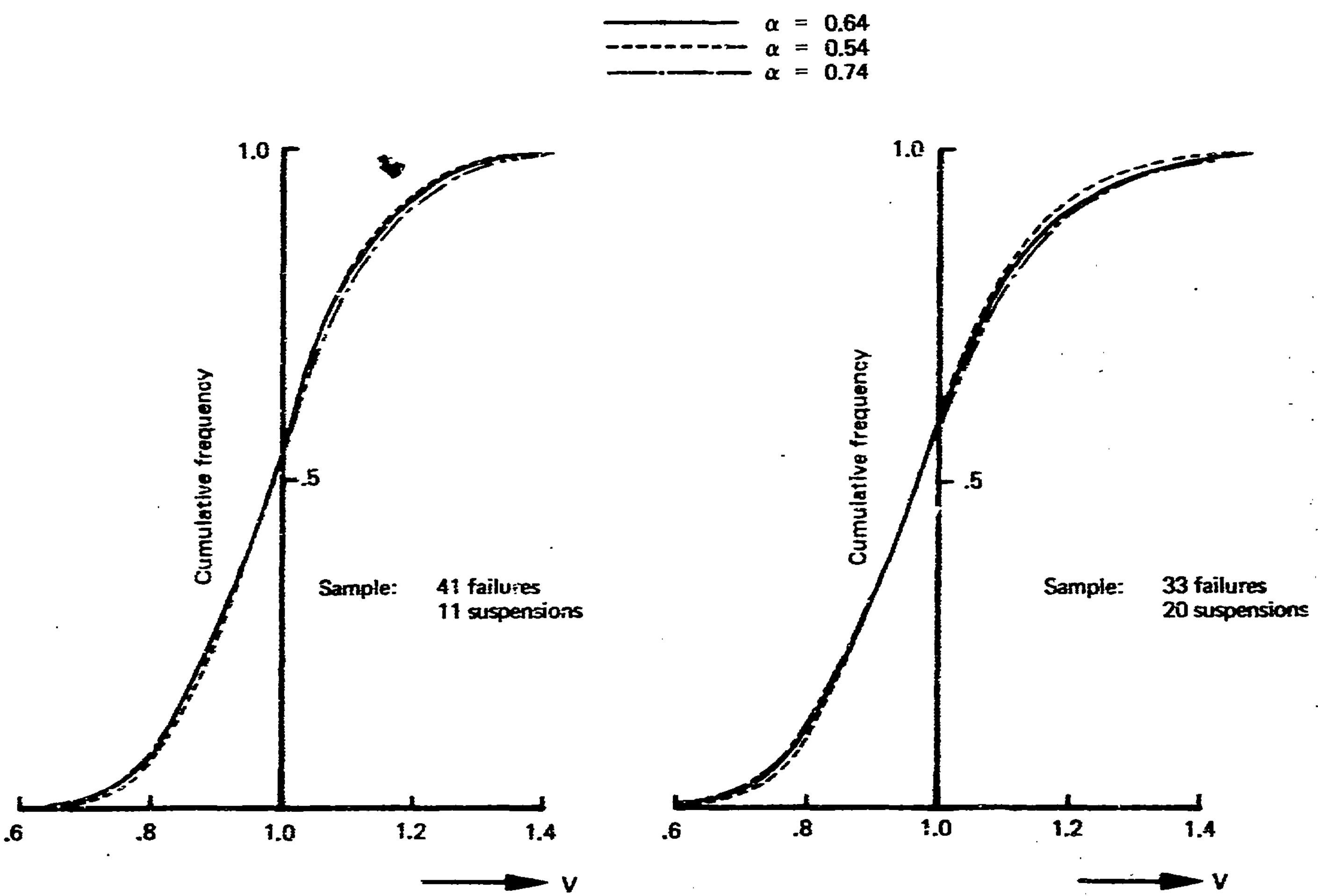

Figure 16.—Simulation of Censored Samples With Various Assumed Flexure Parameters

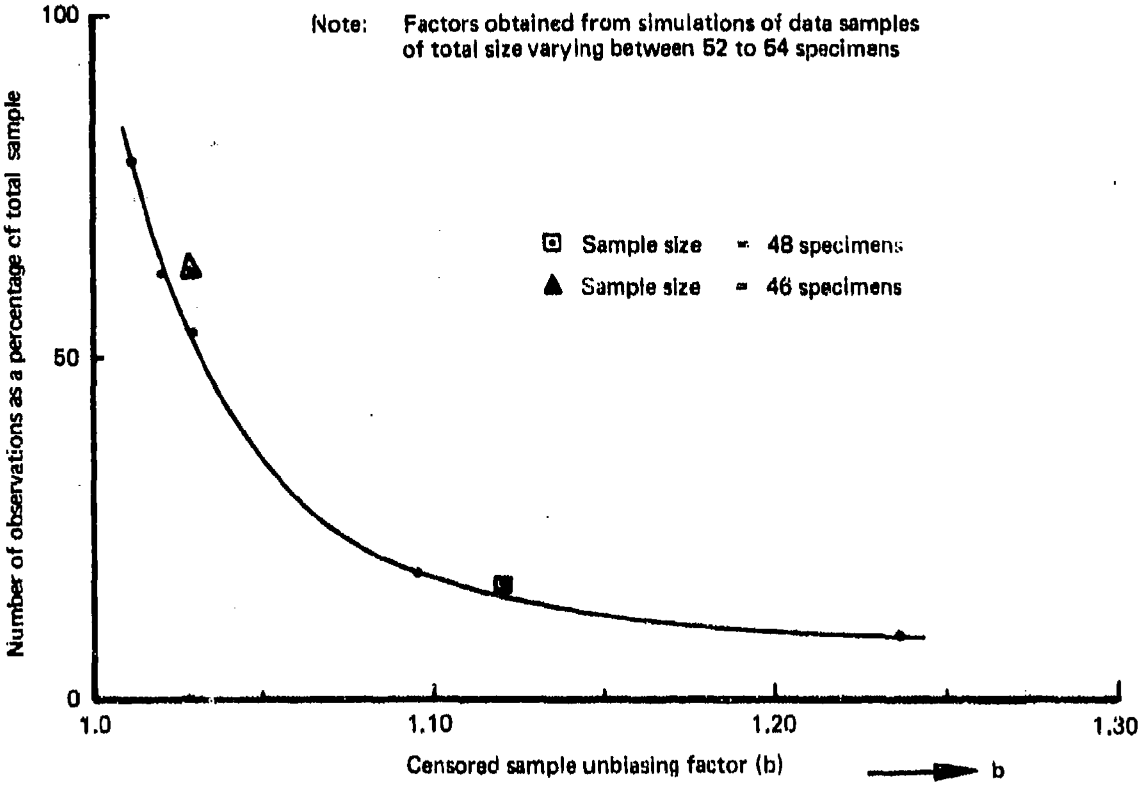

Figure 17.—Example Curve of Unbiasing Factors for the Scale Parameter

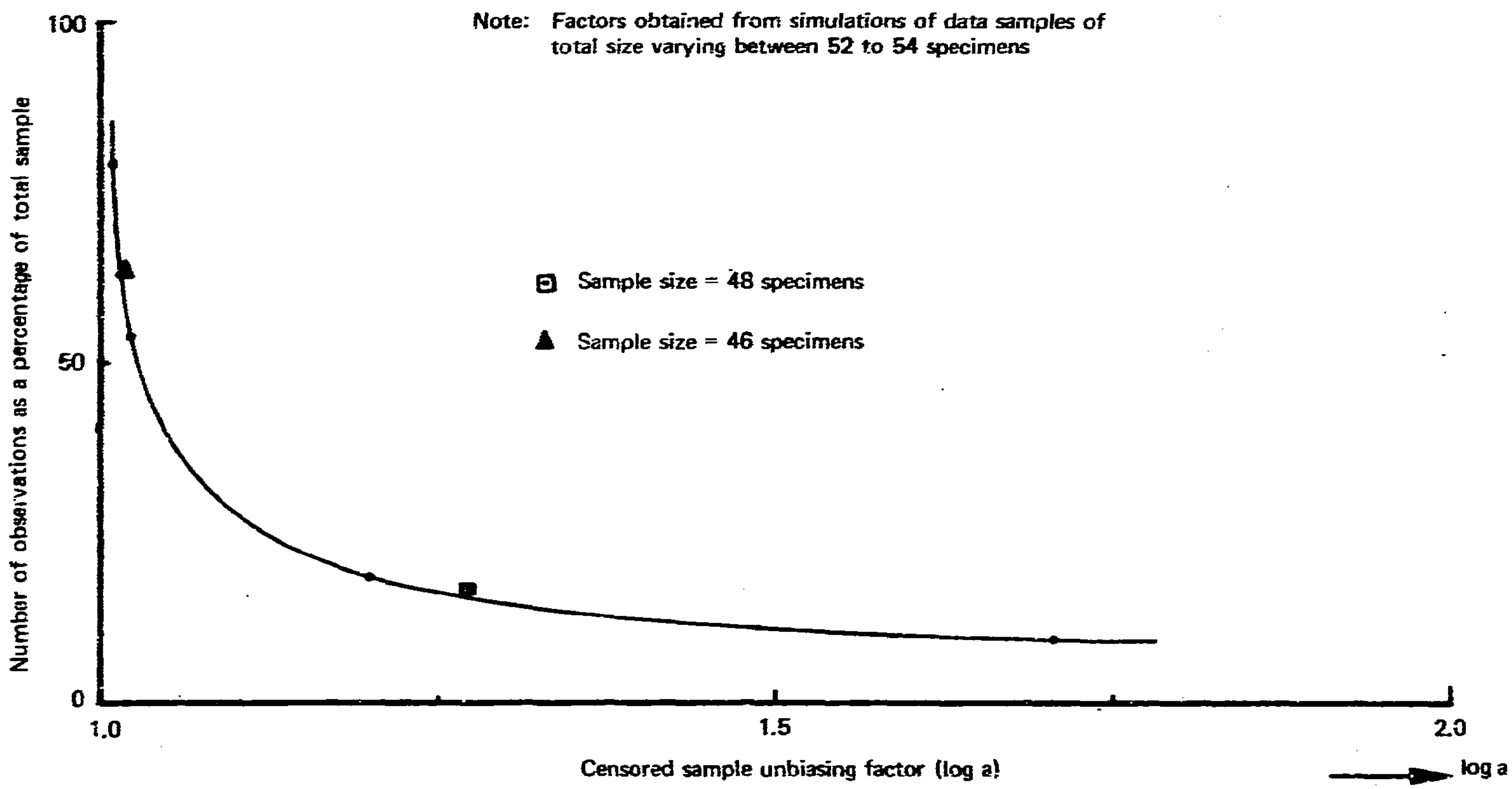

Figure 18.—Example Curve of Unbiasing Factors for the Location Parameter

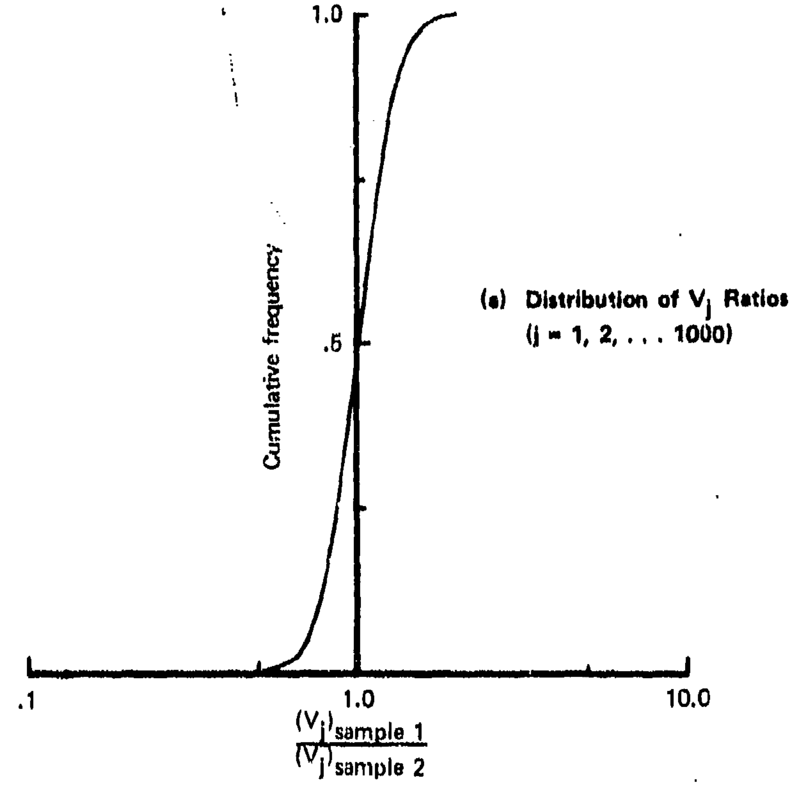

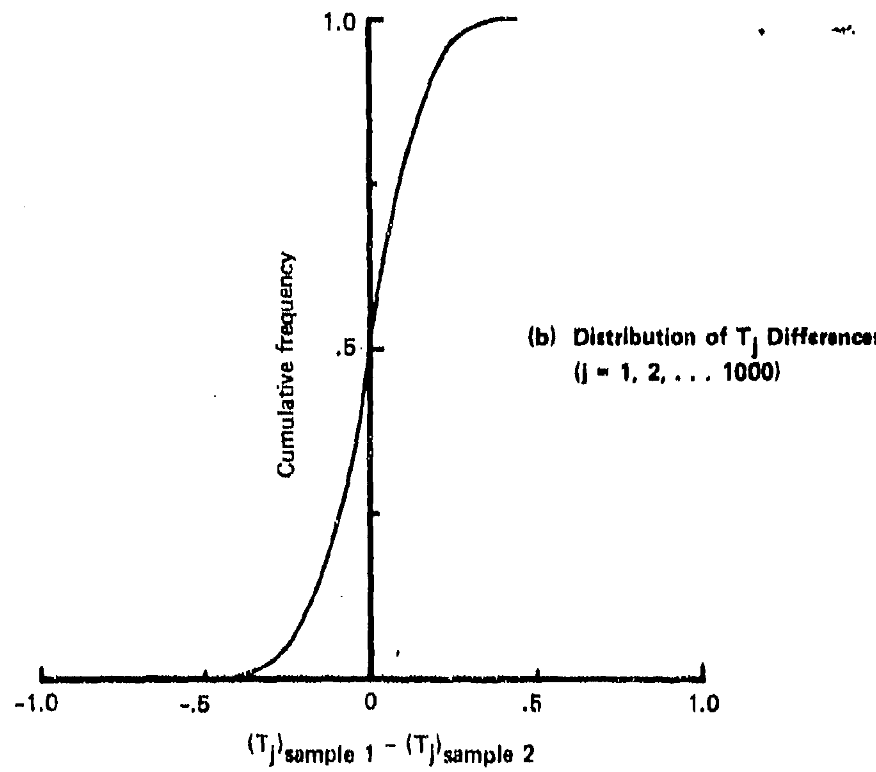

Figure 19.—Distribution of Parameter Statistics for Two Independent Censored Data Samples— Sample 1: 41 Failures, 11 Suspensions; Sample 2: 33 Failures, 20 Suspensions

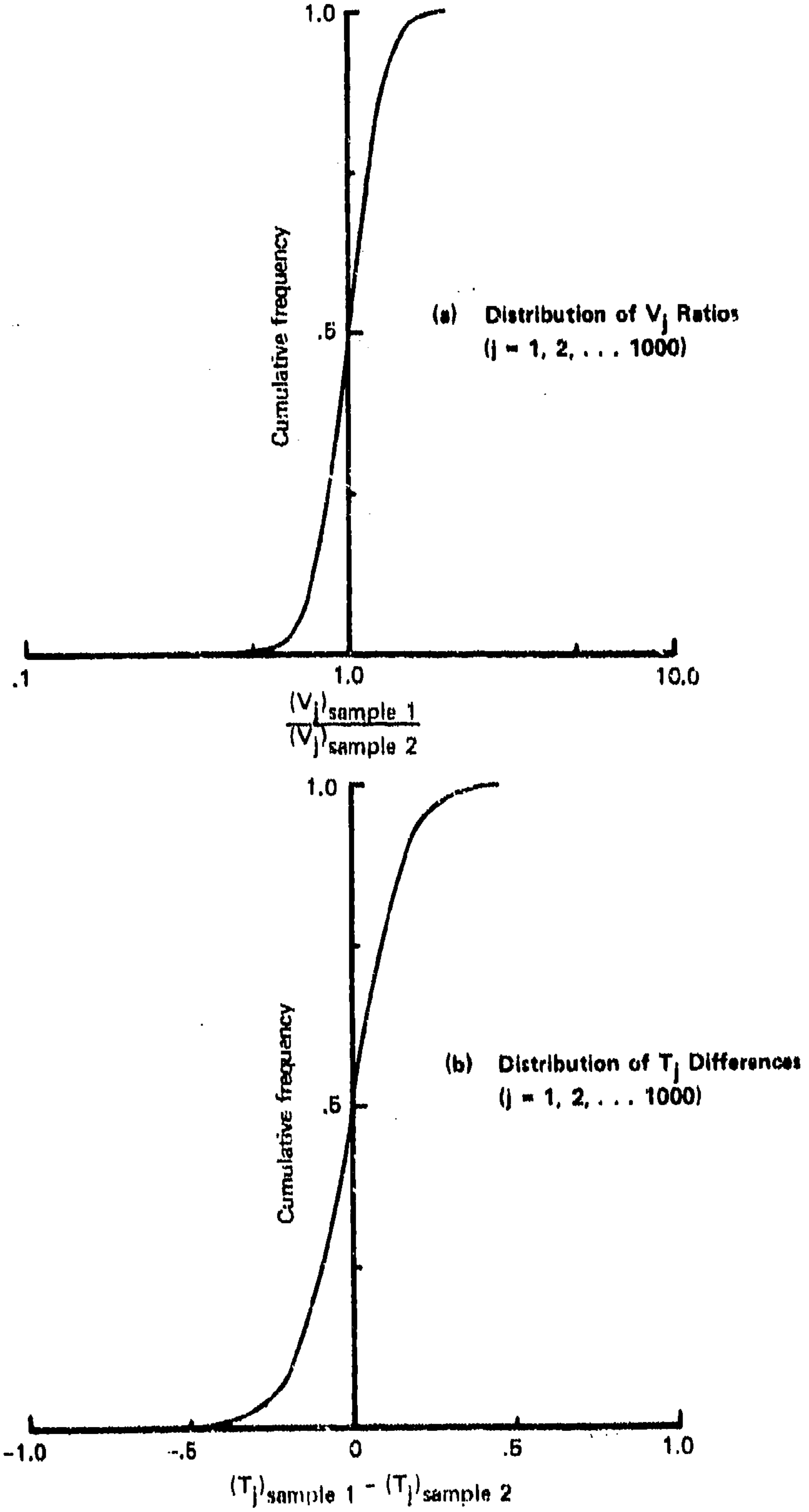

Figure 20.—Distribution of Parameter Statistics for Two Independent Censored Data Samples—Sample 1: 33 Failures, 20 Suspensions; Sample 2: 33 Failures, 20 Suspensions

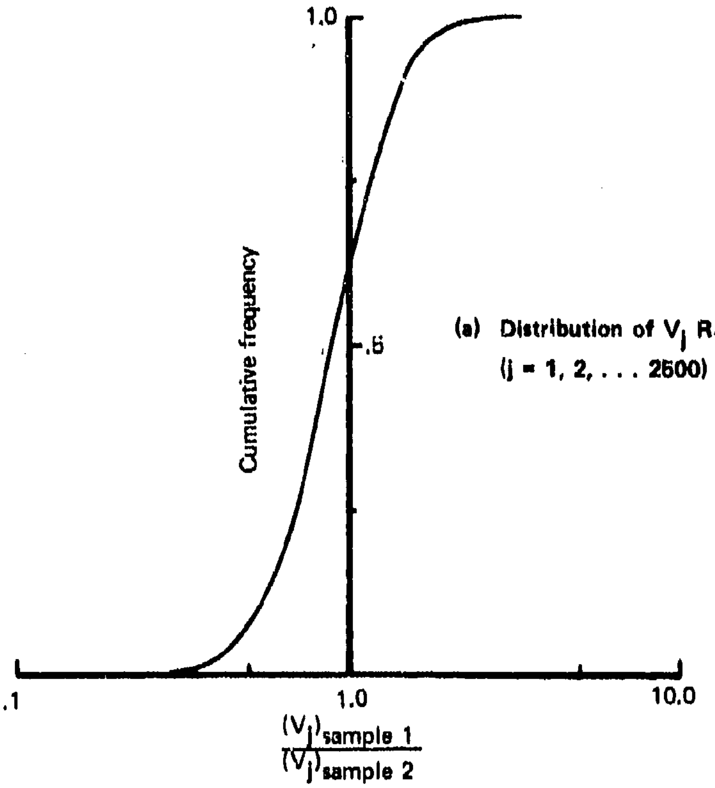

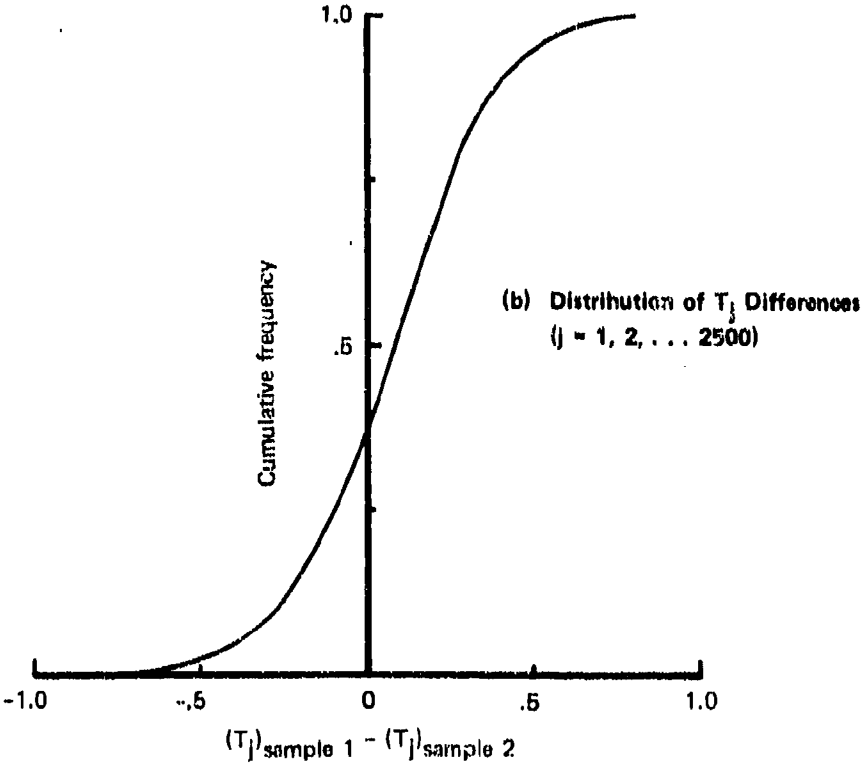

Figure 21.—Distribution of Parameter Statistics for Two Independent Censored Data Samples—Sample 1: 10 Failures, 44 Suspensions; Sample 2: 29 Failures 25 Suspensions

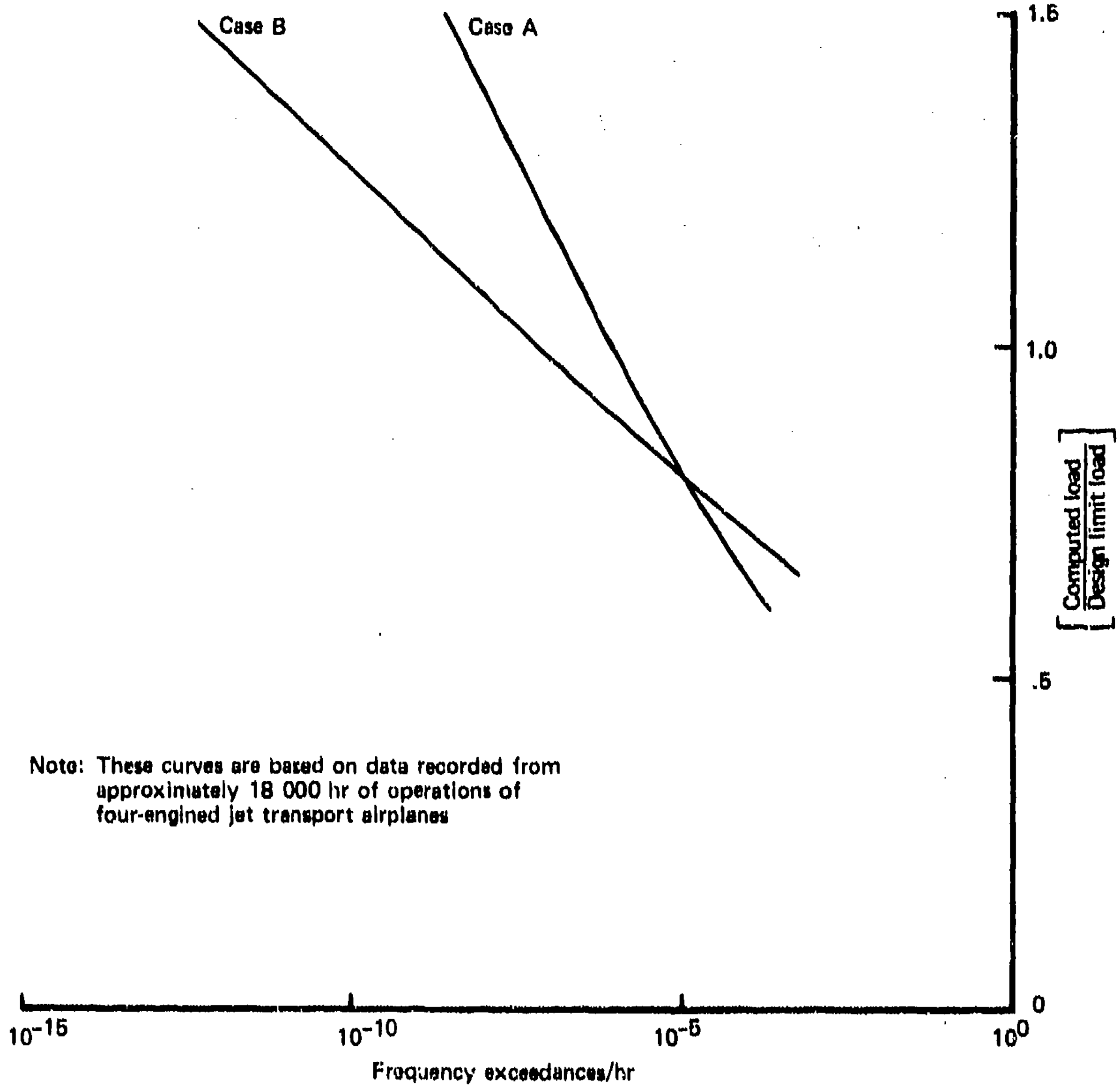

Figure 22.—Exceedances of Gust-Induced Load Ratios for Two Critical Major Locations of a Jet-Engined Tanker/Transport-Type Airplane

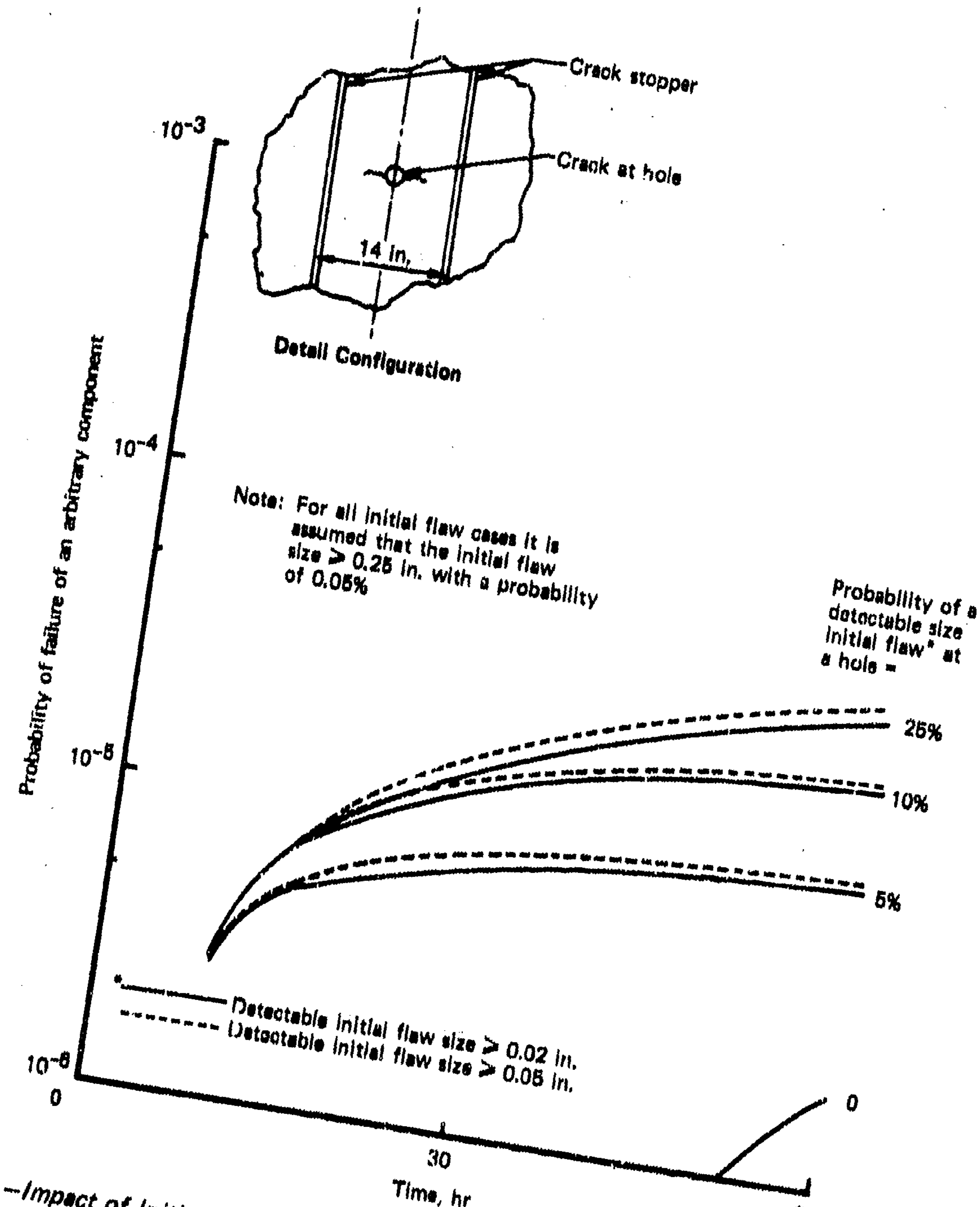

Figure 23.—Impact of Initial Flaws on the Reliability of a Fail-Safe Skin-Type Structure—Type A Loads

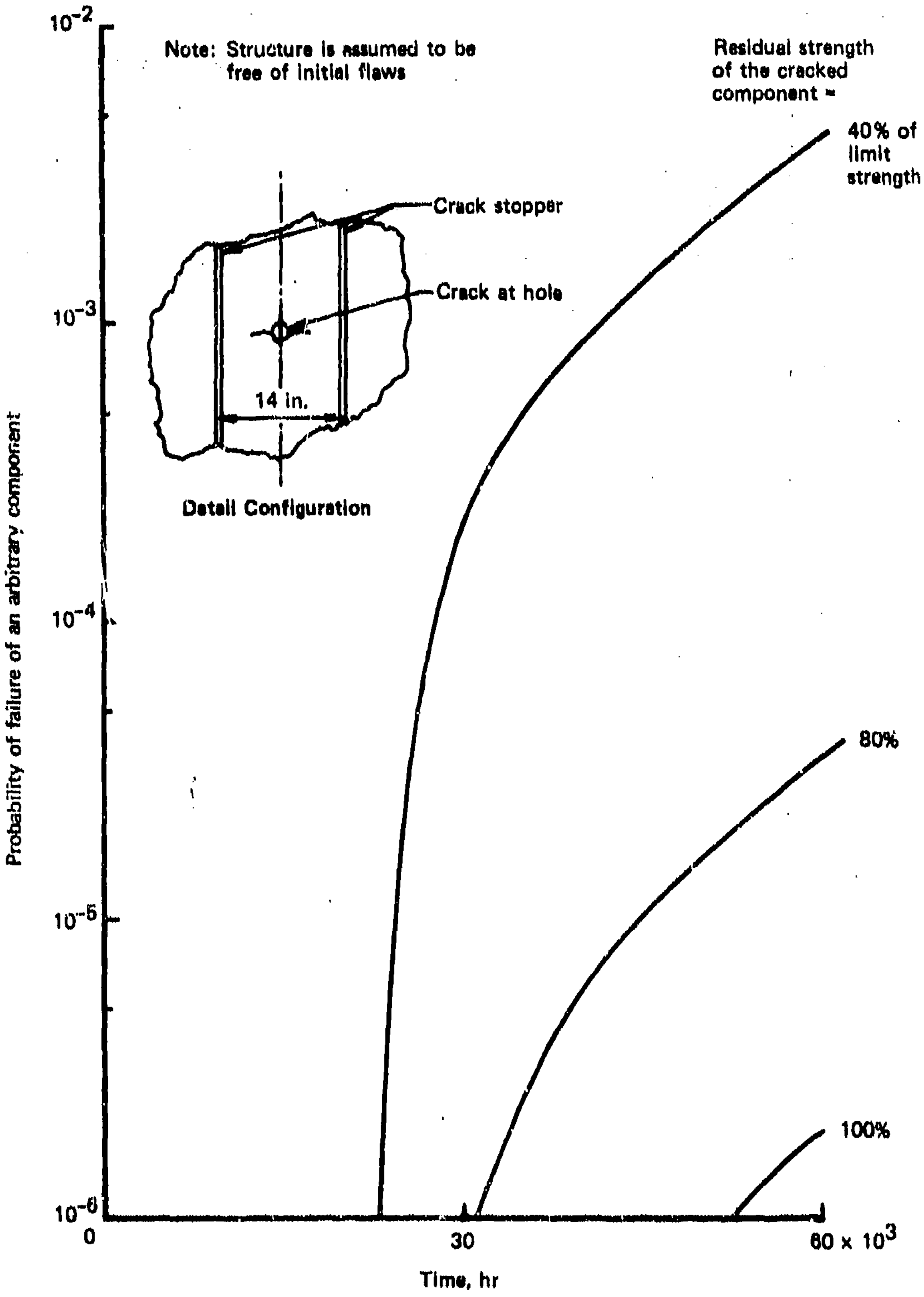

Figure 24.—Impact of Residual Strength on the Reliability of a Skin-Type Structure Without Initial Flaws—Type A Loads

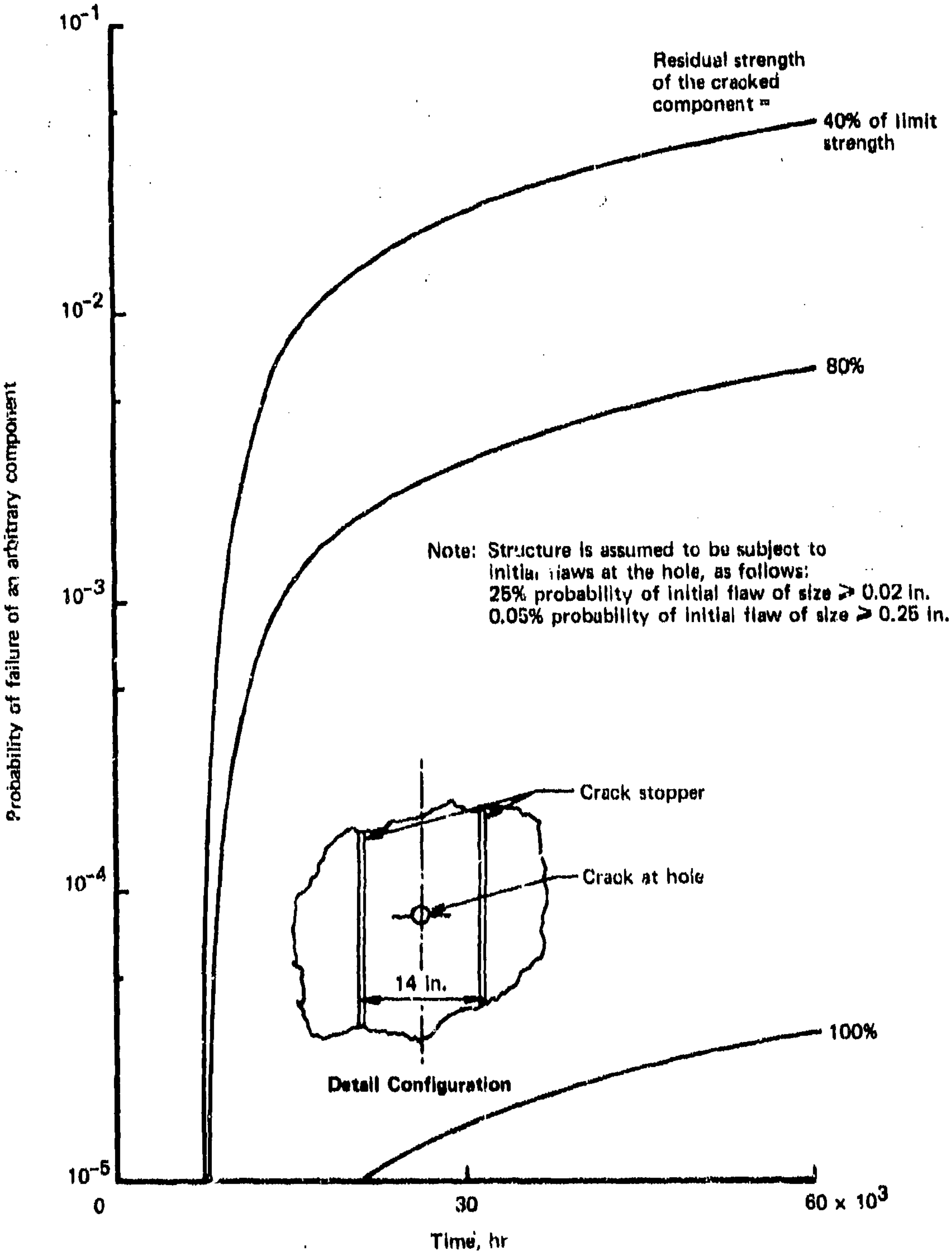

Figure 25.—Impact of Residual Strength on the Reliability of a Skin-Type Structure With Initial Flaws—Type A Loads

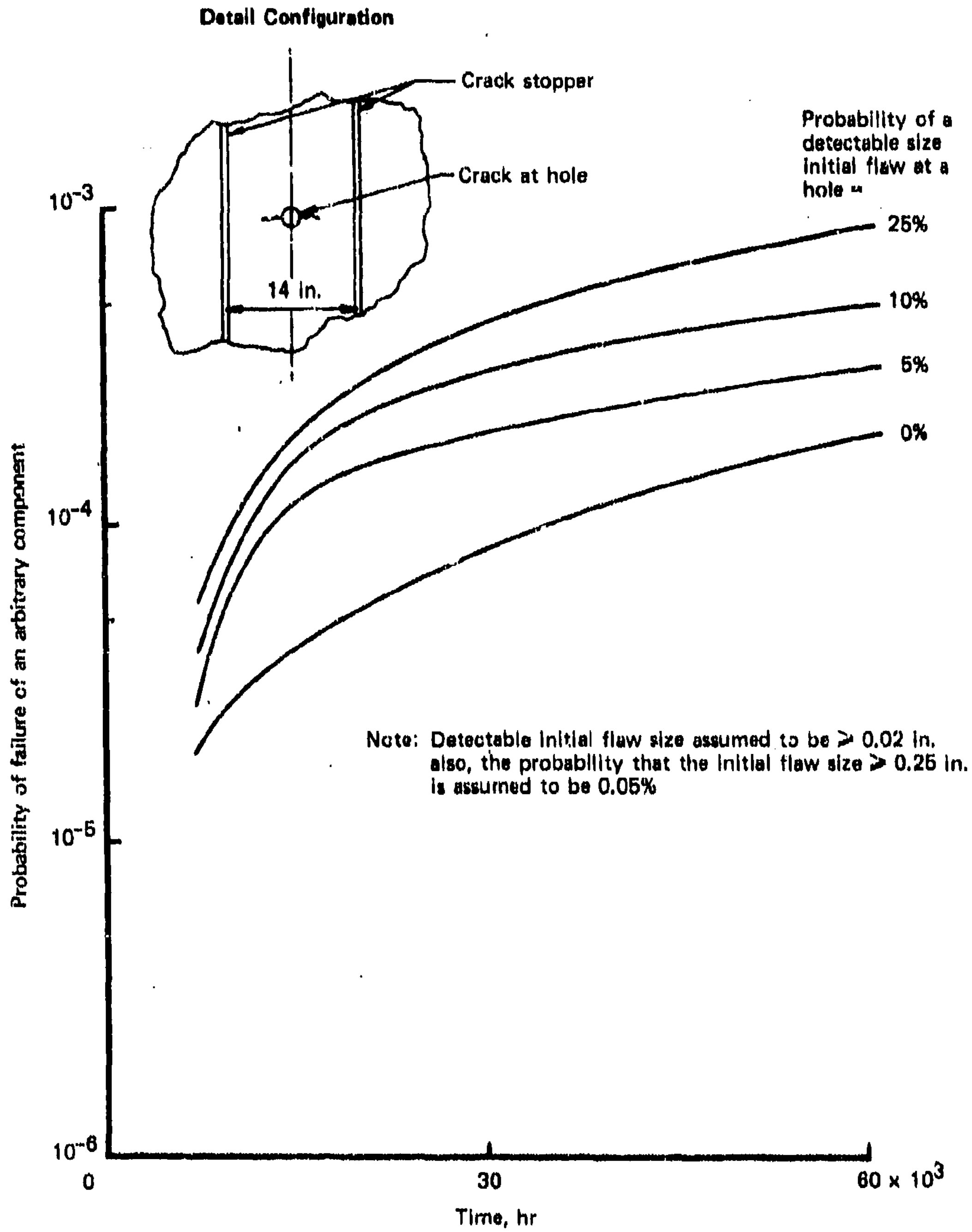

Figure 26.—Impact of Initial Flaws on the Reliability of a Fail-Safe Structure—Type B Loads

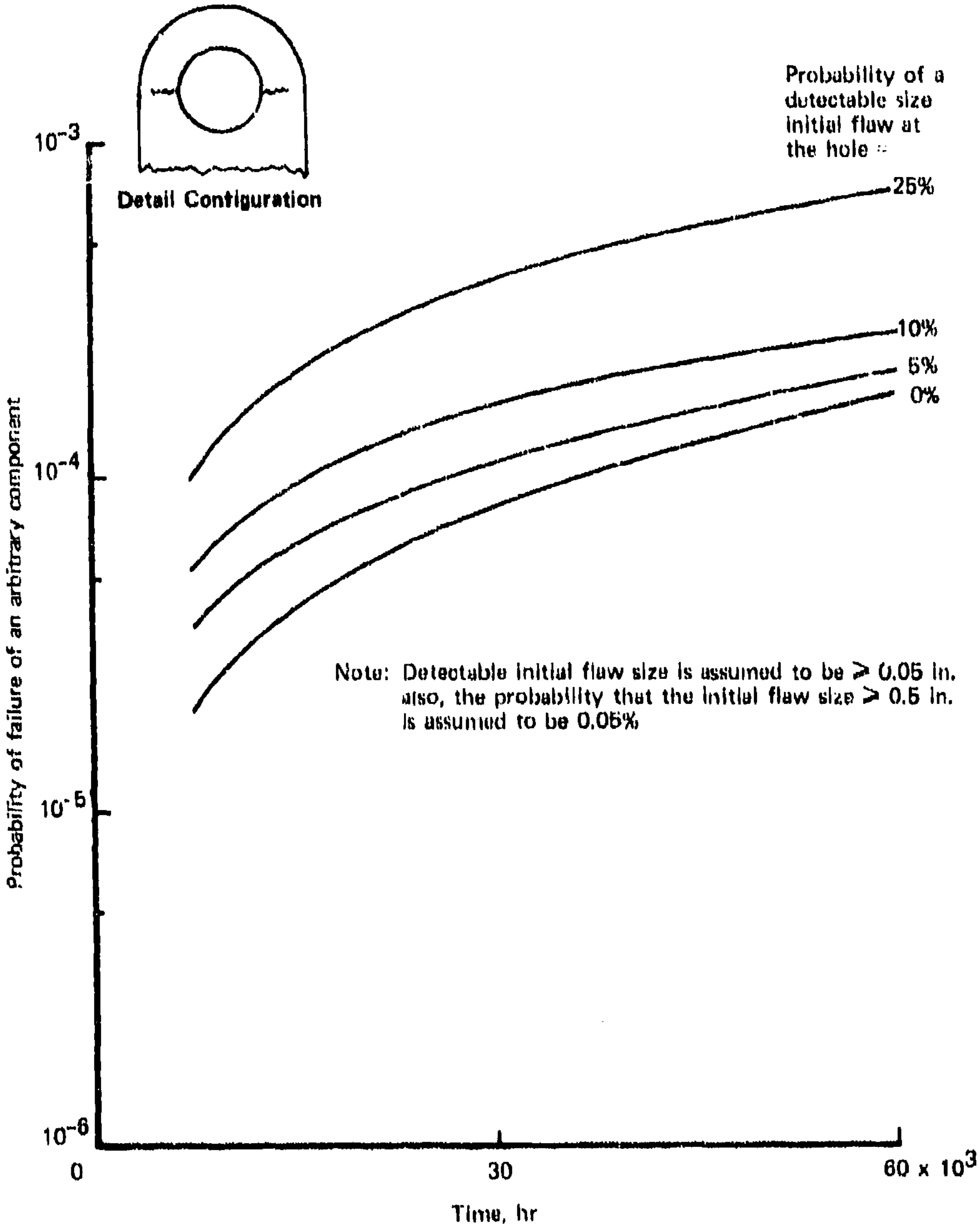

Figure 27.--Impact of Initial Flaws on the Reliability of a Fail-Safe Aluminum Joint-Connection Structure—Type B Loads

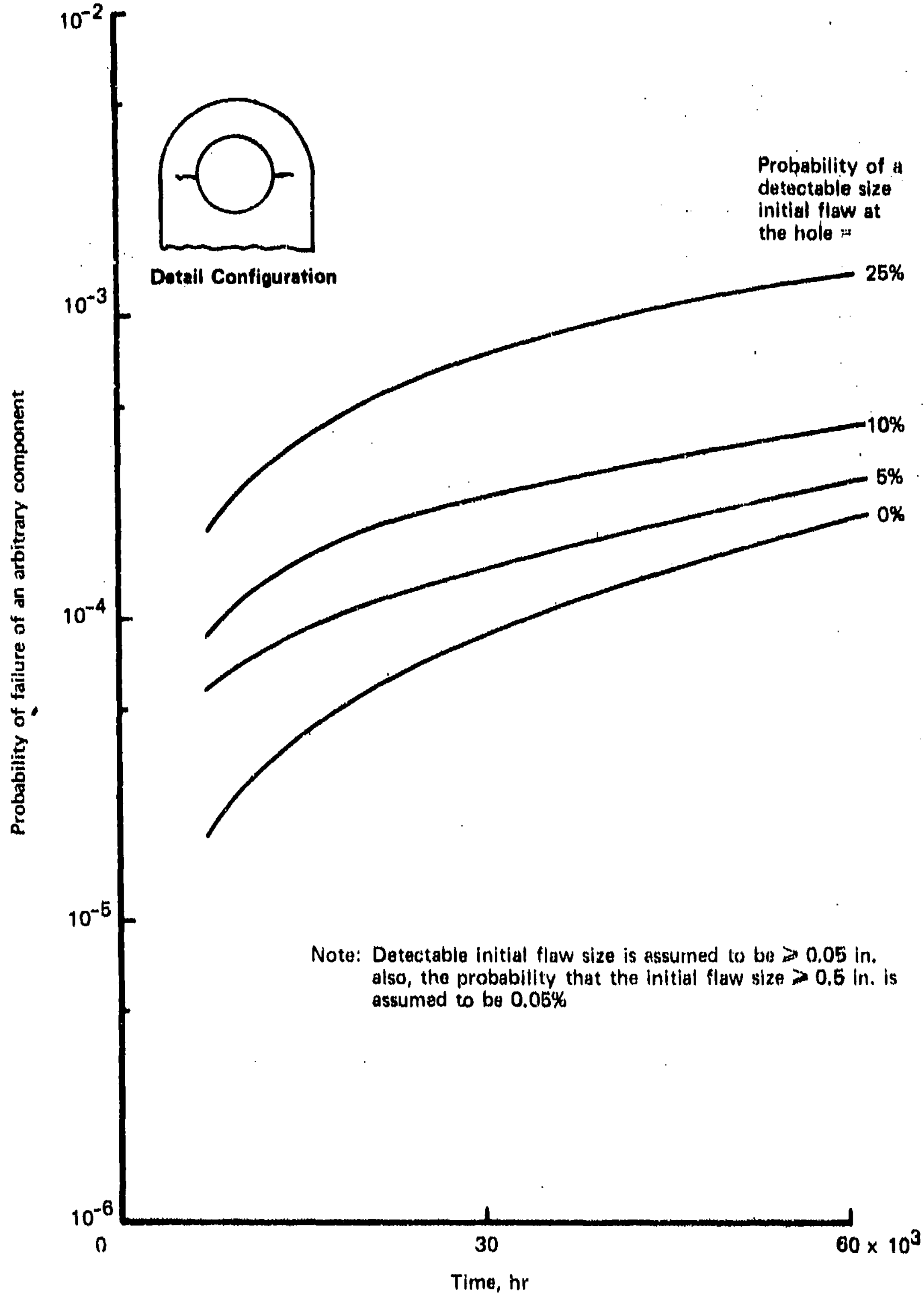

Figure 28.—Impact of Initial flaws on the Reliability of a Fail-Safe Steel Joint-Connection Structure—Type B Loads

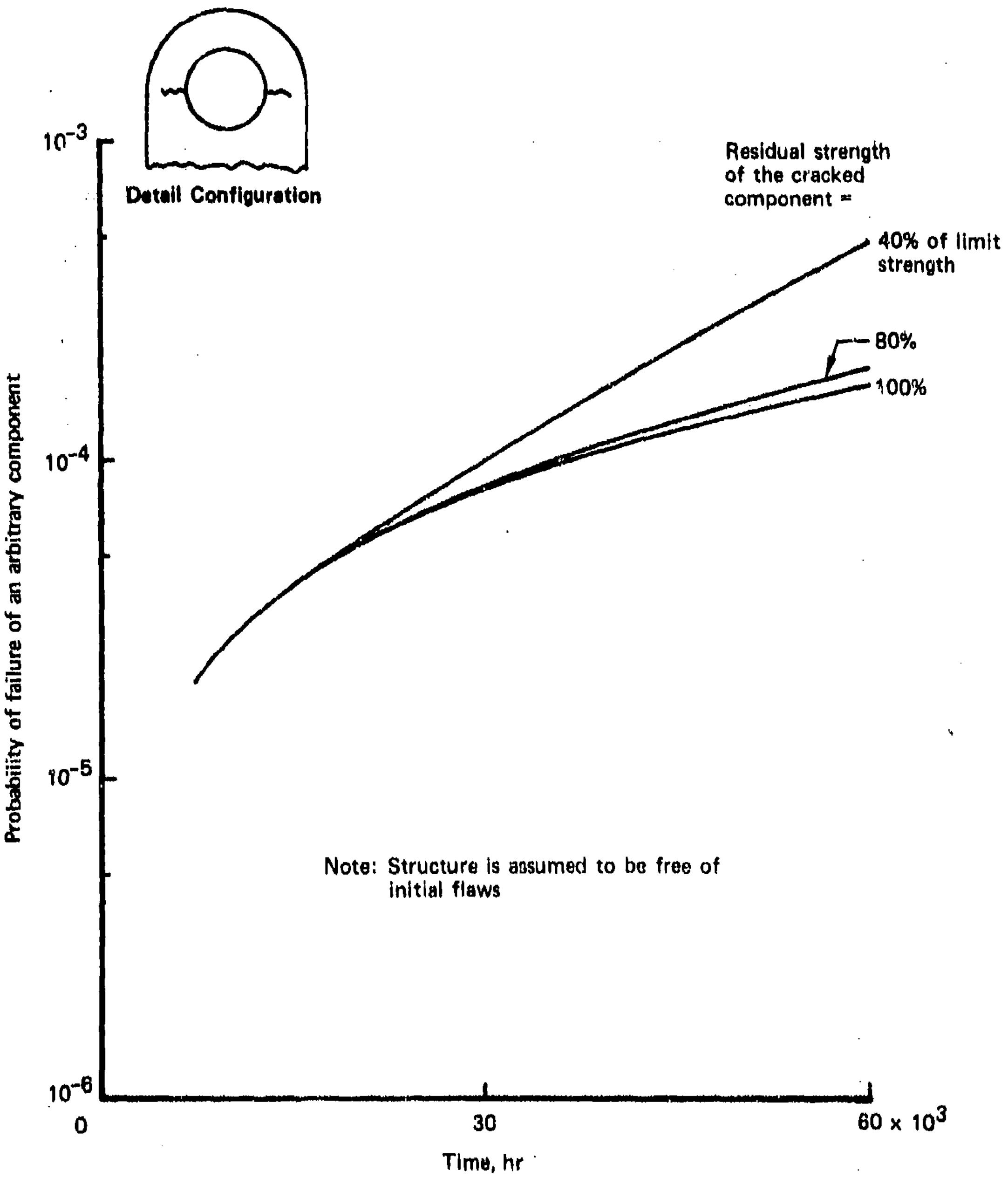

Figure 29.—Impact of Residual Strength on the Reliability of an Aluminum Joint-Connection Structure—Type B Loads

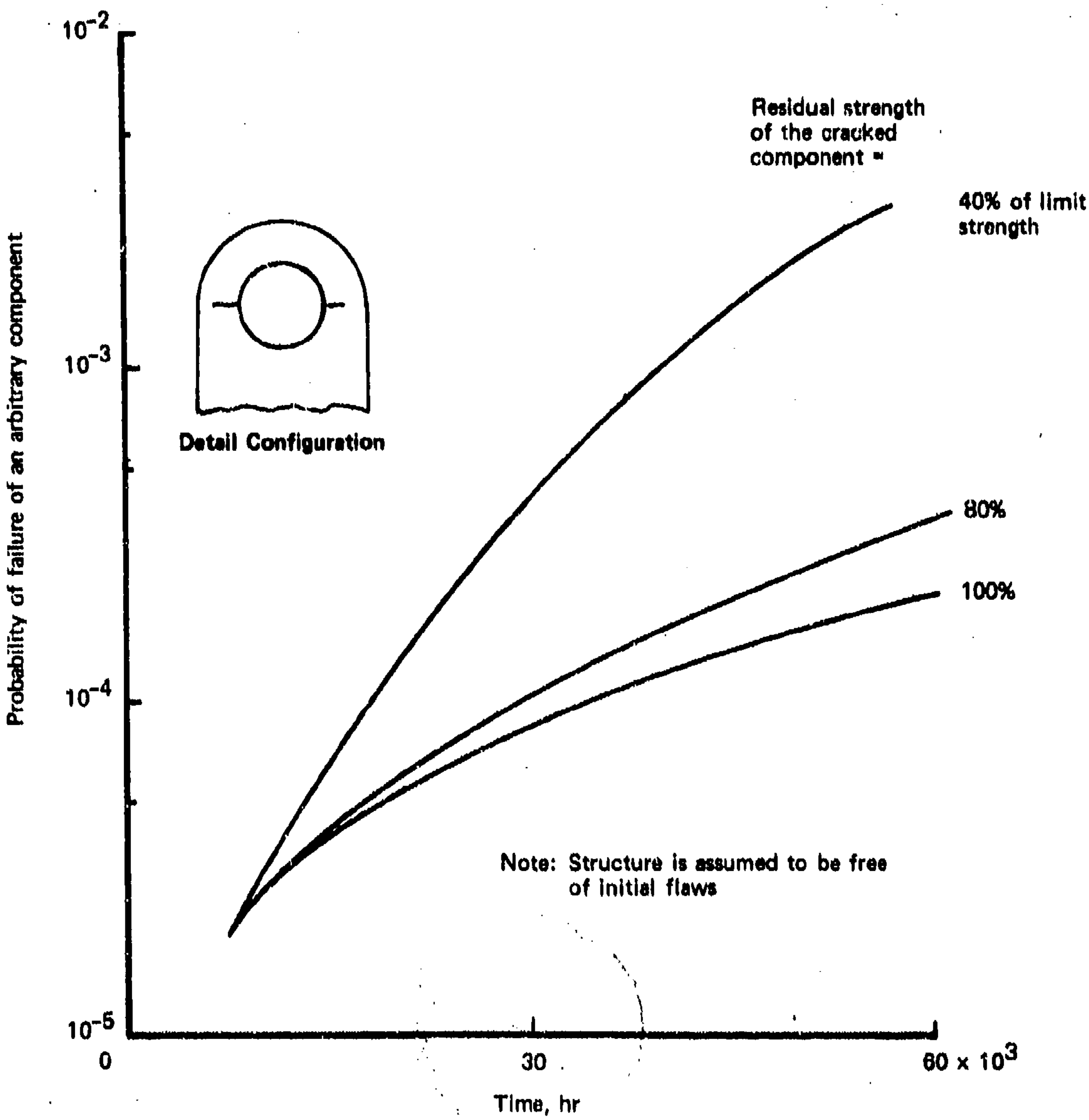

Figure 30.—Impact of Residual Strength on the Reliability of a Steel Joint-Connection Structure—Type B Loads

REFERENCES

1. Freudenthal, A. M., "Reliability Analysis Based on Time to First Failure," published in *Aircraft Fatigue: Design Operational and Economic Aspects* (proceedings of the symposium held in Melbourne, 22-24, May 1967); edited by J. Y. Mann and I. S. Milligan, Pergamon Press, Australia, 1972.

2. Whittaker I. C. and Besuner, P. M., *A Reliability Analysis Approach to Fatigue Life Variability of Aircraft Structures,* AFML-TR-69-65, March 1969.

3. Whittaker, I. C., *Development of Titanium and Steel Fatigue Variability Model for Application of Reliability Analysis to Aircraft Structures,* AFML-TR-72-236, October 1972.

4. Scarphie, C. S. and Watson, R. S., *Evaluation of a Reliability Analysis Approach to a Fatigue Life Variability of Aircraft Structures Using C-130 In-Service Operational Data,* AFML-TR-70-272, February 1971. (Distribution limited.)

5. Impellizzeri, L. F., Siegel, A. E., and McGinnis, R. A., *Evaluation of a Structural Reliability Analysis Procedure as Applied to Fighter Aircraft,* AFML-TR-73-150, September 1973. (Distribution limited.)

6. Whittaker, I. C. and Gerharz, J. J., *A Feasibility Study for Verification of Fatigue Reliability Analysis,* AFML-TR-70-157, September 1970.

7. Butler, J. P. and Rees, D. A., *Development of Statistical Fatigue Failure Characteristics of 0.125 2024-T3 Aluminum Under Simulated Flight-by-Flight Loading,* AFML-TR-74-124, July 1974.

8. Butler, J. P. and Rees, D. A., *Exploration of Statistical Fatigue Failure Characteristics of 0.063-Inch Mill-Annealed Ti-6Al-4V Sheet and 0.050-Inch Heat-Treated 17-7Ph Steel Sheet Under Simulated Flight-by-Flight Loading,* AFML-TR-74-269, January 1974.

9. Birnbaum, Z. W. and Saunders, S. C., "A New Family of Life Distributions," *J. of Applied Probability,* 6, pp 319-327, August 1969.

10. Saunders, S. C., "A Family of Random Variables Closed Under Reciprocation," *J. Amer. Statist. Assoc.,* 69, pp 533-539, June 1974.

11. Abelkis, P. R., *Fatigue Strength Design and Analysis of Aircraft Structures. Part I. Scatter Factors and Design Charts,* AFFDL-TR-66-197, Part I, June 1967.

12. Whittaker, I. C. and Saunders, S. C., *Exploratory Development on Application of Reliability Analysis to Aircraft Structures Considering Interaction of Cumulative Fatigue Damage and Ultimate Strength,* AFML-TR-72-283, January 1973.

13. Whittaker, I. C. and Saunders, S. C., *Application of Reliability Analysis to Aircraft Structures Subject to Fatigue Crack Growth and Periodic Structural Inspection,* AFML-TR-73-92, June 1973.

14. Varanasi, S. R. and Whittaker, I. C., "A Structural Reliability Prediction Method Considering Crack Growth and Residual Strength," *Fatigue Crack Growth Under Spectrum Loads,* ASTM-STP 595.

15. *Airplane Damage Tolerance Design Requirements,* MIL-A-83444 (USAF), July 1974.

16. Weibull, W., *Scatter in Fatigue Life of 24S-T Alclad Specimens With Drilled Holes,* SAAB TN 32, May 1955.

17. Gran, R. J. et al., *Investigation and Analysis Development of Early Life Aircraft Structural Failure,* AFFDL-TR-70-149, March 1971.

☆ U. S. GOVERNMENT PRINTING OFFICE: 1976 — 657-630/666